Institut de Nanociència
i Nanotecnologia
UNIVERSITAT DE BARCELONA

2026 IN²UB Inhouse Meeting

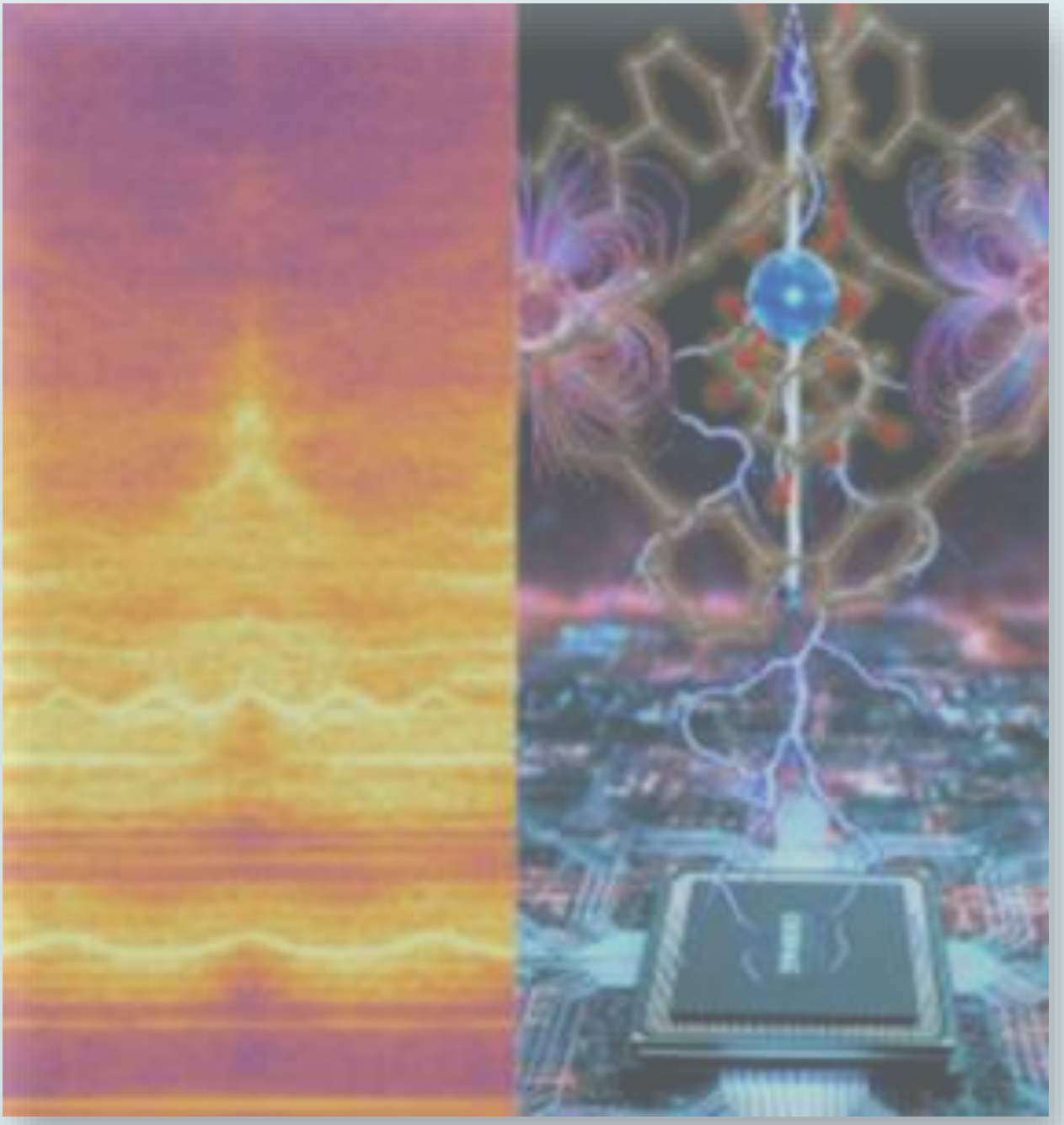

8th July 2026
(Faculties of Chemistry and Physics UB)

Institut de Nanociència
i Nanotecnologia
UNIVERSITAT DE BARCELONA

Editorial Board and Management: IN2UB

Cover images:

Left imatge: Fragment of Magnon population spectrum n(kx, f) of the OMM system with Bext = 150 mT and Bpump = 120 mT at t = 300 ns, The spectra has been obtained by performing the FFT with 4-ns-long time blocs. Kindly provided by, Dario González Diez (First Prize, Poster Awards, IN2UB 2025 Inhouse Meeting).

Right imatge: Tunable Functionalization of Host-Guest Supramolecular Assemblies *via* Selectice Metal Ion Employment. Kindly provided by, Konstantinos Sotirakopoulos, (Second Prize, Poster Awards, IN2UB 2025 Inhouse Meeting).

Content

FOREWORD

Dear IN2UB members,

It is a great pleasure to welcome you to the 2026 IN2UB Annual Workshop. This year marks the beginning of a new chapter for the institute, with a newly appointed Council and my appointment as the new Director. I would like to express my sincere gratitude to all Council members who volunteered to take on this responsibility, as well as for their personal support of my candidacy. I would also like to extend my heartfelt thanks to Prof. Guillem Aromí for his dedication and commitment to the institute. I would not be in this position without Guillem's support, and I believe that his personality, leadership, and charisma have played a fundamental role in keeping the institute cohesive and strong.

Science thrives on collaboration, and this should remain the guiding principle that gives purpose to our institute. Meaningful collaboration, however, requires mutual understanding. The posters and oral presentations at this Workshop play a crucial role in fostering that understanding by showcasing the outstanding research carried out by members of our institute. In this sense, the Annual Workshop is arguably the institute's most important event. I deeply appreciate the time and effort invested by the organizers, as well as by all scientific contributors and participants who make this event possible.

We are currently navigating a period of transition, with new members joining our university and institute while senior colleagues move toward retirement. The newly appointed Council reflects this evolving landscape. Our goal is to preserve and reinforce the qualities that have made the institute successful, including initiatives such as the ART grants and this Annual Workshop. At the same time, we aim to introduce new ideas to further enhance the institute, including improvements to its internal structure and a renewal of the website. Above all, we are committed to ensuring that it remains a vibrant forum for exchange, collaboration, and inspiration, centered on what unites us all: a shared passion for science!

Warm regards,

Martí Duocastella

PROGRAM

8th July 2026

Aula Magna, Solar Atrium and Hall
(Faculties of Chemistry and Physics UB)

9:30h – 10h Registration

10h – 10.10h Welcome&Opening (Prof. Martí Duocastella Solà, IN2UB Elected Director)

SESSION I Chaired by Giancarlo Franzese (Full Professor, Physics)

10.10h – 10.30h Oral 1- Ni-HHTP cMOF for Chemiresitive Gas Sensing of CH4 and CO2: from Crystalline Structure to Mechanism Insight. By, Ignasi Fort-Grandas (Predoctoral Researcher, Physics)

10.30h – 10.50h ART1 – Biophysical Optimization of Targeted Cleavable Nanoparticle as Biosensors for Early Detection of Neuronal Degeneration in Glaucoma. By, Gerard Esteruelas-Navarro (Postdoctoral Researcher, Pharmacy)

10.50h –11.10h Oral 2 – Submicron and Micron 2.5d Contact Guidance Cues for Cardiomyocyte Alignment by Two Photon Polymerization. By, Emma Oriol-Ferrero (Predoctoral Researcher, Physics)

11.10h – 11.50h Break (Atri)

SESSION II Chaired by Marta Estrader Bofarull (Associate Professor, Chemistry)

11.50h – 12.10h Oral 3 – Microwave Assisted Synthesis of Lanthanoid 2d Metal-Organic Frameworks. By, Samuel John Amali (Predoctoral Researcher, Chemistry)

12.10h – 12.30h Oral 4 – Processing-Tuned Energy Storage in $Ba_{1-x}Sr_xTiO_3$ Ceramics. By, Nerea Morante del Pino (Predoctoral Researcher, Chemistry)

12.30h – 12.50h Oral 5 – Advanced Synergistic Delivery Systems in Oncology: The Combination of Apigenin and Melatonin within Rosehip-Based Nanocarriers. By, Lorena Bonilla-Vidal (Postdoctoral Researcher, Pharmacy)

12.50h – 13.10h Oral 6 – Size-Dependent Antiferromagnetism and Direct Observation of Néel Axes in NiO Nanoparticles By XMLD. By, Jorge Ara-Escario (Predoctoral Researcher, Physics)

13.10h – 14h Lunch (Atri)

14h – 14.50h Poster Session I (Martí i Franquès)

SESSION III – Chaired by Xavier Batlle Gelabert (Full Professor, Physics)

14.50h – 15.10h ART2 – Next Generation Elastocaloric Materials for Energy-Efficient Cooling (NEXTCOOL). By, Raúl Díaz-Torres (Tenure-Track Lecturer, Chemistry) & Enric Stern-Taulats (Ramón y Cajal Postdoctoral Researcher, Physics)

15.10h – 15.30h Oral 7 – Controlled Phototaxis of Active Liquid Crystal Emulsions. By, Joel Torres Andrés (Predoctoral Researcher, Chemistry)

15.30h – 16.20h Poster Session II (Martí i Franquès)

16.20h – 17h Break (Atri)

17h – 17.20h Poster recognition

17.20h – 17.30h Closing Remarks (Prof. Guillem Aromí Bedmar, IN2UB Acting Director)

ART

1-Biophysical Optimization of Targeted Cleavable Nanoparticle as Biosensors for Early Detection of Neuronal Degeneration in Glaucoma

G.Esteruelas [1,2*], M.J. Gomara[3], L.Bonilla[1,2], O.Domench[1,2], J.Font[1], I.Haro [3], M.Espina [1,2], M.L.García [1,2], E.Sánchez-López[1,2]

[1] Dep.of Pharmacy, Pharmaceutical Technology and Physical Chemistry, Faculty of Pharmacy and Food Sciences, University of Barcelona; [2] Institute of Nanoscience and Nanotechnology (IN2UB), University of Barcelona; [3] Unit of Synthesis and Biomedical Applications of Peptides, IQAC-CSIC.

gesteruelas@ub.edu

Glaucoma is a progressive neurodegenerative disease and one of the leading causes of irreversible blindness worldwide, with retinal ganglion cell degeneration often progressing silently until permanent visual damage has occurred [1,2]. Since apoptosis represents a key early event in retinal neurodegeneration, the development of non-invasive molecular tools capable of detecting apoptotic activity may provide new opportunities for earlier diagnosis and disease monitoring [3]. In this context, we report the development of a targeted fluorescent nanosensor based on PLGA nanoparticles designed for ocular application and apoptosis-responsive detection in retinal cells.

The sensing mechanism is based on a caspase-3-responsive FRET system, in which a biosensing peptide containing a DEVD cleavable sequence is coupled to a donor/acceptor fluorophore pair. Upon enzymatic cleavage, the distance between both fluorophores is modified, leading to a measurable ratiometric fluorescence change. In parallel, an RGD-based guiding peptide was incorporated to enhance interaction with retinal cells. Both peptides were successfully synthesized and covalently conjugated to the polymeric nanoparticle surface, confirming the feasibility of the multifunctional nanosensor design.

After formulation optimization, the functionalized nanoparticles displayed physicochemical properties suitable for ocular nanomedicine applications, with a mean hydrodynamic diameter of 192.3 ± 2.3 nm, a low polydispersity index of 0.102 ± 0.006, and a positive zeta potential of +32.8 ± 6.3 mV. Transmission electron microscopy confirmed their spherical morphology and the formation of well-defined nanostructures. *In vitro* MTT assays performed in R28 and ARPE cell lines showed good cellular tolerability and low toxicity under the tested experimental conditions, supporting their suitability for retinal cell studies and future ocular application [3].

Apoptosis was induced in R28 retinal precursor cells to establish a disease-relevant *in vitro* model for evaluating nanosensor performance. Functional studies assess the ratiometric fluorescence response associated with DEVD cleavage by caspase-3, together with the ability of the targeted nanoparticles to discriminate apoptotic from non-apoptotic retinal cells. Overall, these results support the potential of this FRET-based PLGA nanosystem as a promising non-invasive fluorescent platform for the early detection of glaucoma-associated retinal neurodegeneration.

References: [1] Al-Wizni A, Saleki M, Lee CYPD, et al. Noninferiority of selective and micropulse laser trabeculoplasties: a meta-analysis and systematic review. Lasers Med Sci. 2025;40:198. [2] Rusciano D, Pezzino S, Mutolo MG, Giannotti R, Librando A, Pescosolido N. Neuroprotection in glaucoma: old and new promising treatments. Adv Pharmacol Sci. 17;2017:4320408. [3] Zhang X, Vadoothker S, Munir WM, Saeedi O. Ocular surface disease and glaucoma medications: a clinical approach. Eye Contact Lens. 2019;45(1):11–18.

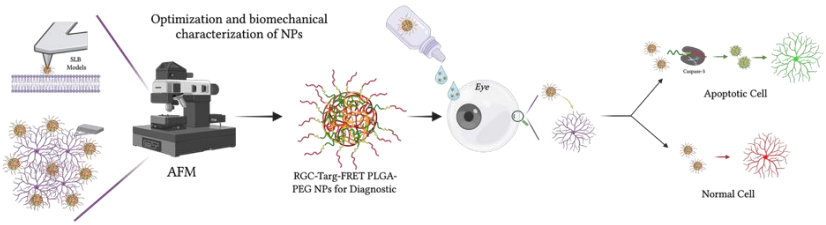

Figure 1. Project key relevant features.

2- NEXT GENERATION ELASTOCALORIC MATERIALS FOR ENERGY-EFFICIENT COOLING (NEXTCOOL)

R. Díaz-Torres[1,2], E. Stern-Taulats[2,3], P. Garcia Sanchez[1]

[1]Departament de Química Inorgànica i Orgànica, Secció de Química Inorgànica, Facultat de Química, Universitat de Barcelona (UB)

[2]Institut de Nanociència i Nanotecnología, Universitat de Barcelona (IN²UB)

[3]Departament de Física de la Matèria Condensada, Facultat de Física, Universitat de Barcelona (UB)

rauldiaz@ub.edu / enric.stern@fmc.ub.edu

Conventional refrigeration technologies based on hydrofluorocarbons (HFCs) are among the largest contributors to greenhouse gas emissions, driving the search for sustainable solid-state cooling alternatives. The elastocaloric (eC) effect — a reversible temperature change induced by uniaxial mechanical stress — is one of the most promising routes towards compact and energy-efficient cooling devices. Spin-crossover (SCO) complexes of Fe(II) are particularly attractive candidates for eC applications: they undergo reversible high-spin (HS) to low-spin (LS) transitions near room temperature, accompanied by large entropy changes at relatively low operating stresses. When incorporated into a polymer matrix, these complexes form a mechanically addressable materials capable of sustaining the stress cycles required for elastocaloric operation — something unfeasible with loose powders or single crystals.

The NEXTCOOL project aims to develop and characterise SCO/polymer composites optimised for elastocaloric cooling. Optimisation efforts focus on two complementary aspects: the molecular design of SCO complexes and the fabrication of the composite. On the molecular side, complexes bearing flexible functional groups are being designed to maximise the entropy change associated with the spin-state transition. On the materials side, key parameters such as matrix rigidity, SCO loading ratio, sample geometry, and the nature of the SCO component are being systematically investigated. As an initial experimental approach, a series of [Fe(qsal-X)$_2$] complexes (X = Cl, Br, I) has been incorporated into polymer matrices and evaluated under mechanical loading. A preliminary temperature drop of ~1 °C upon stress release, consistent with the elastocaloric effect, has been observed. These results establish the basis for further optimisation towards larger and reversible ΔT values.

References:

[1] *Nat. Commun.* 2024, **15**, 6171. [2] *J. Mater. Chem. C* 2026, **14**, 2641.

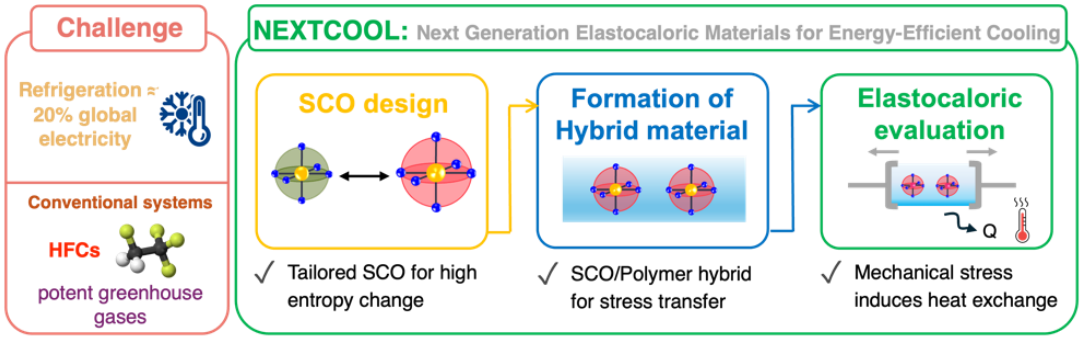

ORALS

O.1. Ni-HHTP cMOF for Chemiresitive Gas Sensing of CH4 and CO2: from Crystalline Structure to Mechanism Insight

Ignasi Fort-Grandas,[1,2,3] Marta Martínez-Belmonte,[4] Jordi Benet-Buchholz,[4] Rosa M. Gomila,[5] An-toni Frontera,[5] Albert Romano-Rodríguez, [1,2] and Anton Vidal-Ferran [3,6]

[1] Department of Electronic and Biomedical Engineering, Universitat de Barcelona, 08028 Barcelona, Catalonia, Spain. [2] Institute of Nanoscience and Nanotechnology (IN2UB), Universitat de Barcelona 08028 Barcelona, Catalonia, Spain.[3] Department of Inorganic and Organic Chemistry, Universitat de Barcelona Catalonia, Spain. [4] Institute of Chemical Research of Catalonia (ICIQ), 43007 Tarragona, Catalonia, Spain.[5] Department of Chemistry, Universitat de les Illes Balears, 07122 Palma de Mallorca, Spain.[6] ICREA (Institució Catalana de Recerca i Estudis Avançats), 08010 Barcelona, Catalonia, Spain.

ignfortgra_9@ub.edu

The importance of monitoring greenhouse gas (GHGs) levels with miniaturized and efficient devices has become an important challenge which remains unresolved. Conductive Metal-Organic Frame-works (cMOFs) have been presented as promising due to their capability to produce chemiresistive responses at room temperature. We report for the first time the crystal structure of Ni-HHTP cMOF and its CH4 and CO2 gas sensing properties. We discuss the gas-MOF interactions and mechanism to justify the significantly higher sensitivity of the sensor towards CH4.

Keywords: Conductive MOFs, crystalline, chemiresistivity, mechanism, CH4 and CO2 sensing.

Background, Motivation and Objective: Currently, most solid-state gas sensing tech-nologies come from devices that are made from semiconducting metal oxides (MOXs). Despite large efforts, two major drawbacks remain for their suitability in integrated sensor applications: their relatively high operating tem-perature (above 150 ºC) and their poor selectiv-ity, i.e., their inability to correctly discriminate and quantify the concentration of a specific gas within a mixture [1]. These limitations, more specifically the former, can be overcome by using cMOFs instead of MOXs as the sensing material in chemiresistive sensors, as they are able to operate at room temperature [2, 3].

Conductive cMOFs are a subfamily of Metal-Organic Frameworks (MOFs), as only by means of specific chemical design of the ligand and the coordination chemistry with the metal can an electronically conductive MOF be formed. Triphenylene-derivative MOFs have attracted attention in recent years for their po-tential applications, including chemiresistive gas sensing [4]. In particular, our research has focused on the coordination of 2,3,6,7,10,11-hexahydroxytriphenylene (HHTP) with nickel salts to yield Ni-HHTP MOF crystals. The lack of reported crystal structures for triphenylene-derivative MOFs makes the discussion of gas-MOF interactions a challenge. By obtaining the single-crystal structure of Ni-HHTP, we aim to discuss the material nature and its interactions with CH4 and CO2 gases, for which we report the chemiresistive gas sensing for the first time.

Description of the New Method or System: Single crystal Ni-HHTP nanoparticles were syn-thesized via hydrothermal MOF synthesis. A coordinating solvent, DMF (n,n-dimethylformamide), was added to modulate the rate of particle formation and, thus, favor crystal growth. The Ni-HHTP crystal structure was resolved using 3D electron diffraction tech-nique.

The conductive MOFs are deposited onto cus-tom-made Au/Cr/SiO2 interdigitated electrodes (IDE) via drop-casting technique to fabricate the gas sensing devices.

Room temperature chemiresistive gas sensing experiments were performed using dry synthet-ic air (SA) as carrier gas, and exposing the sensor to CH4 and CO2 pulses using concentra-tion ranges of the order of their respective am-bient gas levels. Computational studies have been performed with the goal of discussing the analyte gas-MOF interactions and bring insight into the chemiresistive effect [3].

Results: The crystal structure obtained for Ni-HHTP MOF reveals two different layers forming the MOF, as depicted in Fig 1. A polymeric-like layer is formed by extended structure of Ni3(HHTP)2·6H2O. Notably, Ni3(HHTP)1·12H2O units are found in-between layers of Ni3(HHTP)2·6H2O. These discrete units are held together with the polymeric layer by intermolecular interactions, mainly hydrogen bonding and pi-pi stacking, yielding the complete structure of the MOF.

Chemiresistive CH4 and CO2 gas sensing ex-periments at room temperature show the sen-sor response to both analytes (Fig. 2 and Fig. 3). The response is proportional to the concen-tration of the analyte. The studied concentration ranges for both CH4 and CO2 gases compre-hend respective ambient gas levels, postulating Ni-HHTP as a promising greenhouse gas sens-ing material.

References [1] T. Lin, X. Lv, Z. Hu, A. Xu, C. Feng, Semiconduc-tor Metal Oxides as Chemoresistive Sensors for Detecting Volatile Organic Compounds, Sensors 19, 233 (2019); doi: 10.3390/s19020233. [2] Y. Li, A. Xiao, B. Zou, H. Zhang, K. Yan, Y. Lin, Advances of metal–organic frameworks for gas sensing, Polyhedron 154, 83-97 (2018); doi: 10.1016/j.poly.2018.07.028. [3] I. Fort-Grandas, M. Martínez-Belmonte, J. Benet-Buchholz, R. M. Gomila, A. Frontera, A. Romano-Rodríguez, A. Vidal-Ferran Layered Nickel–HHTP Networks for Efficient Chemiresistive Sensing of Greenhouse Gases ACS Small (2026) Manu-script under revision. [4] M. Campbell, S. Liu, T. Swager, M. Dincă, Chemiresistive Sensor Arrays from Conductive 2D Metal–Organic Frameworks J. Am. Chem. Soc. 43, 13780-13783 (2015); doi: 10.1021/jacs.5b09600

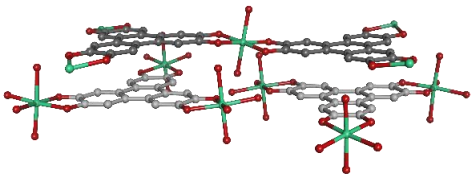

Fig. 1. Illustration obtained from the crystal struc-ture of Ni-HHTP MOF showing the two distinct units of Ni-HHTP layers on top and and Ni fragments at the bottom.

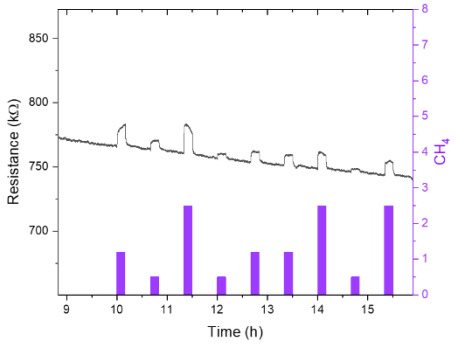

Fig. 2. Room-temperature resistance variation of Ni-HHTP MOF under SA with CH_4 pulses of different concentrations.

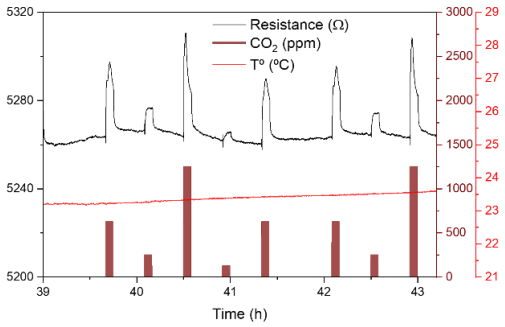

Fig. 3. Room-temperature resistance variation of Ni-HHTP MOF under SA with CO2 pulses of different concentrations.

O.2. SUBMICRON AND MICRON 2.5D CONTACT GUIDANCE CUES FOR CARDIOMYOCYTE ALIGNMENT BY TWO PHOTON POLYMERIZATION

Emma Oriol-Ferrero[1,4], Renato Eduardo-Yanac[1,2,4], Paula Ferrando[1,2,4], Bárbara Borges-Fernandez[1,4], Byron Suárez-Villacres[1,2,4], Elisabeth Engel[5,2,3], Romen Rodríguez[1,3,4], Oscar Castano[1,2,3,4]

[1]Electronics and Biomedical Engineering, Universitat de Barcelona (UB), 08028 Barcelona, Spain
[2]Biomaterials for Regenerative Therapies, Institute for Bioengineering of Catalonia (IBEC), The Barcelona Institute of Science and Technology (BIST), Baldiri i Reixac 10-12, 08028 Barcelona, Spain.
[3]CIBER en Bioingeniería, Biomateriales y Nanomedicina (CIBER-BBN) 28029 Madrid, Spain
[4]Institute of Nanoscience and Nanotechnology, Universitat de Barcelona (UB), 08028 Barcelona, Spain.
[5]Materials Sciences and Engineering, Universitat Politècnica de Catalunya (UPC), 08930, Barcelona, Spain

eoriolfe@ub.edu

Introduction: Current in vitro models remain limited in recapitulating native cardiac tissue connectivity, which depends critically on anisotropic cellular alignment. Here, we aim to engineer a myocardium-like microenvironment through contact guidance using two-photon-polymerized microscale structures. While anisotropically electrospun PLA fibers have demonstrated cardiomyocyte alignment in 2D systems [1], two-photon polymerization (2PP) offers finer geometric control and a pathway toward aligned 3D cardiac tissues for heart-on-a-chip applications.

Materials and Methods: Scaffold geometries were mechanically assessed using COMSOL Multiphysics finite element analysis across a range of Young's modulus and Poisson's ratio values. IP-Visio resin (Nanoscribe GmbH) was selected based on mechanical stability and low autofluorescence. 2.5D micro and submicron patterns were fabricated on glass substrates by 2PP lithography and characterized by scanning electron microscopy (SEM). After a gelatine coating, HL-1 cardiomyocytes were cultured on the substrates until confluence. Samples were fixed and stained for α-actinin, connexin-43, and DAPI, followed by confocal imaging. Sarcomeric alignment was quantified using tensor analysis of α-actinin fluorescence.

Results: Finite element simulations confirmed IP-Visio as mechanically suitable for fabrication. Single-scale periodic micropatterns and hierarchical patterns with secondary features of 700 nm, 1.4 µm, and 3 µm were printed and verified by SEM. Quantitative tensor analysis revealed enhanced cardiomyocyte alignment on all patterned substrates compared to unpatterned controls, with increased alignment for single-scale patterns and those with 3um secondary features.

Discussion: 2PP-fabricated micropatterns provided robust nanoscale-to-microscale guidance cues capable of directing cardiomyocyte organization. These results highlight the potential of high-resolution additive manufacturing for engineering anisotropic cellular microenvironment allowing for systematic variation of feature size, periodicity, and orientation to study contact-guidance effects. However, the high stiffness of IP-Visio (GPa range) relative to native myocardium may influence cell–material interactions. Future work will explore softer, 2PP-compatible resins and fully 3D architectures for integration into microphysiological and lab-on-chip systems.

References

[1] López-Canosa A, Perez-Amodio S, Yanac-Huertas E, Ordoño J, Rodriguez-Trujillo R, Samitier J, Castaño O, Engel E. A microphysiological system combining electrospun fibers and electrical stimulation for the maturation of highly anisotropic cardiac tissue. Biofabrication. 2021;13(3). doi:10.1088/1758-5090/abff12.

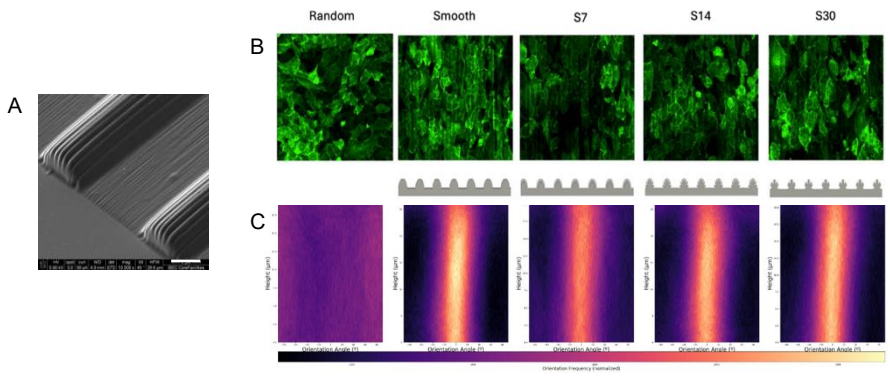

Figure 1. (A) SEM image of 2PP nanopatterned structure with 700nm-wide features (scale bar: 5um). (B) Confocal images of cells cultured on the patterned substrate. (C) Analysis of cellular orientation angles measured across different z-planes.

O.3. MICROWAVE ASSISTED SYNTHESIS OF LANTHANOID 2D METAL-ORGANIC FRAMEWORKS

Samuel John Amali[1,3], Chaima Arfa[1,2], E. Carolina Sañudo[1,3*]

[1]Departament de Química Inorgànica i Orgànica, Secció de Química Inorgànica, C/Martí i Franqués 1-11, 08028, Barcelona, Spain.
[2]University of Carthage, Faculty of Sciences of Bizerte, LR13ES08, Laboratory of Chemical Materials, 7021, Bizerte, Tunisia
[3]Institut de Nanociències i Nanotecnologia, Universitat de Barcelona (IN2UB), 08028 Barcelona, Spain.

esanudo@ub.edu

Metal-Organic Frameworks (MOFs) are highly porous crystalline materials composed of metal ions coordinated to organic ligands, known for their exceptional thermal stability, large surface area, variable pore sizes and tuneable properties, making them ideal for applications in, sensing [1], Carbon capture [2], drug delivery, and catalysis [3]. Despite their potential, traditional synthesis methods, such as solvothermal and hydrothermal processes, are time consuming and often result in low yields and poor phase purity. This study explores microwave-assisted synthesis to produce heterometallic lanthanoid 2D MOFs, which led to the discovery of novel MOFs with the general formula $[(Ln_xLn_{1-x})_4(PhCOO)_9(MeCOO)_3(MeOH)_3(H_2O)]\cdot MeOH\cdot MeCN$, the study include both homonuclear (Ln=La, Ce, Pr) and heterometallic compounds ([LaEu]), ([LaGd]), ([LaTb]) with varying lanthanide molar ratios.

The microwave-assisted method offers rapid and uniform heating, significantly reducing synthesis times from hours to minutes while enhancing the quality and yield of the MOFs. Characterization of the synthesized MOFs revealed good thermal stability and potentially significant gas sorption properties, including promising sensing capabilities and potential for application in quantum qubits

The implications of this research are significant, indicating that microwave-assisted synthesis can produce high quality MOFs with enhanced properties suitable for various applications. This study has opened avenues for testing the potential applications of the new MOFs.

References:

[1] F. Moghzi, J. Soleimannejad, E. C. Sañudo, and J. Janczak, "Dopamine Sensing Based on Ultrathin Fluorescent Metal-Organic Nanosheets," ACS Appl. Mater. Interfaces, vol. 12, no. 40, pp. 44499–44507, Oct. 2020, doi: 10.1021/acsami.0c13166.

[2] D. Sengupta et al., "Integrated CO2 Capture and Conversion by a Robust Cu(I)-Based Metal-Organic Framework," J. Am. Chem. Soc., vol. 146, no. 39, pp. 27006–27013, Oct. 2024, doi: 10.1021/jacs.4c08757.

[3] D. Li, A. Yadav, H. Zhou, K. Roy, P. Thanasekaran, and C. Lee, "Advances and Applications of Metal-Organic Frameworks (MOFs) in Emerging Technologies: A Comprehensive Review," Global Challenges, vol. 8, no. 2, Feb. 2024, doi: 10.1002/gch2.202300244

O.4. PROCESSING-TUNED ENERGY STORAGE IN $Ba_{1-x}Sr_xTiO_3$ CERAMICS

N. Morante[1,2], S. Lopez-Blanco[3], J. Garcia[3], L. Mestres[1,2], X. Vendrell[1,2]

[1] Department of Inorganic and Organic Chemistry, University of Barcelona
[2] Institute of Nanoscience and Nanotechnology, University of Barcelona
[3] Department of Physics, Universitat Politècnica de Catalunya

nerea.morante@ub.edu

The transition to low-carbon energy technologies relies heavily on advancements in energy-efficient processing techniques and sustainable energy storage materials. Conventional solid-state method often involves high temperatures, greater than 1000°C, and extended dwell times, hours or even days, resulting in substantial energy consumption and limited control over the final microstructure. Flash Sintering (FS) has emerged as a promising alternative,[1] enabling rapid densification at significantly reduced temperatures through the application of an external electric field, thereby minimizing the overall energy footprint of ceramic processing. A further refinement of this technique, known as Reactive Flash Sintering (RFS), combines the synthesis and sintering processes into a single step.[2]

This research explores the impact of processing route and composition on the energy storage performance of lead-free barium strontium titanate derivatives ($Ba_{1-x}Sr_xTiO_3$, BST), a material of considerable interest for dielectric energy storage applications.[3] BST compositions with strontium concentrations ranging from x = 0.3 to 0.6 were synthesized via both conventional solid-state and FS/RFS methods. Structural characterisation was carried out by powder X-ray diffraction (PXRD) with Rietveld refinement, while the microstructure was examined via scanning electron microscopy (SEM) and Electrochemical Impedance Spectroscopy (EIS) was used to analyse the electrical performance of the materials. The findings demonstrate clear correlations between the material's composition, the specific processing conditions employed, and its resulting dielectric and ferroelectric behaviour. Notably, flash-sintered BST ceramics exhibit competitive functional properties, as shows Figure 1, while substantially reducing the thermal processing demands associated with traditional methods. These results highlight the potential of flash sintering as an energy-efficient manufacturing route for advanced dielectric ceramics and position BST materials as viable candidates for contributing to sustainable electrostatic energy storage technologies.

References: [1] M. Cologna, *et al. J. Am. Ceram. Soc.*, **2010**, *93*, 3556. [2] S. López-Blanco, *et al. Mater. Chem. C*, **2025**, *13*, 3578. [3] H. Yang, *et al. ACS Appl. Mater Interfaces.*, **2020**, *12*, 43942.

Figure 1. Improvement of ferroelectric properties by using flash sintering method.

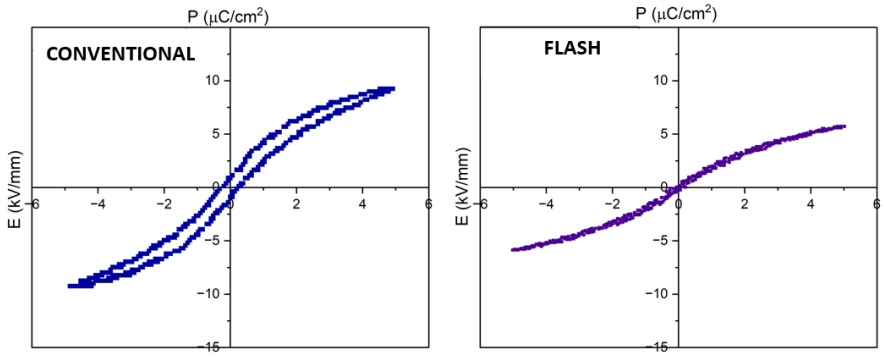

O.5. Advanced Synergistic Delivery Systems in Oncology: The Combination of Apigenin and Melatonin within Rosehip-Based Nanocarriers

L. Bonilla-Vidal [1,2], G. Esteruelas[1,2], M. Espina [1,2], María Luisa García [1,2], A. Gliszczyńska [3], E. Sánchez-López[1,2]

[1]Department of Pharmacy, Pharmaceutical Technology and Physical Chemistry, Faculty of Pharmacy and Food Sciences, University of Barcelona, 08028, Barcelona, Spain
[2] Institute of Nanoscience and Nanotechnology (IN²UB), University of Barcelona, 08028 Barcelona, Spain
[3] Department of Food Chemistry and Biocatalysis, Wrocław University of Environmental and Life Sciences, Norwida 25, 50-375 Wrocław, Poland

Lbonilla95@ub.edu

Cancer remains one of the primary global health challenges, accounting for approximately nine million deaths annually. While pharmacological advancements have improved survival rates, the clinical utility of conventional chemotherapy is often hindered by systemic toxicity and a lack of tumor selectivity [1]. Although natural compounds such as the flavone Apigenin (APG) and the neurohormone Melatonin (MEL) have shown significant anti-cancer potential, their clinical utility is hampered by poor aqueous solubility and rapid metabolic degradation [2,3]. To address these limitations, this research developed an advanced delivery system using Nanostructured Lipid Carriers (NLC) formulated with rosehip oil. This natural lipid matrix not only serves as a vehicle but also provides intrinsic antioxidant and anti-inflammatory properties that potentially enhance the overall therapeutic profile.

The methodology involved the optimization of the lipid matrix through high-pressure homogenization, utilizing a Design of Experiments approach to ensure ideal physicochemical characteristics. The resulting APG-MEL-NLCs were characterized through dynamic light scattering and electron microscopy, revealing highly stable spherical particles with an average diameter below 200 nm and a negative surface charge. High encapsulation efficiency was achieved for both compounds, ensuring that the bioactive molecules remained protected from light degradation and premature clearance [4]. Biopharmaceutical evaluations demonstrated a sustained release. The biological activity was validated through *in vitro* cytotoxicity assays across various cancer cell lines. Results indicated that the co-encapsulation of APG and MEL produces a significant additive effect, particularly in a leukemia cells model [5]. This rosehip-based nanotechnological platform offers a sophisticated, multi-target approach that could redefine modern cancer management.

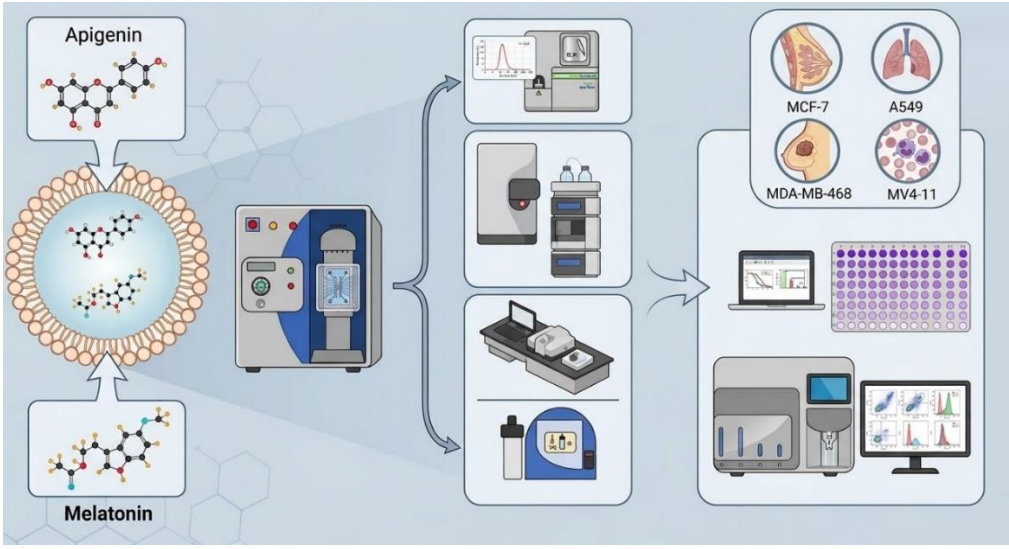

References: [1] Gavas S, *et al*. Nanoparticles for cancer therapy: current progress and challenges. Nanoscale Res Lett. 2021;16(1):1–21. [2] Nozhat Z, *et al*. Chemoprotective and chemosensitizing effects of apigenin on cancer therapy. Cancer Cell Int. 2021;21(1):1–26. [3] Wang L, *et al*. Use of melatonin in cancer treatment: where are we? Int J Mol Sci. 2022;23(7):3779. [4] Bonilla-Vidal L, *et al.* Melatonin loaded nanostructured lipid carriers for the treatment of uveal melanoma. J Drug Deliv Sci Technol. 2024;106057. [5] Bonilla-Vidal L, *et al.* Nanostructured lipid carriers co-encapsulating Apigenin and Melatonin: An innovative strategy against cancer. Mater Des. 2025;250(3):113573.

O.6. SIZE-DEPENDENT ANTIFERROMAGNETISM AND DIRECT OBSERVATION OF NÉEL AXES IN NiO NANOPARTICLES BY XMLD

J. Ara,[1,2] C. Moya,[2,3] M. García del Muro,[1,2] A. I. Figueroa, M. X. Aribó [1,2] Ò. Iglesias,[1,2] A. Kleibert,[4] A. Labarta,[1,2] A. F. Rodríguez,[1,2] and X. Batlle[1,2]

[1]Departament de Física de la Matèria Condensada, Universitat de Barcelona, Martí i Franquès 1, 08028 Barcelona, Spain
[2]Institut de Nanociència i Nanotecnologia (IN2UB), Universitat de Barcelona, 08028 Barcelona, Spain
[3]Departament de Química Inorgànica i Orgànica, C/Martí i Franquès 1-11, 1era planta, 08028 Barcelona, Spain
[4]Swiss Light Source, Paul Scherrer Institut, Villigen, PSI CH-5232, Switzerland

jorge_ara@ub.edu

Antiferromagnetic nanoparticles (NPs) have attracted significant interest due to their unique magnetic ordering and potential multifunctionality in applications ranging from electronics to catalysis and biomedicine. Despite extensive studies, a comprehensive understanding of antiferromagnetism at the nanoscale remains elusive, particularly regarding the role of uncompensated spins and their impact on magnetic ordering [1],[2]. In this context, NiO NPs constitute a model system to explore size-dependent effects, where decreasing particle size leads to deviations from bulk magnetic behaviour.

Here, we investigate the size-dependent antiferromagnetic properties of highly crystalline NiO NPs with mean diameters of 6, 20, and 34 nm. Structural characterization confirms single-phase particles with high crystalline quality across all sizes. From a magnetic point of view, a clear evolution is observed: the largest particles exhibit behaviour close to bulk antiferromagnetism, whereas the smallest show a superparamagnetic contribution superimposed on the antiferromagnetic background, with 20 nm particles displaying intermediate characteristics.

To directly probe antiferromagnetic order at the single-particle level, we employ synchrotron-based X-ray photoemission electron microscopy combined with X-ray magnetic linear dichroism (XMLD). This approach enables a quantitative determination of the three-dimensional orientation of the Néel axes in individual 34 nm NiO NPs. The XMLD contrast, analysed as a function of polarization and sample orientation, reveals stable Néel axis orientations at room temperature, stochastically distributed among the twelve allowed easy directions defined by the particle crystallography [3]. Importantly, the results are consistent with a single-domain, two-sublattice antiferromagnetic structure, rather than multi-sublattice spin configuration models [4].

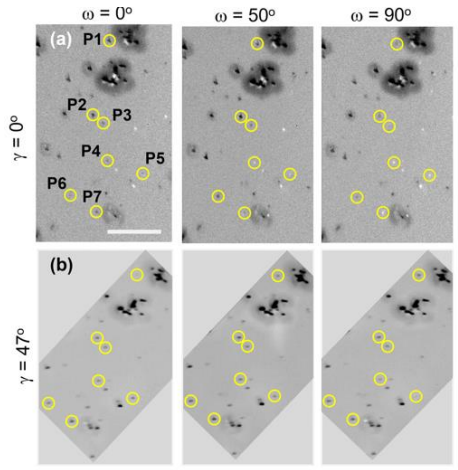

Figure 1. Representative XMLD–XPEEM images of NiO nanoparticles at different polarization angles (ω = 0°, 50°, 90°) and sample orientations (γ = 0° and 47°). Highlighted particles exhibit contrast variations associated with different Néel axis orientations.

References: [1] X. Batlle, C. Moya, M. Escoda-Torrella, Ò. Iglesias, A. Fraile Rodríguez, A. Labarta; J. Magn. Magn. Mater., 2022, 543, 168594. [2] C. Moya, J. Ara, A. Labarta, X. Batlle; Magnetism, 2024, 4(3), 252–280. [3] J. Ara, C. Moya, M. García del Muro, A. I. Figueroa, M. X. Aribó, Ò. Iglesias, A. Kleibert, A. Labarta, A. Fraile Rodríguez and X. Batlle, Nanoscale, 2025, 17, 17719-17732. [4] R. H. Kodama, S. A. Makhlouf, A. E. Berkowitz; Phys. Rev. Lett., 1997, 79(7), 1393–1396.

O.7. CONTROLLED PHOTOTAXIS OF ACTIVE LIQUID CRYSTAL EMUSLIONS

J. Torres-Andrés[1,2], J. Lardiés[1], M. Bossoms[1], F. Sagués[1,2], J. Ignés-Mullol[1,2]

[1]Departament de Ciència de Materials i Química Física, Facultat de Química, Universitat de Barcelona, Barcelona, 08028.
[2]Institut de Nanociència i Nanotecnologia de la Universitat de Barcelona (IN²UB), Universitat de Barcelona, Barcelona, 08028.

joel.torres@ub.edu

Microswimmers are microscale entities capable of converting environmental free energy or external stimuli into directed motion in liquid media. They are ubiquitous across complex systems, ranging from biological environments to synthetic active matter [1]. Among the various realizations of microswimmers, self-propelling droplets based on active liquid crystal (LC) emulsions constitute a particularly versatile platform due to their intrinsic anisotropy. In highly concentrated ionic surfactant solutions, LC droplets exhibit spontaneous self-propulsion driven by Marangoni flows arising from asymmetric solubilization at the droplet interface [2]. While external electric or magnetic fields enable controlled driving of such droplets, their applicability is often limited in microfluidic environments, restricting precise and scalable control strategies.

Here, we present a novel, fully light-based driving methodology using ultraviolet (UV) illumination [3]. By employing a photoresponsive liquid crystal as the dispersed phase, we achieve remote and reversible control over both the velocity and spatial position of individual self-propelling droplets. This approach further enables collective driving of multiple droplets, allowing systematic exploration of emergent collective behaviors in active emulsions. Additionally, we demonstrate that similar control can be extended to double-emulsion architectures, enabling the transport of both oil or water-based cargo. Our results establish light-controlled LC emulsions as a powerful and flexible platform for programmable active matter, with promising implications for microfluidic technologies, controlled micro-cargo delivery, and model systems for photoresponsive active materials.

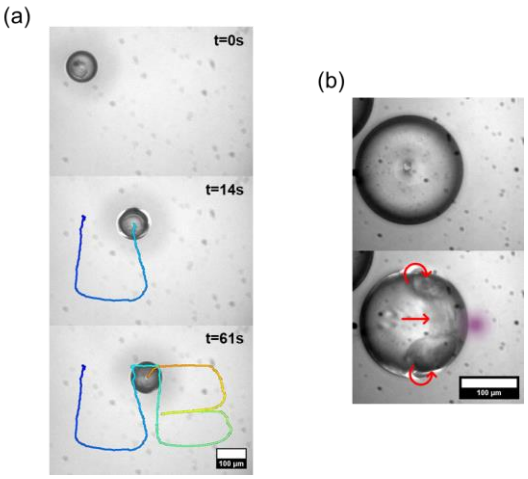

Figure 1. (a) Control of a MBBA droplet using a UV-light spot (λ=385 nm-ρ≈3.1 W·cm^{-2}). The droplet's trajectory writes the letters UB. (b) Emergence of Marangoni flows (red arrows) under the application of UV light (purple circle) over an homeotropically aligned MBBA droplet.

References:

[1] Birrer, S., et al., Current Opinion in Colloid & Interface Science, 2022, 61, 101623. [2] Concellón, A., Angewandte Chemie, 2023, 135, e202308857. [3] Dogishi, Y., et al., Soft Matter, 2018,14, 8085-8089.

POSTERS

NanoMet

P1. Computational Modelling of Protein Corona Formation on Lipid Nanoparticles: Hard Corona and Polydispersity Effects

Fiona Gallach[1,2*], Oriol Vilanova[1,2], Alberto Martinez-Serra[3], Marco Monopoli[4], Giancarlo Franzese[1,2]

[1]Departament de Física de la Matèria Condensada, Facutat de Física, Universitat de Barcelona, Marti i Franques 1, 08028 Barcelona, Spain
[2]Institute of Nanoscience and Nanotechnology (IN2UB), Universitat de Barcelona, Marti i Franques 1, 08028 Barcelona, Spain
[2] Barcelona Supercomputing Center (BSC), Barcelona, Spain
[3] Royal College of Surgeons in Ireland (RCSI), Dublin, Ireland

fgallach7@alumnes.ub.edu

Introduction

When lipid nanoparticles (LNPs) enter biological fluids, proteins adsorb onto their surface, forming a biomolecular corona that consists of a tightly bound hard corona (HC) and a loosely associated soft corona (SC). This corona influences their pharmacokinetics and cellular fate. Computational modeling of HC formation is essential for the rational design of LNP-based drug delivery systems [1].

Materials & Methods

A coarse-grained (CG) model was employed to describe human serum albumin (HSA)–LNP interactions using a potential that combines van der Waals attraction, electrostatic repulsion, and Born repulsion. The interaction strength was calibrated by fitting simulated adsorption isotherms to experimental surface coverage data (0–10 mg/mL HSA) for an LNP with radius R = 90 nm, yielding an optimal interaction strength of 7.25 kBT. Additional simulations at R = 87 nm and R = 93 nm were performed to mimic the experimental polydispersity [2].

Results and Discussion

The calibrated model closely matches the experimental HSA adsorption isotherm, accurately capturing both initial adsorption and surface saturation. Simulations at R = 87 nm and R = 93 nm align well with the baseline case, suggesting that a polydispersity of ±3 nm has minimal impact on HC formation. Consistently, the potential wells for R = 50 nm, 90 nm, and 93 nm are nearly identical in depth and position, indicating that the binding energy landscape remains largely unaffected by small changes in curvature within this size range. Ongoing analysis, including cooperative effects from three-body protein–protein–NP interactions, aims to further refine the model's alignment with experimental results. These preliminary findings confirm the effectiveness of the CG framework for modeling HSA corona formation and pave the way for future research on Vroman-type competitive exchange under physiological conditions.

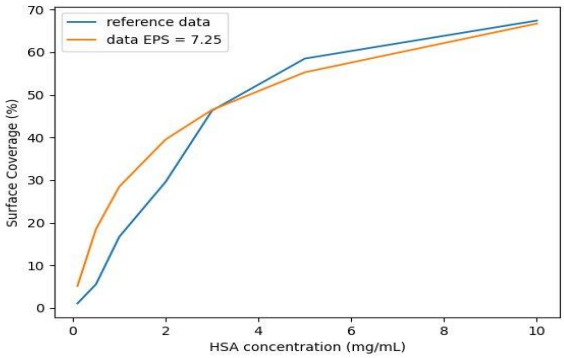

Fig. 1. HSA Surface coverage of LNP: model (orange) vs. experimental data (blue).

References

[1] F. Spinozzi, P. Moretti, D. R. Perinelli, G. Corucci, P. Piergiovanni, H. Amenitsch, G. A. Sancini, G. Franzese, and P. Blasi. Small-angle x-ray scattering unveils the internal structure of lipid nanoparticles. *Journal of Colloid and Interface Science*, **662**, 446 (2024).

[2] O. Vilanova, A. Martinez-Serra, M. P. Monopoli, and G. Franzese. Characterizing the hard and soft nanoparticle-protein corona with multilayer adsorption. *Frontiers in Nanotechnology*, **6**, 1531039, (2025).

P.2. Viscosity and Diffusion in ionic auqueous solutions.

S. Pelosso[1], G. Franzese[1]
[1]Department of Condensed Matter Physics,Universitat de Barcelona, Marti i Franques 1, 08028 Barcelona, Spain

SpelossoR@ub.edu

Introduction

Many soft and biological systems operate in ionic environments where salts significantly influence water transport and stability. In aqueous electrolyte solutions, viscosity and diffusivity are often described by the empirical Jones–Dole relation and commonly discussed in terms of structure-making (kosmotropic) or structure-breaking (chaotropic) ions [1]. However, the physical basis and the robustness of these trends remain subjects of debate. Therefore, we aim to develop a computationally efficient framework to capture these transport behaviors and extend the analysis to less-explored regimes with limited experimental data.

Materials & Methods

We modify a cooperative coarse-grained water model, previously demonstrated to qualitatively reproduce key water anomalies [2], to include ionic effects in a mean-field manner without explicit ions. Ionic influences are incorporated through concentration-dependent changes in: (i) the directional hydrogen-bond interactions between water molecules and (ii) the effective volume associated with hydrogen-bond fluctuations, guided by experimental data [3]. Simulations are conducted within a Monte Carlo NPT ensemble, enabling efficient sampling and extraction of transport properties such as viscosity and diffusivity.

Results and Discussion

The proposed framework qualitatively captures Jones–Dole-like trends in viscosity and diffusivity over a wide concentration range, including deviations at higher concentrations that are consistent with experimental findings. Extending the study to varying pressures reveals an asymmetric response: structure-making behavior remains stable across the conditions examined, while structure-breaking behavior becomes pressure-dependent, exhibiting a crossover at elevated pressures. In conclusion, the model successfully reproduces the key trends related to structure-making and structure-breaking ions, providing predictive insights even in regimes with sparse experimental data.

Funding

We acknowledge the Grant n.PID2024-157478NB-C31 funded by MCIN/AEI/10.13039/501100011033 and ERDF, EU.

References

[1] Jones, G.; Dole, M. **J. Am. Chem. Soc.** 51 (1929) 2950–2964. DOI: 10.1021/ja01385a012.

[2] de los Santos, F.; Franzese, G. **J. Phys. Chem. B** 115 (2011) 14311–14320. DOI: 10.1021/jp206197t.

[3] Corridoni, T.; et al. **J. Phys. Chem. B** 115 (2011) 14008–14013. DOI: 10.1021/jp202755u.

P.3. Geomicrobiological Controls on Gold Rim Formation: TEM Evidence for Biomediated Au Nano-Precipitation in Pyrenean Fluvial Nuggets

Josep Roqué-Rosell[1], Ana Clarisa Matute Ordoñez[1], Sergi Plana Ruiz[2], Jordi Ibáñez-Insa[3], Soledad Álvarez-Pousa[2], Abigail Jiménez-Franco[2].

[1]Universitat de Barcelona, Facultat de Ciències de la Terra
C/Martí i Franquès s/n, 08028 Barcelona. E-
Universtiat Rovira i Virgili, Servei de Recursos Científics i Tècnics
Av Països Catalans, 26-Campus Sescelades, Ed N2.
[3]Geosciences Barcelona (GEO3BCN-CSIC)
C/Lluís Solé i Sabarís s/n, 08028 Barcelona.

josep.roque@ub.edu

Fluvial gold nuggets are dynamic supergene systems that record the combined effects of mechanical recycling, chemical reworking, and biologically mediated mineralization processes operating down to the nanoscale. This study focuses on gold nuggets recovered from the fluvial terraces of the Segre River, in the Plana del Corb area (NE Spain, province of Lleida), a sector currently exploited for alluvial aggregates by the company Sorigué, which has enabled systematic recovery of auriferous material. These nuggets represent valuable mineralogical archives for investigating supergene gold evolution in active fluvial environments.

Seven representative nuggets encompassing all recognized morphologies—spongy, kidney-shaped, flat, folded, and barrel-shaped—were selected for detailed study. SEM–EDS and EMPA analyses reveal variable degrees of mechanical recycling and supergene modification. Kidney-shaped and spongy nuggets represent mechanically semi-evolved stages and preserve hypogene electrum cores with As–Fe–S–Cu inclusions, whereas folded and barrel-shaped nuggets exhibit advanced mechanical and chemical transformation, characterized by well-developed pure gold rims and stronger supergene signatures. Quartz is ubiquitous but shows progressive grain-size reduction with increasing mechanical evolution. Core compositions define three geochemical families: (1) As–Ag–Sb–rich nuggets with Ag contents >15 wt.%, mainly kidney-shaped; (2) low-Ag (<15 wt.%) spongy and flat nuggets with Te–Cu signatures; and (3) folded and barrel-shaped nuggets characterized by Sb–Hg signatures, suggesting affinities with epithermal environments.

Dominant flat and folded discoidal morphologies indicate long-distance fluvial transport, whereas kidney-shaped and spongy nuggets reflect more limited transport and lower degrees of mechanical reworking. Across all morphologies, polished-section observations reveal the systematic coexistence of electrum cores and pure gold rims. Ultrathin sections extracted from the electrum–gold interface were investigated by TEM, providing direct nanoscale evidence of biofilm-related textures and the development of Au nanoparticles. These observations demonstrate that biomediated dissolution and reprecipitation processes are directly responsible for the nucleation and growth of Au-rich rims during early stages of supergene evolution.

TEM–PED analyses further allowed crystalline domain sizes to be quantified and provided a detailed nanoscale characterization of phase boundaries (**Figure 1**). The results reveal the coexistence of two supergene evolution mechanisms: biomediated Au precipitation dominating in less mechanically evolved nuggets, and chemical–mechanical recrystallization prevailing in highly transformed flat and folded nuggets. These findings underscore the importance of nanoscale approaches for identifying biologically mediated processes that control

the mineralogical evolution of gold nuggets in fluvial supergene environments.

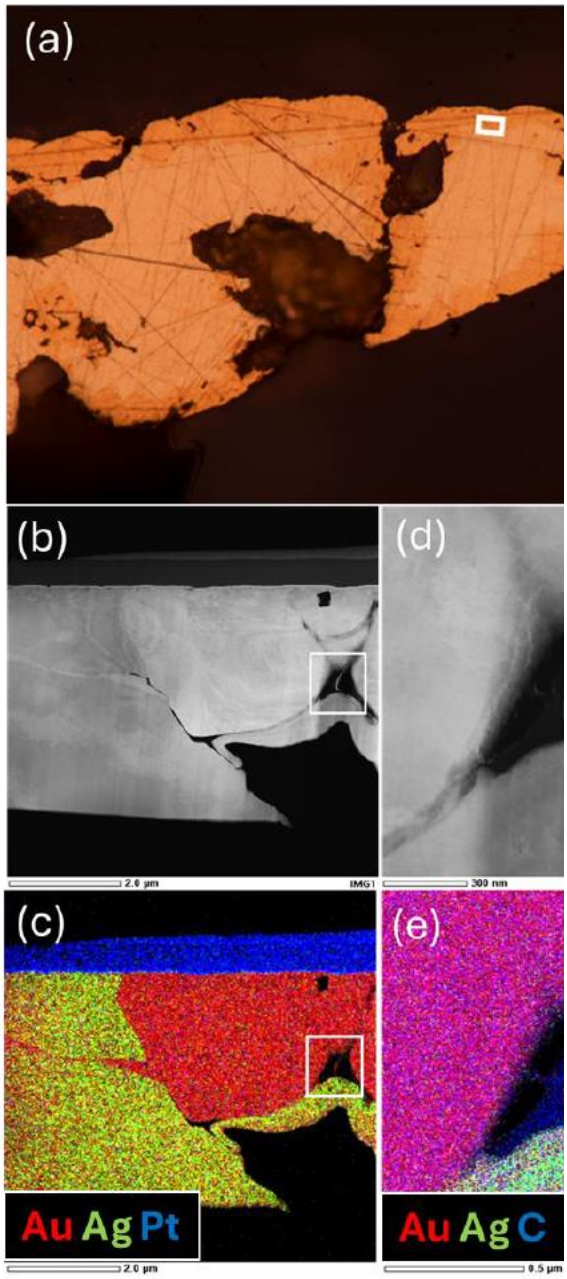

Figure 1. TEM–EDS study of sample GA-03-ARR-1 showing a metallographic polished section with the area selected for focused ion beam (FIB) lamella extraction, the corresponding FIB lamella imaged by field-emission scanning electron microscopy (FE-SEM), and TEM–EDS elemental maps revealing compositional domains of native gold (Au) and electrum (Ag–Au). The figure also illustrates a porous zone developed between the native gold rim and the electrum core, where chemical mapping indicates the presence of an amorphous C–N–O-rich substance. High-magnification TEM imaging documents gold nanoparticles migrating from the electrum toward the native gold, and EDS maps of these nanoparticles show their composition and close spatial association with the organic material, suggesting a biomediated or biogeochemical transport process.

P.4. Many-body contributions to polymorphism and polyhexaticity in a water monolayer.

O. Vilanova, G. Franzese

Física Estadística i Interdisciplinària–Departament de Física de la Matèria Condensada, Facultat de Física, Universitat de Barcelona
Institut de Nanociència i Nanotecnologia de la Universitat de Barcelona (IN2UB)

ovilanga7@alumnes.ub.edu

Nanoconfined water plays a crucial role in nanofluidics, biology, and cutting-edge technologies. The process of melting water monolayers and quasi-two-dimensional confined water involves, as an intermediate stage, the hexatic phase—a state that lies between solid and liquid and is characterized by quasi-long-range orientational order and short-range translational order. However, the influence of hydrogen bond (HB) cooperativity in this process has not been thoroughly investigated. This gap hampers our understanding of the phase behavior of confined water and limits the accuracy of our models. To address this, we extend the water model developed by Franzese and Stanley, which explicitly includes many-body interactions (MBIs) of HBs. We distinguish the contributions of three-body and five-body HB-MBIs. Our Monte Carlo calculations in the isobaric–isothermal ensemble produce a detailed pressure–temperature phase diagram, revealing polymorphism and polyhexaticity: low-density square ice and high-density triangular ice are separated from the liquid phase by distinct hexatic phases. Three-body interactions notably promote crystallization and can destabilize the low-density hexatic phase, while cooperative five-body interactions help restore it, thus modifying the thermodynamic landscape. These findings demonstrate that HB-MBIs are key to determining the phase behavior of confined water, influencing phenomena such as non-monotonic specific heat, maximum-density lines, and the accessibility of the liquid–liquid critical point. Beyond advancing theoretical understanding, these results have wide-ranging implications for nanofluidics, interfacial science, and applications in biology, food technology, and pharmaceutics, where controlling water under confinement is essential.

References:

[1] O. Vilanova, G. Franzese, Journal of Chemical Physics 164, 174503 (2026).

[2] L. E. Coronas, O. Vilanova, and G. Franzese, Journal of Molecular Liquids 434, 128032 (2025).

[3] L. E. Coronas, O. Vilanova, and G. Franzese, Frontiers in Nanotechnology 7, 1637828 (2025).

P.5. Simulating the Multiple-Exposure Protein Corona Protocol

Raad Felemban[1,2], Alberto Martinez-Serra[3], Oriol Vilanova[1,2], Marco Monopoli[4], Montserrat Mitjans[1,2], Giancarlo Franzese[1,2]

[1]Departament de Física de la Matèria Condensada, Facutat de Física, Universitat de Barcelona, Marti i Franques 1, 08028 Barcelona, Spain
[2]Institute of Nanoscience and Nanotechnology (IN2UB), Universitat de Barcelona, Marti i Franques 1, 08028 Barcelona, Spain
[2] Barcelona Supercomputing Center (BSC), Barcelona, Spain
[3] Royal College of Surgeons in Ireland (RCSI), Dublin, Ireland

rffelemban@ub.edu

Introduction

Sequential "multiple-exposure" protocols, in which a biological fluid is repeatedly exposed to fresh batches of nanoparticles (NPs), can generate a reproducible, cycle-dependent protein corona fingerprint. Martinez-Serra et al. observed systematic changes in SDS-PAGE and densitometry across nine exposure cycles, consistent with competitive adsorption and the gradual depletion of key plasma proteins [1]. Understanding the mechanism behind this cycle-dependent reshaping is crucial for replicating the protocol, adapting it to new conditions, and evaluating its potential as a controlled, depletion-driven protein selection ("filtering") strategy.

Materials & Methods

We replicate the multiple-exposure process using coarse-grained simulations based on Vilanova et al.'s framework [2]. Proteins are modeled as effective ellipsoidal particles that interact with the silica NP surface and each other through experimentally calibrated potentials. To mimic the sequential protocol, simulations are run iteratively, updating the bulk composition between cycles based on a depletion mass balance that accounts for proteins removed from solution by adsorption. Given computational limitations, simulations cannot reach laboratory time scales, especially when three or more proteins compete in suspension. Following Vilanova et al., we plan to apply the Non-Langmuir Differential Rate Equation theory as presented in Ref.[2] to extrapolate results beyond 30 minutes.

Results & Discussion

Our simulations establish a baseline for corona evolution by sequentially tracking hard-corona composition and reference-normalized metrics (bound fractions). Results allow comparison with experimental SDS-PAGE fingerprints. These metrics aim to replicate the experimental trend patterns and facilitate cycle-by-cycle analysis of depletion-driven selection. Ongoing work will complete the analysis of fingerprint trends and develop generalization tests for other nanoparticle materials and exposure conditions to guide further experiments.

Funding

We acknowledge Grant No. PID2024-157478NB-C31 funded by MCIN/AEI/10.13039/501100011033 and ERDF, EU. R.F. acknowledges the support of the Cultural Attaché Office of the Embassy of the Kingdom of Saudi Arabia in Spain (Madrid).

References

[1] A. Martinez-Serra, J. Cheeseman, A. Saorin, M. G. Soliman, M. Dobricic, D. I. R. Spencer, and M. P. Monopoli. Multiple exposures of plasma to nanoparticles: A novel tool to personalize biomolecular coronas and fractionate fluids. Analytical Chemistry, *Analytical Chemistry,* **97,** 14132 (2025).

[2] O. Vilanova, J. J. Mittag, P. M. Kelly, S. Milani, K. A. Dawson, J. O. Rädler, and G. Franzese. Understanding the kinetics of protein–nanoparticle corona formation, *ACS Nano*, **10**, 10842, (2016).

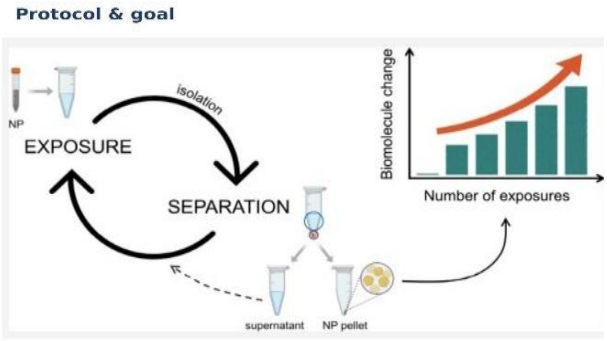

Figure 1. Multiple-exposure protocol schematic. Adapted from Ref. [1].

P.6. UMAP for dimensionality reduction of multidimensional spectroscopic data?

V. Costa-Ledesma[1], F. Peiró[1], S. Estradé[1]

[1]LENS-MIND, Department of Electronics and Biomedical Engineering and Institute of Nanoscience and Nanotechnology (IN2UB), University of Barcelona (UB), 08028, Barcelona, Spain

vcostale@ub.edu

Introduction

EELS spectrum images are becoming increasingly large as acquisition technology continues to advance faster than data-processing and storage capabilities. Modern instruments allow recording richer datasets with higher spatial resolution, finer energy dispersion, and longer acquisition times, which translates into ever-growing file sizes and more demanding computational requirements. This growth in data volume creates an important challenge for researchers, since processing, transferring, and exporting these datasets becomes progressively more difficult. In this context, dimensionality reduction methods offer a promising path to reduce storage and transmission costs while preserving the essential information content of the spectra. UMAP has already been introduced as a dimensionality reduction approach for spectroscopic data, yielding good results for clustering when combined with HDBSCAN in core-loss acquisitions [1] and moreover, with low-loss acquisitions [2]. However, these studies have mostly focused on the forward projection into the latent space, exploiting its structure for analysis and visualization. The behavior of the inverse transformation directly from UMAP space for spectroscopic datasets remains an open question. It is not yet clear how well the original spectral and spatial information can be reconstructed after compressing the data into a few embedding dimensions.

Materials & Methods

EELS spectrum images were acquired using a NEOARM-TEM, resulting in high-dimensional arrays that combine spatial and spectral information. To reduce dimensionality while preserving spectral structure, UMAP was applied with various embedding dimensions. The inverse-transformed data were then compared to the original images to assess the retention of spectral features, intensity distributions, and spatial contrast. This allowed us to evaluate whether UMAP can produce a compact, low-dimensional representation suitable for accurate reconstruction, and thus serve as a practical compression strategy for EELS data.

[1] Javier Blanco-Portals, F. Peiró, and S. Estradé. Strategies for eels data analysis. Introducing umap and hdbscan for dimensionality deduction and clustering. Micros. Microanal., 28(1):109–122, 2022

[2] Vanessa Costa-Ledesma, F.Perió and S. Estradé. Highly Efficient Machine Learning Strategy for Low-Loss EELS Characterization: Nanophotonic Resonances as a Case Study , Unpublished

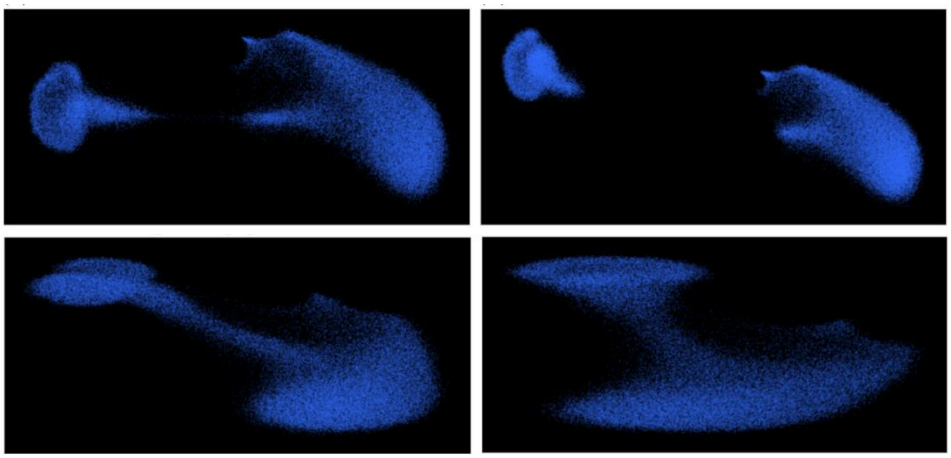

Figure 1: Differences in the UMAP embedding considering different hyperparameters.

P.7. TEM CHARACTERIZATION OF THE NANOSCALE STRUCTURE OF FREE-STANDING LSM-SDC VERTICALLY ALIGNED NANOCOMPOSITES

O. Falcó[1,2], M. Anzengruber[3], K. Kreka[3], F. Chiabrera[3], F. Biautti[3], J.C. González[3], A. Tarancón[3], S. Estradé[1,2], F. Peiró[1,2], C. Coll[2,4], L. Yedra[1,2]

[1]Department of Electronics and Biomedical Engineering, Faculty of Physics, University of Barcelona, Spain
[2]LENS-MIND, Institute of Nanoscience and Nanotechnology (IN²UB), University of Barcelona, Spain
[3]Department of Advanced Materials for Energy Applications, Catalonia Institute for Energy Research (IREC), Spain
[4]Department of Applied Physics, Faculty of Physics, University of Barcelona, Spain

ona.falco@ub.edu

Free-standing oxide membranes (FSMs) have recently emerged as promising platforms for the study of complex oxide heterostructures, enabling the decoupling of epitaxial thin films from their original substrates while preserving their structural integrity. In particular, vertically aligned nanocomposite (VANs) structures based on mixed ionic-electronic conductors are of great interest for electrochemical applications due to their large interfacial area and tuneable nanoscale structure.

Complex oxide systems based on perovskite structures are widely investigated for energy technologies, where interface density and nanoscale design strongly influence their functional response [1]. In this context, FSMs provide an effective route to study these systems beyond substrate-imposed constraints.

In this work, FSMs based on a $La_{0.8}Sr_{0.8}MnO_3$-$Ce_{0.8}Sm_{0.2}O_2$ (LSM-SDC) VAN system were investigated using advanced transmission electron microscopy (TEM) techniques. The membranes were prepared through a sacrificial layer release strategy and subsequently transferred onto an alternative substrate.

The use of oxide sacrificial layers, such as brownmillerite $SrCoO_{2.5}$ (SCO), enables selective removal of the underlaying layer while preserving the nanocomposite structure, allowing the fabrication of free-standing films with retained nanoscale organization [2].

Cross-sectional and top-view TEM observations reveal the characteristic VAN morphology, consisting of two columnar phases corresponding to LSM and SDC extending across the film thickness. High-resolution TEM (HRTEM) imaging confirms a high degree of crystallinity across the membrane, with well-defined lattice fringes observed in multiple regions. Scanning TEM and electron energy-loss spectroscopy (STEM-EELS) analysis provides clear compositional contrast between Mn-rich LSM and the Ce-rich SDC pillars and an estimation of their relative distribution. In addition, EELS spectra suggest the presence of La in regions where it would not be expected. This behaviour may be related to an underlying layer or to local compositional effects within the nanocomposite.

Overall, these results help to better understand the nanoscale structure and composition of free-standing VAN systems, relevant for energy-related applications such as solid oxide cells, where a high density of controlled interfaces can significantly enhance performance.

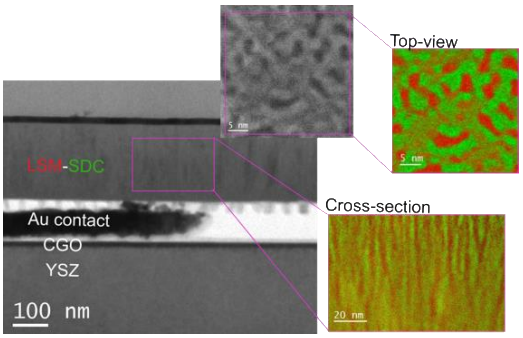

FIGURE 1. Low magnification image of the free-standing sample, showing a top view and cross-section of the LSM-SDC columns, highlighted in red and green, respectively.

References: [1] M. P. Wells et al., Nano Energy, 2024. [2] F. M. Chiabrera et al., Ann. Phys., 2022.

P.8. Unveiling the entropic role of hydration water in biomolecular condensates.

L. E. Coronas[1], S. Timr[2,3], F. Sterpone[2], and G. Franzese[1,]

[1]Institute of Nanoscience and Nanotechnology (IN2UB), & Departament de Física de la Matèria Condensada, Facutat de Física, University of Barcelona, Martí i Franquès 1, Barcelona 08028, Spain
[2]Université Paris Cité, CNRS, Laboratoire de Biochimie Théorique, 13 rue Pierre et Marie Curie, 75005 Paris, France
[3]J. Heyrovsky Institute of Physical Chemistry, Czech Academy of Sciences, Dolejskova 2155/3, 182 00 Prague, Czechia

gfranzese@ub.edu

Introduction

Biological processes such as the sequestration of superoxide dismutase 1 (SOD1) into biomolecular condensates, including fused in sarcoma (FUS) and stress granules, are vital for understanding disease mechanisms, including amyotrophic lateral sclerosis (ALS). Moreover, protein–crowder interactions within these condensates are recognized as fundamental to cellular phase separation and disease-related processes. However, the specific role of the hydration environment in governing SOD1's behavior and transition dynamics within these condensates remains poorly understood, limiting our ability to accurately model these critical biological systems [1].

Materials & Methods

We incorporate explicit water into an implicit solvent model (OPEP) to investigate how water influences SOD1's behavior, residence times, and transition rates among associative states. We employ the advanced CVF water model, which accurately captures hydrogen-bond networks at the molecular level [3, 4].

Results and Discussion

While the OPEP model indicates that bovine serum albumin (BSA) crowders reduce SOD1's partition coefficient (PC) into FUS condensates primarily through non-specific interactions, our explicit-water approach points to hydration entropy in BSA as a key contributor to the observed PC reduction (**Fig. 1**). This result offers a new perspective on the system's free-energy landscape, complementing those obtained from OPEP alone. Our research supports the notion that explicitly modeling water can enhance our understanding of protein–crowder interactions and their biological implications, further emphasizing the potential role of water in cellular phase separation and disease-related processes [5].

References

[1] N. Samanta, S. S. Ribeiro, M. Becker, E. Laborie, R. Pollak, S. Timr, F. Sterpone, and S. Ebbinghaus, J. Am. Chem. Soc. **143**, 19909 (2021).
[3] L. E. Coronas and G. Franzese, J. Chem. Phys. **161**, 164502 (2024).
[4] L. E. Coronas, O. Vilanova, and G. Franzese, J. Mol. Liq. **434**, 128032 (2025).
[5] L. E. Coronas, S. Timr, F. Sterpone, and G. Franzese, J. Chem. Phys. **164**, 094910 (2026).

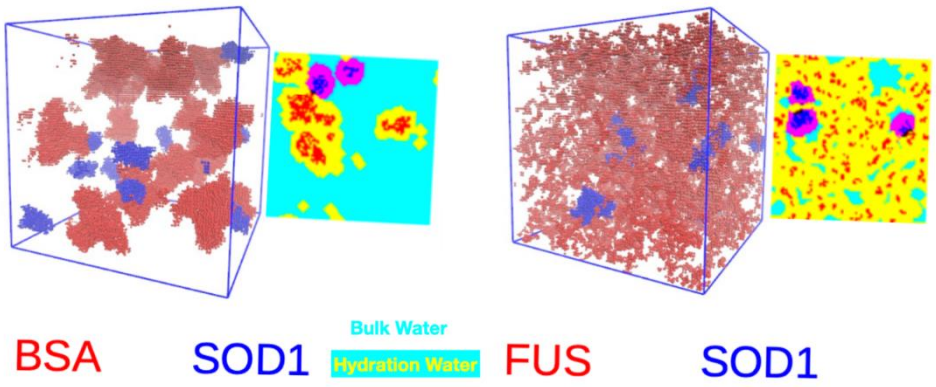

Fig.1 Simulation snapshots of SOD1 in contact with BSA (left) and FUS (right) are shown in their 3D implicit-water representation (with SOD1 in blue and the other protein in red) or as 2D sections with water (turquoise for bulk and yellow or purple for hydration water).

P.9. Hydration Water in Biomolecular Condensates.

I. Rabal[1], G. Franzese[1,2]

[1]Departament de Física de la Matèria Condensada, Facutat de Física, Universitat de Barcelona, Marti i Franques 1, 08028 Barcelona, Spain
[2]Institute of Nanoscience and Nanotechnology (IN2UB), Universitat de Barcelona, Marti i Franques 1, 08028 Barcelona, Spain

irabalsa8@alumnes.ub.edu

Introduction

Biomolecular condensates are associated with numerous cellular functions, including modulating biochemical reactions, participating in signaling pathways, storing or sequestering molecules, and patching membranes. They play a vital role in genomic activities and are linked to neurodegenerative diseases and cancer. Liquid-liquid phase separation (LLPS) has emerged as a key mechanism driving condensate assembly [1].

Materials & Methods

A coarse-grained (CG) model of hydrated proteins in water, capturing water's complexity, was adopted to explicitly consider water's role in protein-protein interactions and phase behavior. This approach allows the study of biomolecular condensate formation as a function of temperature, pressure, and protein concentration [2]. A Flory-Huggins mean-field model of the system [3] can be developed based on Monte Carlo (MC) simulations involving four components: folded proteins (F), unfolded proteins (U), hydration water (H), and bulk water (W). The F-U equilibrium depends on thermodynamic conditions, affecting the H-W balance, mixing energy, and interactions.

Results and Discussion

We present the preliminary steps within this mean-field framework to study the influence of hydration water on LLPS, focusing on changes in the hydrogen-bond network, volume, and entropy. Free energy landscapes will be derived from the Flory-Huggins approximation and combined with numerical data from MC simulations to analyze coexistence conditions and phase transitions in the system.

Funding

We acknowledge the Grant n.PID2024-157478NB-C31 funded by MCIN/AEI/10.13039/501100011033 and ERDF, EU.

References

[1] Alberti, S., Arosio, P., Best, R. B., et al. *Nat. Commun.* **16**, 7730 (2025). DOI:10.1038/s41467-025-62055-8

[2] V. Bianco, G. Franzese, and I. Coluzza, *ChemPhysChem* **21**, 377–384 (2020). DOI:10.1002/cphc.201900904

[3] O. Adame-Arana, C. A. Weber, V. Zaburdaev, J. Prost, and F. Jülicher, *Biophys. J.* **119**, 1590–1605(2020). DOI:10.1016/j.bpj.2020.07.044

P.10. Analysis of Electronic structure of Vanadium-Doped ZnO using Scanning Transmission Electron Microscopy.

B. Vargas [1], P. Estarlich [2], S. Plana-Ruiz[1,3], G. Alvarez [2], C. Voz [2], G. Masmitjà [2], J. Puigdollers [2], P. Benítez[4,5], C. López [4,5], C. Cazorla Silva [4,5,6], S. Estradé [1], L. López-Conesa [1,7], F. Peiró [1].

[1.] LENS, Department of Electronics and Biomedical Engineering and Institute of Nanoscience and Nanotechnology (IN2UB), University of Barcelona (UB). Barcelona, Spain.
[2.] Dept Enginyeria Electrònica, Universitatat Politecnica de Catalunya (UPC). Barcelona, Spain.
[3.] Servei de Recursos Científics i Tècnics, Universitat Rovira i Virgili. Tarragona, Spain.
[4.] Department of Physics, Universitat Politècnica de Catalunya. Barcelona, Spain.
[5.] Research Center in Multiscale Science and Engineering, Universitat Polictènica de Catalunya. Barcelona, Spain.
[6.] Institució Catalana de Recerca i Estudis Avançats (ICREA). Barcelona, Spain.
[7.] TEM MAT Laboratory - Scientific and Technological Centers of the University of Barcelona (CCiTUB). Barcelona, Spain.

bvargas@ub.edu

Vanadium-doped zinc oxide (ZnO:V) thin film, deposited via the atomic layer deposition (ALD) technique with 14:1 dopant ratio, was investigated as functional layers in transparent photovoltaic (TPV) solar cells. The ZnO:V layer was characterized using (S)TEM to study its crystallographic and physical properties at the nanoscale. Four-dimensional STEM (4D-STEM) mapping was performed to analyze grain orientation and local structural variations. Electron energy-loss spectroscopy (EELS) was employed to investigate the chemical composition and spatial distribution of vanadium, as well as to probe nanoscale electronic properties such as the band gap, dielectric function, and vanadium oxidation states.

The band gap values obtained from EELS measurements show good agreement with X-ray photoelectron spectroscopy (XPS) results. These experimental findings will be further compared with density functional theory (DFT) calculations to confirm the presence of the different vanadium oxidation states and to elucidate their influence on the formation of intermediate bands in ZnO at the nanoscale.

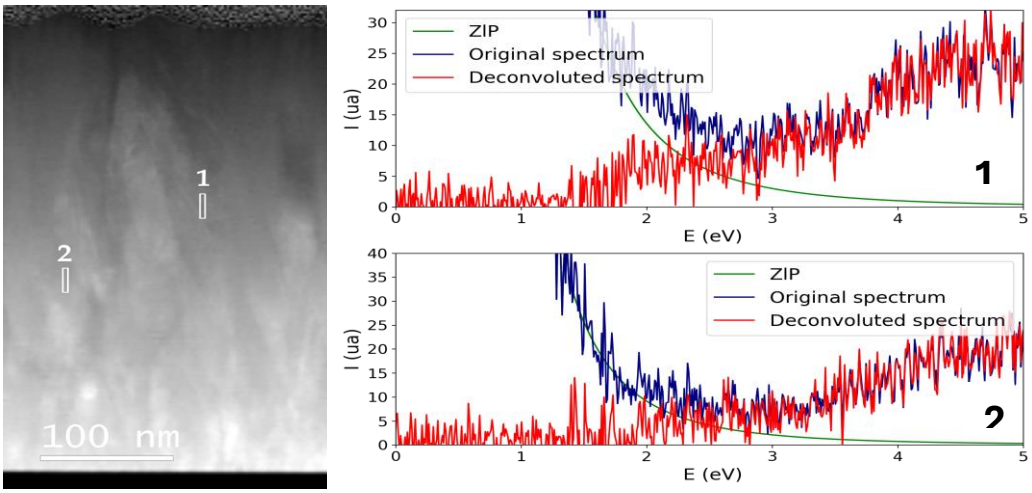

Figure:Calculation of the band gap of ZnO:V using low-loss EELS in two different areas corresponding to different oxidation states of vanadium.

P.11. BEYOND THE CATALYST: THE ROLE OF POLLUTANT AGGREGATION AND pH IN TiO_2-MEDIATED WASTEWATER CLEANING

M. von Einem[1], S. Köppen-Hannemann[1,2], G. Franzese[3,4]

[1] Hybrid Materials Interfaces Group, Faculty of Production Engineering and Bremen Center for Computational Materials Science, University of Bremen, Germany
[2] MAPEX Center for Materials and Processes, University of Bremen, Germany
[3] Institut de Nanociència i Nanotecnologia, Universitat de Barcelona, Spain
[4] Secció de Física Estadística i Interdisciplinària – Departament de Física de la Matèria Condensada, Universitat de Barcelona, Spain

gfranzese@ub.edu

Advanced oxidation processes (AOPs), i.e. heterogeneous photocatalysis based on titanium dioxide (TiO_2), have emerged as promising strategies for sustainable water remediation. While extensive research has focused on enhancing the photocatalytic activity of TiO_2 through material modifications, the influence of the aqueous interfacial environment — particularly the complex interactions among water, dissolved pollutants, and ions — remains underexplored. The efficiency of direct pollutant degradation is dependent on the adsorption of target contaminants at the catalyst surface, a process governed by molecular mobility and interfacial dynamics. In a previous study, we demonstrated that pollutant clustering in solution can act as a competing mechanism hindering surface adsorption [1]. Building upon these findings, this study investigates how the aggregation behavior of pollutants in aqueous solution affects their surface mobility and subsequent adsorption on TiO_2. Furthermore, we examine the role of pH in modulating cluster formation and stability, and how the TiO_2 surface influences the aggregation dynamics of pollutant species. These insights contribute to a more comprehensive understanding of the interfacial processes governing photocatalytic efficiency, offering valuable guidance for optimizing TiO_2-based water treatment systems under realistic environmental conditions.

Figure 2: Cluster of ibuprofen in water surrounded by sodium and chloride ions.

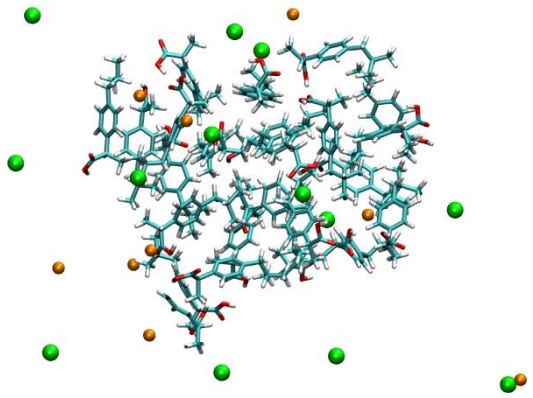

[1] M. von Einem, F. Balzaretti, M. Romero, W. Dononelli, L. Colombi Ciacchi, G. Franzese, S. Köppen-Hannemann (2026). Mater. Adv., 7, 2017-2038, DOI: 10.1039/d5ma01085c

NanoBio

P.12. SCULPTING SUPER-OSCILLATORY DOUGHNUT BEAMS FOR SUPER RESOLUTION MICROSCOPY

C. Agazzi[1], N. Toledo-García[1,2], J. Tiana-Alsina[1,2] , R. Martínez-Herrero[3], M. Montes-Usategui[1,2], D. Maluenda[1,2], E. Martín-Badosa[1,2], A. Carnicer[1]

[1]Departament de Física Aplicada, Facultat de Física, Universitat de Barcelona, Carrer de Martí i Franquès 1, 08028 Barcelona, Spain.[2]Institut de Nanociència i Nanotecnologia (IN2UB), Universitat de Barcelona, 08028 Barcelona, Spain.
[3]Departamento de Óptica, Facultad de Ciencias Físicas, Universidad Complutense de Madrid, Plaza de las Ciencias 1, 28040 Madrid, Spain

costanza.agazzi@ub.edu / artur.carnicer@ub.edu

Stimulated emission depletion (STED) and reversible saturable optical fluorescence transitions (RESOLFT) microscopy achieve super-resolution by overlaying the excitation focus with a doughnut-shaped depletion beam whose central intensity zero selectively preserves fluorescence at the very center [1, 2]. The polarization state and the spatial confinement of this zero are both fundamental to depletion performance: azimuthally polarized beams produce a more robust and symmetric central null under high numerical aperture focusing, while a narrower null generally yields finer resolution and lower depletion power requirements [3].

In this work, we explore super-pupil engineering as a route to improving this confinement. Super-pupils are structured amplitude patterns at the entrance pupil of an optical setup that exploit interference in the focal plane to shape the intensity distribution beyond what conventional beam families can achieve [4]. Working within this framework, we optimize the pupil profile of an azimuthally polarized vector beam to approximate a Bessel-like focal distribution [5]. The design balances two competing demands: tightening the central minimum while keeping the inevitable sidelobes, a well-known drawback of super-oscillatory fields [4], at a level that does not compromise the depletion performance. The result is a central minimum that is both narrower and more sharply defined than those of standard Laguerre-Gaussian or azimuthally polarized beams.

The design is implemented experimentally on a phase-only spatial light modulator in a double-pass configuration, which provides independent control of both orthogonal polarization components and enables full vector-field synthesis within a single device [6]. Encoding such a complex, structured field onto a phase-only device introduces non-trivial implementation challenges, which we systematically address through hologram design optimization [7] and careful characterization of the experimental setup.

Focal characterization via raster-scanning of sub-diffraction fluorescent beads confirms a reduction in doughnut diameter relative to the reference beams, in good agreement with numerical predictions.
Complementary measurements with 23 nm beads are consistent with a more spatially confined on-axis minimum, although a full quantitative characterization of the central zero remains experimentally challenging, as probe size, signal level, and photobleaching impose competing constraints on measurement fidelity.

These results establish super-pupil engineering as a promising route to improving depletion beam confinement, with analytical modelling predicting a resolution gain of approximately 27% and a depletion power reduction of approximately 46% relative to a canonical Laguerre-Gaussian beam, paving the way

for their experimental verification in a full STED or RESOLFT imaging configuration.

References:

[1] S. W. Hell and M. Kroug, *Appl. Phys. B* **60**, 495 (1995).

[2] M. Hofmann et al., *Proc. Natl. Acad. Sci.* **102**, 17565 (2005).

[3] B. Harke et al., *Opt. Express* **16**, 4154 (2008).

[4] G. Chen, Z.-Q. Wen, and C.-W. Qiu, *Light: Sci. Appl.* **8**, 56 (2019).

[5] F. M. Huang et al., *Opt. Lett.* **32**, 1995 (2007).

[6] I. Moreno et al., *Opt. Express* **20**, 364 (2012).

[7] V. Arrızón, *Opt. Lett.* **28**, 1359 (2003).

P.13. GENE SILENCING OF LncRNA H19 USING PPRH THERAPEUTIC OLIGONUCLEOTIDES IN HT29 COLORECTAL CANCER CELLS

N. Urgell [1], A. Delgado [1,2], E. López-Aguilar [1,2], C. J. Ciudad[1,2], V. Noé [1,2]

[1]Department of Biochemistry and Physiology, School of Pharmacy and Food sciences, University of Barcelona [2] IN2UB

cciudad@ub.edu

INTRODUCTION

The human genome contains a wide variety of non-coding RNAs (ncRNAs), that play important regulatory functions in gene expression even if they do not encode for proteins. They are classified into small ncRNAs and long non-coding RNAs (lncRNAs) depending on their length, shorter or longer than 200 nucleotides, respectively [1]. NcRNAs regulate gene expression by modulating fundamental mechanisms, such as transcription and translation. Nevertheless, dysregulated expression of lncRNAs has been involved in tumorigenesis and metastatic progression [2]. Particularly, in colorectal cancer, the aberrant expression of lncRNAs has been associated with advanced disease stage, unfavorable prognosis, and drug resistance [3]. Among these, lncRNA H19 is frequently overexpressed in a variety of solid tumors [4] exerting key regulatory functions in the initiation and progression of colorectal cancer. H19 acts as a competitive endogenous RNA (ceRNA) sponging microRNAs involved in the regulation of malignant phenotypes. The purpose of this study was to analyze the effect of silencing H19 in the HT29 colorectal cancer cell line. Therefore, we designed 4 Polypurine Reverse Hoogsteen (PPRH) hairpins directed against this lcnRNA to perform studies with these PPRHs and in combination with the antifolate drug methotrexate (MTX).

MATERIAL & METHODS

The HT29 cell line was used as a representative cell line for human colorectal cancer and grown in selective medium RPMI (lacking hypoxanthine and thymidine). Transfection of the PPRHs was performed using DOTAP. RT-qPCR analyses using the SYBR-Green method were performed to evaluate the RNA levels of H19 lncRNA in control and transfected cells. Cell viability assays using the MTT method were conducted to evaluate the effect of MTX or PPRHs, either alone or in combination.

RESULTS & DISCUSSION

We designed four PPRHs targeting polypurine-rich sequences within the H19 lncRNA gene. The gene silencing efficacy of these PPRHs was confirmed by RT-qPCR also observing a decrease in cell viability. Finally, we demonstrated that the combinatorial treatment of PPRHs targeting H19 together with MTX enhanced the effectiveness of the antifolate drug and further potentiated its effect [5]

ACKNOWLEDGEMENT

Work supported by grant MICIIN/MCIU (Grant PID2021- 122271OB-I00- MICIU/AEI /10.13039/501100011033 & FEDER, UE.),

RERERENCES

[1] V.A. Ferretti, I.E. León, Long Non-coding RNAs in Cisplatin Resistance in Osteosarcoma, Curr. Treat. Options Oncol. 22 (2021) 41.

[2] M. Wang, J. Gu, X. Zhang, J. Yang, X. Zhang, X. Fang, Long Non-coding RNA DANCR in Cancer: Roles, Mechanisms, and Implications, Front. Cell Dev. Biol. 9 (2021).

[3] P.R. Chowdhury, S. Salvamani, B. Gunasekaran, H.B. Peng, V. Ulaganathan, H19: An Oncogenic Long Non-coding RNA in Colorectal Cancer, Yale J. Biol. Med. 96 (2023) 495–509.

[4] L. Bolha, M. Ravnik-Glavač, D. Glavač, Long Noncoding RNAs as Biomarkers in Cancer, Dis. Markers 2017 (2017) 1–14.

[5] A. Delgado, E. López-Aguilar, J. Cullell, N. Mencia, C.J. Ciudad, V. Noé, Identification of hub genes and lncRNAs driving the transition from early response to methotrexate resistance in HT29 colon cancer cells, Biochem. Pharmacol. 250 (2026) 117943

P.14. Selective Delivery of PPRHs to Hepatocytes Using Trigalfapys

Maria Martínez-Gallardo[1], Rosa Griera[2], Núria Llor[2], Carlos Ciudad[1], Véronique Noé[1]

[1]Department of Biochemistry and Physiology, [2]Department of Pharmacology, Toxicology and Therapeutic Chemistry, School of Pharmacy and Food Sciences, University of Barcelona

vnoe@ub.edu

Transfection agents are essential for the delivery of therapeutic oligonucleotides; however, their application remains limited by low efficiency, instability, and lack of cell-type selectivity (1). Thus, in this study we synthesized and validated a family of lipid-based compounds named Trigalfapys for the transfection of Polypurine Reverse Hoogsteen (PPRHs) hairpins with the aim of achieving selective delivery to hepatocytes. PPRHs are highly stable and sequence-specific gene-silencing molecules that do not rely on cellular RNA-processing machinery, but their therapeutic potential depends on the availability of efficient delivery systems (2). The asialoglycoprotein receptor (ASGPR), a C-type lectin highly expressed on hepatocytes, mediates the endocytosis of ligands containing terminal galactose or *N*-acetylgalactosamine (GalNAc), making it an attractive target for liver-specific delivery (3).

Materials and Methods.

A series of Trigalfapys compounds with varying alkyl chain lengths were synthesized. These molecules were designed to combine the hepatocyte-targeting ability of GalNAc with the transfection properties of pyridinium groups. The compounds were prepared using nucleophilic substitution and glycosylation reactions, resulting in tricationic GalNAc-conjugated structures. The binding affinity of these new compounds with PPRHs was evaluated by

agarose gel retardation assays. Cytotoxicity was assessed in PC3, MCF7, T47D, HT29, HeLa and HepG2 as a hepatoma representative cell line. Cellular uptake of Trigalfapy–PPRH complexes labelled with FAM was analyzed by fluorescence microscopy and quantified by flow cytometry. The involvement of ASGPR in the internalization process was studied through competition assays with GalNAc. Functional effects were evaluated by cell viability assays and mRNA quantification following transfection.

Results and Discussion.

Among the compounds tested, Trigalfapy C18 showed the most efficient complex formation with PPRHs. Trigalfapy C18 was used up to a concentration of 3 µg/mL, not showing cytotoxicity or reducing cell viability. Selective internalization of the complexes was observed in HepG2 cells, whereas no uptake or effect was detected in other cell lines served as negative controls lacking the ASGPR. Fluorescent microscopy confirmed higher levels of internalization in HepG2 cells. Transfection with Trigalfapy C18 and PPRHs targeting oncogenes involved in cell proliferation (c-MYC, KRAS) resulted in a decrease in cell viability, indicating effective gene silencing. These results highlight the importance of receptor-mediated uptake to achieve selective delivery.

Acknowledgement. Work supported by grant MICIIN/MCIU (Grant PID2021- 122271OB-I00-MICIU/AEI /10.13039/501100011033 & FEDER, UE.).

References:

1. Ali Zaidi SS, Fatima F, Ali Zaidi SA, Zhou D, Deng W, Liu S. Engineering siRNA therapeutics: challenges and strategies. J Nanobiotechnology. 2023 Oct 18;21(1):381.
2. Ciudad CJ, Rodríguez L, Villalobos X, Félix AJ, Noé V. Polypurine Reverse Hoogsteen Hairpins as a Gene Silencing Tool for Cancer. Curr Med Chem. 24(26):2809–26.
3. Rao N P, Ajish JK, Kumar KSA. Asialoglycoprotein receptor-1 mediated targeted drug delivery to liver cancer cells using stimuli responsive galactosylated electrospun nanofibers. Int J Biol Macromol. 2025 Nov 1;329:147793.

P.15. Shear Stress Transmission in Micro and Nanoporous Hydrogels for Angiogenesis on a Chip Applications

Jorge Eduardo López Ávila[1,2,3], Mamta Jotkar[1], Elisabeth Engel[4,2,5], Oscar Castaño Linares[1,2,3,5]

[1] Universitat de Barcelona (UB), Barcelona, Spain
[2] Institute for Bioengineering of Catalonia (IBEC), Barcelona, Spain
[3] Institut de Nanociència i Nanotecnologia (IN²UB), Barcelona, Spain
[4] Materials Sciences and Engineering, Universitat Politècnica de Catalunya (UPC), Barcelona, Spain
5 CIBER-BBN, Madrid (Spain)

jlopezav8@alumnes.ub.edu

Fluid shear stress regulates cellular behavior through mechanotransduction pathways operating at subcellular length scales, influencing migration, proliferation, differentiation, and angiogenesis. However, in hydrogel-based microfluidic systems and organ-on-a-chip platforms, shear transmission is strongly shaped by the micro- and nanoporous structure of the extracellular matrix (ECM), in addition to channel geometry. This coupling remains difficult to control and can lead to misleading estimations of the mechanical stimuli experienced by cells.

In this work, a numerical investigation was conducted to analyze fluid flow and shear stress distribution in a microfluidic chip containing a central fibrin hydrogel. Finite element simulations were performed in COMSOL Multiphysics, coupling laminar flow in the free channel with porous flow inside the hydrogel using a Brinkman formulation.

By progressively refining the interface geometry between the channel and the micro- and nanoporous gel, hydrogel permeability was shown to be a dominant factor governing both volumetric flow rate and shear transmission. Pore-scale resistance alters macroscopic flow behavior and local shear exposure, while classical microchannel scaling effects, such as the influence of channel height, become significantly reduced due to porous resistance.

The transition from pressure-driven to flow-controlled operation highlighted that syringe-pump-driven flow provides reliable control for achieving biologically relevant shear regimes. Additionally, structured channel-gel interfaces redistribute shear stress within the hydrogel, generating either localized high shear regions or spatially uniform stimulation depending on design. These effects emerge from pore-scale flow redirection rather than bulk channel features.

These findings indicate the importance of jointly considering material properties, flow conditions, and nanoscale geometry in the design of microfluidic systems for controlled mechanical stimulation in biological applications relevant for further assessment.

References

[1] Huber D., Oskooei A., Casadevall i Solvas X., deMello A., Kaigala G.V. *Hydrodynamics in Cell Studies*. Chem Rev. 2018;118:2042–2079.
[2] López-Canosa A., Pérez-Amodio S., Engel E., Castaño O. *Microfluidic 3D platform to evaluate endothelial progenitor cell recruitment by bioactive materials*. Acta Biomater. 2022;151:264–277.

P.16. Antifungal impact on Candida albicans membrane nanomechanics

A. Botet-Carreras[1]; Ò. Domènech[1]

[1]Physical Chemistry Section, Faculty of Pharmacy and Food Sciences; university of Barcelona

odomenech@ub.edu

Cutaneous fungal infections, such as candidiasis caused by *Candida albicans*, can be serious illnesses in immunocompromised patients or in cases of superficial burns [1]. First-line drugs for treating candidiasis are azole antifungals, but the emergence of resistance to these drugs hinders effective treatment. Amphotericin B (AmB) is a broad-spectrum, highly active polyene macrolide with demonstrated efficacy against azole-resistant fungi [2]. It is poorly soluble in water, amphoteric, amphiphilic, and difficult to dissolve in organic solvents.

In this work, we evaluated the effect of three different AmB formulations against the fungus *Candida albicans* using atomic force microscopy in force spectroscopy mode (FS-AFM). Individual fungal cells were trapped on a polyethylene filter to preserve their curvature and roughness (Fig. 1). The modulus of elasticity (Young's modulus) was evaluated before and after treatment, along with the effect of excipients in the AmB-free formulation.

All three formulations studied altered the elastic modulus of the fungal cell membrane, but only the formulation containing Transcutol® showed an effect of the AmB formulation beyond the effect of the excipients, suggesting that Transcutol® destabilizes the cell membrane and facilitates the permeation of AmB into the cell.

In this kind of experiments the drug incubation time was short compared to the time required to kill the fungus, so it was possible to observe which formulation allowed faster initial permeation of AmB through the fungal cell membrane through nanomechanical properties of the cell membrane.

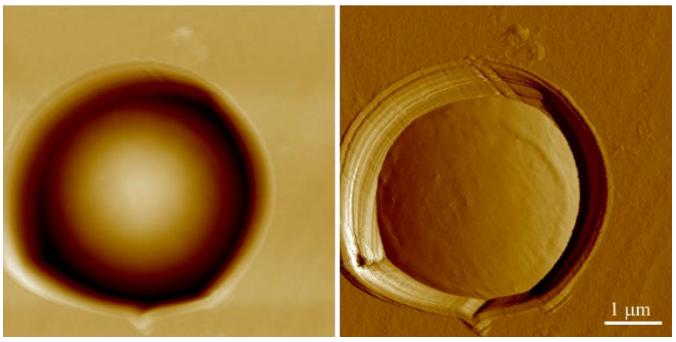

Figure 1. AFM image of an individual fungal cell trapped in a pore left) topographic and right) deflection images.

References:

[1] Sanchez, D.A. et al. Nanomedicine 2014, 10, 269–277.

[2] Vincent, B.M. et al. PLoS Biol. 2013, 11, e1001692.

P.17. FLUCTUATION THEOREMS IN DNA-TRANSLOCATING MOLECULAR MOTORS

V. Rodríguez Franco[1,2], I. Pérez Castillo[3], M. Mañosas[1,2], F. Ritort[1,2]

[1]Facultat de Física, Universitat de Barcelona, Diagonal 645, 08028 Barcelona, Spain
[2]Institut de Nanociència i Nanotecnologia (IN2UB), Universitat de Barcelona, 08028 Barcelona, Spain.
[3]Departamento de Física, Universidad Autónoma Metropolitana-Iztapalapa, San Rafael Atlixco 186, Ciudad de México 09340, Mexico

vrodrifr7@alumnes.ub.edu

Introduction

Helicases are molecular motors that unwind double-stranded DNA using the energy of ATP hydrolysis. Single-molecule experiments with Magnetic Tweezers (MT) or Optical Tweezers (OT) allow tracking the helicase displacement in real time. A key question is if fluctuation relations (FRs) from non-equilibrium statistical mechanics can be tested and exploited using these displacement measurements.

Materials and Methods

We use MT and OT to follow the unzipping of a DNA hairpin by a helicase at different forces. The motion of the helicase can be modelled as a biased random walk in a one-dimensional lattice, with probabilities P_+ and P_- for forward and backward steps. The model is validated through numerical simulations and compared with experimental traces. A more complex model to account for the Brownian fluctuations of the bead is developed where we propose a Poisson process with additive Gaussian noise, $D(t) = \mu N(t) + \varepsilon$, where $N(t) \sim \text{Poisson}(\lambda t)$ represents the helicase steps and $\varepsilon \sim N(0,\sigma^2)$ captures the thermal noise of the bead.

Results and Discussion

For the biased random walk, we analytically derive and verify the fluctuation relation $L(\Delta x, t) = \log\left(\frac{P(\Delta x)}{P(-\Delta x)}\right) = \Delta x \log\left(\frac{P_+}{P_-}\right)$. Comparison with experimental data shows qualitative agreement, but the experimental displacement distributions present heavier tails than the Gaussian predicted by the simple model, and the slope of the FR deviates from the theoretical prediction. To address this, we develop the Poisson-Gaussian model, for which we derive an exact log-ratio $L(\Delta x, t)$. This extended model yields a fluctuation relation that naturally incorporates the effect of thermal noise offering a more realistic description of the experimental system.

P.18. Programmable Structured Light for Fast and High-Fidelity Depletion Microscopy

N. Toledo-García[1,2], C. Agazzi[1,2], J. Tiana-Alsina[1,2], D. Maluenda-Niubó[1,2], M. Montes-Usategui[1,2], A. Carnicer[1,2], E. Martín-Badosa[1,2]

[1]Departament de Física Aplicada, Facultat de Física, Universitat de Barcelona, Carrer de Martí i Franquès 1, 08028 Barcelona, Spain
[2]Institut de Nanociència i Nanotecnologia (IN2UB), Universitat de Barcelona, 08028 Barcelona, Spain

nicktoledogarcia@ub.edu

The development of high-speed, high-resolution fluorescence microscopy is essential for observing dynamic biological processes at the nanoscale. However, two major hurdles limit the effectiveness of current depletion super-resolution techniques like RESOLFT [1]: the degradation of the depletion beam quality and the slow acquisition speeds inherent in point-by-point scanning. We present two imaging platforms designed to tackle these challenges, one platform for the generation of programmable vector beams and another platform for parallelized laser scanning using acousto-optic deflectors.

The first platform presented in this work provides a solution for high-fidelity depletion through a versatile platform based on a single spatial light modulator (SLM) in a double-pass configuration [2]. This setup enables the precise generation of vector beams, which offer significant advantages over conventional scalar beams in high-numerical-aperture microscopy. Specifically, azimuthally polarized beams produce a tighter and more symmetric doughnut intensity profile at the focus. Furthermore, these beams exhibit an enhanced resilience to aberrations, ensuring that the central intensity minimum, critical for effective fluorescence depletion, remains stable even under non-ideal imaging conditions.

The second platform tackles the limitation of scanning speed using a scanning system based on acousto-optic holography. By employing acousto-optic deflectors (AODs) as spatial light modulators [3], we generate programmable arrays of Gaussian and Laguerre-Gaussian beams and scan them across the sample at kHz rates without the movement of any mechanical element. This programmability offers a significant benefit, as the illuminating matrix can be dynamically adapted to different samples; for example, a more sparse array can be used to improve contrast in dense samples, while a denser pattern can be employed to optimize acquisition speed for thinner samples.

The performance of these platforms has been validated through subtraction microscopy [4] on biological samples demonstrating a clear resolution improvement over the standard confocal modality. Building on these results, we are currently working on the full implementation of these platforms for actual RESOLFT imaging. These developments in beam shaping and programmable parallelized scanning offer a practical path toward making super-resolution microscopy more efficient and adaptable for live-cell studies.

References

[1] M. Hofmann, C. Eggeling, S. Jakobs, and S.W. Hell, Proc. Natl. Acad. Sci. 102, 17565–17569 (2005).

[2] I. Moreno, J. Davis, D. Cottrell, and R. Donoso Floody, *Appl. Opt.* 53, 5493–5501 (2014).

[3] M. Montes-Usategui, R. Bola, E. Martín-Badosa, and D. Treptow, PCT/EP2019/067517 (2019).

[4] C. Kuang, S. Li, W. Liu, et al., *Sci. Rep.* 3, 1441 (2013).

NanoPharmaMed

P.19. Metal Crosslinking of Peptide Hydrogels: Structural and Mechanical Effects

Nevil Jose[1], Pol Barcelona[2], Brandon Victorio[1], Elena Xuriguera[2], Patrick Gamez[1] and Ana B. Caballero[1]

[1]Departament de Química Inorgànica i Orgànica. Facultat de Química, UB
[2]Departament de Ciencia dels Materials i Química Física. Facultat de Química, UB
[3] Catalan Institution for Research and Advanced Studies (ICREA), Passeig Lluís Companys 23, 08010, Barcelona, Spain

ana.caballero@ub.edu

Hydrogels are hydrophilic polymeric networks characterized by high water content, permeability, and tunable properties, which make them attractive materials for biomedical applications such as drug delivery, tissue engineering, wound healing, biosensors, bioinks, and catalysis [1].

Within this framework, peptide-based hydrogels are particularly appealing due to their mild fabrication conditions, biocompatibility, biodegradability, and functional versatility. However, their limited mechanical strength and slow gelation kinetics remain major challenges that restrict their biomedical applicability [2].

Herein, we describe how a tightly-controlled crosslinking with copper ions impacts on the structure and on the mechanical performance of peptide hydrogels.

References:

[1] Yu Shrike Zhang, Ali Khademhosseini, Advances in engineering hydrogels. Science356, eaaf3627 (2017). https://doi.org/10.1126/science.aaf3627

[2] Gallo, E., Diaferia, C., Smaldone, G. *et al. Sci Rep* 14, 9940 (2024). https://doi.org/10.1038/s41598-024-60145-z

P.20. Synthesis of Gemini BODIPY Dyes for Mitochondrial Labelling and Drug Delivery

S. Bagherpour[1,2], M. Amabilino-Pérez[1], C. Gallardo-Roselló[1], A. Pereda-Velarde[3,4,5], M. Calvo[6], S. Gines[3,4,5] and L. Pérez-García[1,2]

[1]Departament de Farmacologia, Toxicologia i Química Terapèutica, Universitat de Barcelona, Av. Joan XXIII 27-31, Barcelona, 08028 Spain.
[2]Institut de Nanociència i Nanotecnologia IN2UB, Universitat de Barcelona, Barcelona, 08028 Spain.
[3]Departament de Biomedicina, Facultat de Medicina i Ciències de la Salut, Institut de Neurociències, Universitat de Barcelona, Barcelona, 08036, Spain.
[4]Institut d'Investigacions Biomèdiques August Pi i Sunyer (IDIBAPS), Barcelona, Spain.
[5]Centro de Investigación Biomédica en Red sobre Enfermedades Neurodegenerativas (CIBERNED), Madrid, Spain.
[6]Advanced Optical Microscopy Unit, Centres Científics i Tecnològics de la Universitat de Barcelona, Facultat de Medicina, Universitat de Barcelona, Barcelona, Spain.

saman.bagherpour@ub.edu/mlperez@ub.edu

Mitochondria are crucial for essential cellular functions, and their dysfunction has been associated with numerous human clinical disorders.[1] Fluorescent dyes that stain mitochondria enable the tracking of disease progression and cellular processes by allowing examination of mitochondrial morphology. However, organic fluorophores face several challenges in bioimaging, including solubility issues that require toxic solvents, aggregation-caused quenching, interference with biological processes due to their reactive nature, poor cellular uptake, and photostability problems in aqueous environments.[2]

In the current work, cationic gemini BODIPY dyes were synthesized for mitochondrial imaging in living cells. All synthesized cationic gemini BODIPY dyes were characterized by $^{1}H/^{13}C$ NMR and HR-ESI-MS. The self-assembly behaviour of the water-soluble synthesized dyes was studied using fluorescence spectroscopy, surface tension measurements, and cryogenic transmission electron microscopy. In vitro experiments in HeLa cells revealed excellent internalization, low cytotoxicity, and exceptional mitochondrial labelling by the completely water-soluble cationic gemini BODIPY dye.

Acknowledgment: Project PID-2023-146658NB-C32 was funded by MICIU/AEI/10.13039/501100011033 and by FEDER, EU. We are very grateful to Ana Lopez (María de Maeztu Unit of Excellence, Institute of Neurosciences, University of Barcelona, MDM-2017-0729, Ministry of Science, Innovation and Universities) for technical assistance. We also thank Dr. Teresa Rodrigo and Dr. Lara Sedó and the staff of the animal care, as well as Gemma Martín and Fernando Unzueta from the Advanced Optical Microscopy Unit from Scientific and Technological Centers for image acquisition assistance.

References: [1] P. Norat, S. Soldozy, J. D. Sokolowski, C. M. Gorick, J. S. Kumar, Y. Chae, K. Yağmurlu, F. Prada, M. Walker, M. R. Levitt, R. J. Price, P. Tvrdik, M. Y. S. Kalani, "Mitochondrial dysfunction in neurological disorders: Exploring mitochondrial transplantation" NPJ Regen. Med. 2020, 5, 22.[2] S. Bagherpour, P. Vázquez, M. Duch, J. Pablo Agusil, J. A. Plaza, M. Red ondo-Horcajo, T. Suárez, L. Pérez-García, "Silicon oxide microchips functionalized with fluorescent probes for quantitative real-time glutathione sensing in living cells" J. Mater. Chem. B 2025, 13, 1630–1642.

Figure 1. (a) Cryo-TEM images of self-assembled cationic gemini BODIPY, (b) HeLa cell incubated with synthesized cationic BODIPY.

a)

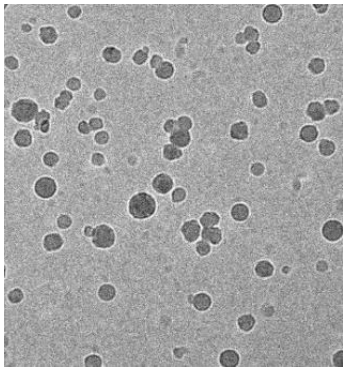

b)

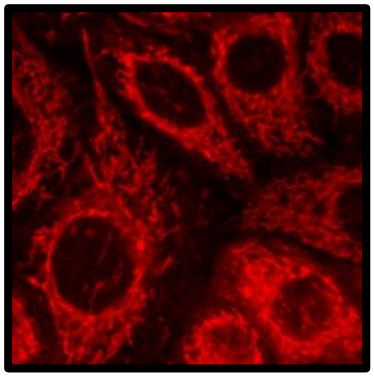

P.21. Light-induced molecular motion in supramolecular fibres

Daniela Dupkalová[a], Aysha Fasna[ab], Zakir Ullah[c], David B. Amabilino[b], Monika Gupta[d] and Lluïsa Pérez-García[a]

[a] Departament de Farmacologia, Toxicologia i Química Terapèutica, Universitat de Barcelona, Av. Joan XXIII 27-31, Barcelona, 08028, Spain and Institut de Nanociència i Nanotecnologia UB (IN2UB)

[b] Institut de Ciència de Materials de Barcelona (ICMAB-CSIC), Carrer del Til.lers, 08193 Bellaterra, Spain

[c] Department of Materials Science and Engineering (MSE), Chungnam National University (CNU), Gwangju, 61186, South Korea

[d] Department of Chemistry, Indian Institute of Technology Jodhpur, Rajasthan, 342030, India

afasnafa73@alumnes.ub.edu /mlperez@ub.edu

Various synthetic stimuli-responsive microscopic systems with impressive control in relative molecular motion have been created [1] to imitate naturally occurring movement of biomolecules. Our group developed a purely supramolecular system where a molecular 'traveller' (TCPP) moved along gemini bis-imidazolium gelator fibers over several microns when irradiated with visible light in the presence of photoswitch (Azo) [2]. Real-time imaging of the motion in the solvated state was recorded using total internal reflection fluorescence (TIRF) microscopy.

In this work, we present a modified system with different azobenzene derivative (AzoF4) incorporated as a photoswitch. Because of higher cis:trans ratio, AzoF4 could change the extent of observed TCPP movement. Moreover, cis-isomer population can be easily replenished using visible light, allowing repeated energy release.

Acknowledgments

We thank the MICIU/AEI/10.13039/501100011033 for financing projects PID2021-123873NB-I00 and PID-2023-146658NB-C32 as well as the "Severo Ochoa" program for Centre of Excellence CEX2023-001263-S. We also thank the Agència de Gestió d'Ajuts Universitaris i de Recerca (AGAUR), Grant 2021SGR01085. DD thanks the predoctoral program AGAUR-FI ajuts (2024 FI-1 00769) Joan Oró.

REFERENCES

1. Baroncini, M; Silvi, S; Credi, A. "Photo- and Redox-Driven Artificial Molecular Motors," Chem. Rev. 2020, 120, 200.

2. Samperi, M.; Bdiri, B.; Sleet, C. D.; Markus, R.; Mallia, A. R.; Pérez-García, L.; Amabilino, D. B. "Light-controlled micron-scale molecular motion," Nat. Chem. 2021, 13, 1200.

Figure 1: a) TIRF microscopy image of hydrogel with **AzoF4** and **TCPP** incorporated in the fibers. b) Molecular structure of **AzoF4** in *trans* and *cis* state.

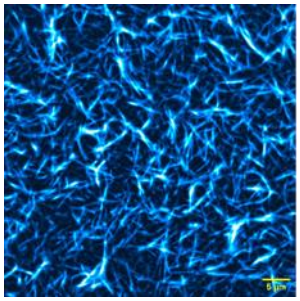

P.22. Niacinamide Water-in-Water Emulsions for Dermal Delivery: Formulation and Preservative Efficacy Evaluation

Claudia Garriga[1]; Elvira Escribano-Ferrer[1,2]; Ana María Marqués Villavecchia[3]; María Jose García-Celma[1,4]

1Department of Pharmacy and Pharmaceutical Technology and Physical Chemistry, Faculty of Pharmacy and Food Sciences. R+D Associated Unit to CSIC. Instituto of Nanoscience and Nanotechnology (IN2UB). University of Barcelona, Joan XXIII, 08028, Barcelona, Spain.

2CIBER 06/003 Physiopathology of Obesity and Nutrition (CIBER-OBN), Institute of Health Carlos III, Madrid, Spain

3Department of Biology, Healthcare and the Environment, Faculty of Pharmacy and Food Sciences. University of Barcelona, Joan XXIII, 08028, Barcelona, Spain.

4Biomedical Research Networking Center in Bioengineering, Biomaterials and Nanomedicine (CIBER-BBN), Institute of Health Carlos III, Madrid, Spain

clgarrio7@alumnes.ub.edu

Niacinamide (NA) is a key active ingredient in dermatology for treating acne, skin aging, and UV-induced damage, among others [1]. Due to its high hydrophilicity, it can be incorporated into water-in-water (W/W) emulsions, which offer an eco-sustainable alternative to conventional systems by avoiding organic solvents and surfactants [2]. This study aims to develop a biocompatible W/W emulsion for dermal application using Transcutol® as a permeation enhancer and eco-friendly preservatives.

W/W emulsions were prepared in PBS (pH 5.5) by dispersing a sodium caseinate (5% w/w) solution into a sodium alginate (2% w/w) solution by high-speed homogenization (25,000 rpm), followed by the addition of NA and Transcutol®. They were prepared using a factorial design (with/without NA, Transcutol®, and various preservatives), and evaluated for up to 1 year through macroscopic inspection. Microbiological safety was assessed via the Challenge Test (EN ISO 11930:2012) against five standard microorganisms for 28 days [3].

Stability tests revealed a strong influence of composition on homogeneity. The optimized formulation (with NA and Transcutol®) remained stable for 1 year, significantly outperforming the control (without NA or Transcutol®), which showed phase separation after 3 weeks. This suggests a stabilizing effect induced by the active ingredient and the permeation enhancer. Regarding preservatives, choice they also influenced physical stability: Leucidal® and potassium sorbate extended control stability to 8 weeks, whereas Phenonip®, Cosgard®, and sorbic acid failed at 3 weeks. The Challenge Test confirmed that all studied preservatives, including eco-friendly options (Leucidal®, Cosgard®, sorbic acid), met the required logarithmic reduction values of the ISO standard [3], ensuring microbial safety throughout the 28-day period.

A kinetically stable W/W caseinate-in-alginate emulsion containing 8% NA and 10% Transcutol® was successfully developed. The results demonstrate that NA and Transcutol® not only acted as active/enhancer but improved the physical stability of the emulsions. This system represents a promising, eco-friendly alternative for the topical delivery of hydrophilic actives.

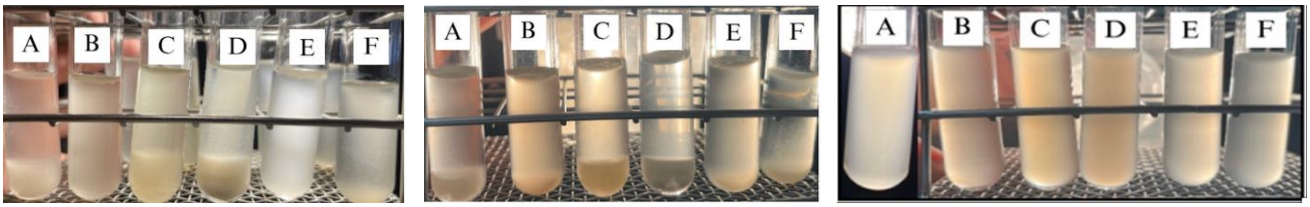

Figure 1. Macroscopic visual stability of W/W emulsions. Left: Control emulsion (without NA or Transcutol®) after 3 weeks. Center: Control emulsion after 8 weeks. Right: Optimized formulation (with NA and Transcutol®) after 1 year. In all cases, letters indicate the preservative used: (A) Phenonip®, (B) Leucidal®, (C) Cosgard™, (D) Sorbic acid, (E) Potassium sorbate, and (F) No preservative.

References

[1] Marques, C., Hadjab, F., Porcello, A., Lourenço, K., Scaletta, C., Abdel-Sayed, P., Hirt-Burri, N., Applegate, L.A., & Laurent, A. Mechanistic insights into the multiple functions of niacinamide: therapeutic implications and cosmeceutical applications in functional skincare products, Antioxidants 13, 425 (2024).

[2] Esquena, J. Water-in-water (W/W) emulsions, Curr. Opin. Colloid Interface Sci. 25, 109-119 (2016).

[3] UNE-EN ISO 11930. Cosmetics. Microbiology. Evaluation of the antimicrobial protection of a cosmetic product.

P.23. BODIPY-Based Probes for Biological Sensing and Mitochondria Targeting

Ruxin Li[1,2], Saman Bagherpour[1,2], Lluïsa Pérez-García[1,2,]

[1] Departament de Farmacologia, Toxicologia i Química Terapèutica, Universitat de Barcelona, Av. Joan XXIII 27-31, Barcelona, 08028, Spain
[2] Institut de Nanociència i Nanotecnologia IN2UB, Universitat de Barcelona

liruxin@ub.edu/mlperez@ub.edu

Mitochondria are central to cellular energy production and redox regulation. Adenosine triphosphate (ATP) reflects cellular energy status and is mainly generated in mitochondria, while glutathione (GSH) serves as a major antioxidant maintaining redox balance. Therefore, developing mitochondria-targeted fluorescent probes for ATP detection and GSH sensing is of great importance for real-time monitoring of mitochondrial function.

The intermediates of both probes contain a terminal alkyne moiety, serving as a clickable handle for further functionalization through click chemistry. The ATP probe contains imidazolium positive charge moiety, using electrostatic interaction strategy for intracellular ATP detection. The GSH probe contains an electron-withdrawing diethyl malonate moiety, enabling reversible Michael addition with GSH for real-time monitoring of mitochondrial redox adaptation.[1-3]

A series of BODIPY-based probes were synthesized and structurally characterized by NMR and MS analyses, followed by UV–Vis absorption and fluorescence spectroscopic studies. The BODIPY core exhibited a characteristic absorption around 500 nm, while conjugation with the malonate moiety induced a significant bathochromic shift of the absorption band to approximately 600 nm, indicating an altered electronic structure and extended conjugation effect. Current studies are focused on evaluating the optical response of these probes toward ATP and GSH sensing. Subsequent investigations will involve in vitro experiments using cellular models to assess their potential for intracellular and mitochondria-related bioimaging applications.

ACKNOWLEDGMENTS

Project PID-2023-146658NB-C3 was funded by MCIN/AEI/10.13039/501100011033. R.L. thanks the FPI predoctoral contract 404 funded by MICIU/AEI /10.13039/501100011033 and FSE+.

References:

[1] Kumar, R.; Sandhu, S.; Singh, P.; Kumar, S. *Chem Rec* **2017**, *17* (4), 441-471.
[2] Xu, Z.; Kim, S. K.; Yoon, J. *Chem Soc Rev* **2010**, *39* (5), 1457-1466.
[3] Bagherpour, S.; Vazquez, P.; Duch, M.; Pablo Agusil, J.; Plaza, J. A.; Redondo-Horcajo, M.; Suarez, T.; Perez-Garcia, L. *J Mater Chem B* **2025**, *13* (5), 1630-1642.

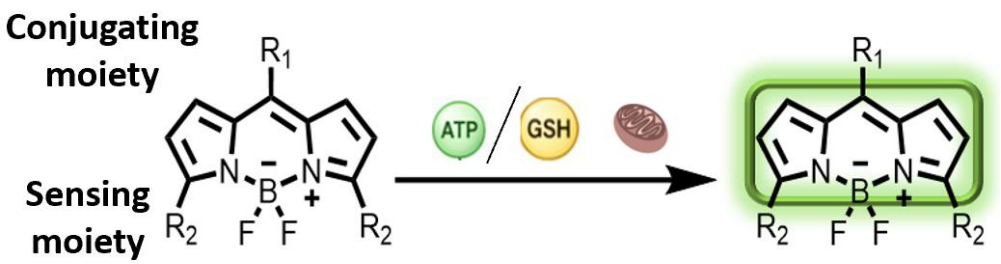

Figure 3. Schematic illustration of the probe response toward ATP/ GSH.

P.24. Development and optimization of Baricitinib Microemulsion as Topical Therapy for PSORIASIS

R. Mohammadi Mey Abadi[1,2], A.C. Calpena[1,2], M. Mallandrich[1,2]

[1]Department of Pharmacy and Pharmaceutical Technology and Physical Chemistry, Faculty of Pharmacy and Food Sciences, UB.
[2] Institute of Nanoscience and Nanotechnology of the University of Barcelona (IN²UB)

rmohammo31@alumnes.ub.edu

Introduction: Baricitinib (BCT) is a JAK inhibitor with very low aqueous solubility (< 1 mg/mL), which limits its formulation development and can cause inconsistent bioavailability [1]. There are several strategies to enhance drug solubility, such as nanoparticles and nanosystems, including nano and microemulsions. Anhydrous microemulsions are thermodynamically stable, transparent, isotropic mixtures of oil, surfactant, and a non-aqueous polar phase that form nanometer-sized droplets. In the absence of water, these systems are designed to protect hydrolysis-sensitive compounds and enhance drug solubility. This work aimed to develop a microemulsion suitable for the topical delivery of baricitinib for the treatment of psoriasis.

Materials & Methods: The optimisation was carried out by pseudo-ternary phase diagrams considering 3 main phases: (A) non-aqueous polar phase composed of Transcutol® P + propylene glycol (3:2), (B) Labrafac lipophile as the oily phase, and (C) Lauroglycol + sulfadone (5:2) as the surfactant and co-surfactant components. The microemulsions were prepared by weighing 5 mg of Baricitinib and dissolving it in the mixture of phase A (Transcutol® P: PEG), followed by sonication for 15 minutes, and the proper amount of phase C was added, followed by a 10-minute sonication, and finally, the Labrafac was added, and a final sonication for 15-20 minutes took place [2]. A total of 20 formulations were obtained as microemulsions and were characterised in terms of visual appearance, pH, droplet size, polydispersity index, and viscosity. The optimal formulations were selected based on the droplet size and physical stability (homogeneous, transparent, and showing no sign of precipitation or phase separation).

Results: Four out of twenty formulations were selected as candidates. The microemulsions resulted in transparent solutions with no signs of phase separation, and their droplet size was within the range 69 - 126 nm, with a polydispersity index of about 0.1 and pH values within the range 4.3 - 5.5, which is within the natural human skin pH values [3]. The viscosity of the microemulsions ranged from 6.7 - 13.8 mPa · s. This range of viscosity values is excellent for covering large surface areas; it indicates a very thin, liquid, and sprayable consistency, and the microemulsions spread rapidly with very little friction.

Discussion: The selected microemulsions exhibited suitable physicochemical properties for topical delivery. However, further characterisation, including assessment of their stability, should be performed before in vitro efficacy evaluation.

Acknowledgment

The authors would like to thank Ismael Abo Horan for assistance with conducting the tests.

References:

[1] Mohammadi-Meyabadi et al. Pharmaceutics 2022.

[2] R. Yehia and D. Attia, Asian Journal of Pharmaceutical and Clinical Research, 2019.

[3] Mijaljica et al. Cosmetics 2025.

P.25. DEVELOPMENT OF PLGA NANOPARTICLES LOADING BARICITINIB FOR ALOPECIA AREATA TREATMENT

S. Sanz [1], S. Soroush [1], M. Mallandrich [1,2]

[1] Department de Pharmacy and Pharmaceutical Technology, and Physical Chemistry, Faculty of Pharmacy and Food Sciences, University of Barcelona, 08028, Barcelona, Spain
[2] Institute of Nanoscience and Nanotechnology of the University of Barcelona (IN²UB), 08028 Barcelona, Spain

ssanzgon7@alumnes.ub.edu

Alopecia Areata (AA) is a chronic inflammatory and autoimmune dermatosis, characterized by non-scarring hair loss. It is one of the most common immune-mediated dermatological pathologies, affecting approximately 2% of the world's population at some point in their lives, without significant ethnic distinction [1].

Baricitinib is a JAK inhibitor approved by the EMA and FDA for adults with severe alopecia areata. It effectively promotes hair regrowth, including eyebrows and eyelashes, but often requires continuous, long-term treatment [2]. However, when taken orally, it presents common systemic side effects. Additionally, Baricitinib is a poor water-soluble drug and using PLGA (poly lactic-co-glycolic acid) nanoparticles is a promising strategy to overcome baricitinib's poor aqueous solubility and inconsistent bioavailability [3].

PLGA nanoparticles (NPs) are highly effective in encapsulating drugs, providing sustained release, and can better penetrate hair follicles, which are the primary site of inflammation in alopecia areata [4]. The aim of this work was to develop PLGA nanoparticles loading Baricitinib in order to offer a topical treatment for alopecia areata.

NPs were prepared following the solvent displacement method, briefly, 0.025 % baricitinib and 0.25 % PLGA was dissolved in ethyl acetate and added drop by drop to an aqueous solution of PVA. The NPs suspension was gelified with 15 % of Pluronic F-127 and 0.5% HPMC. NPs were characterized visually and physicochemically and the nanogel formulation was also characterized by its extensibility showing a result of 30,19 cm^2 applying a weight of 36 g for a minute. The NPs suspension resulted in 254 nm. Nanoparticles in the range of 200–500 nm are ideal for accumulating in the hair follicle openings and reaching deeper. The NPs enhance drug delivery to the hair follicles while acting as reservoirs for prolonged therapeutic action in skin treatments [4].

In conclusion, the developed baricitinib-loaded PLGA nanoparticles showed suitable physicochemical properties for follicular delivery, with particle size within the optimal range for hair follicle targeting and successful incorporation into a topical nanogel formulation. These results support the potential of this nanosystem as a promising topical strategy for localized alopecia areata treatment while minimizing systemic exposure.

References:

[1] Sibbald C. et al J Cutan Med Surg. 2023 doi: 10.1177/12034754231168839

[2] King et al. N Engl J Med, 2022. DOI: 10.1056/NEJMoa2110343

[3] Ansari et al. Saudi Pharm J. 2019. doi: 10.1016/j.jsps.2019.01.012

[4] Yueting et al. Asian Journal of Pharmaceutical Sciences, 2022, https://doi.org/10.1016/j.ajps.2022.04.003

P.26. Liposome-based gels NANOCARRIERfor skin barrier RECOVERY: DEVELOPMENT AND ASSESSMENT.

S. Soroush[1], A. Rico[3], R. Bitar[3], A. Bitar[3], C. Folle[2,3], M. Mallandrich[1,4]

[1] Department of Pharmacy, Pharmaceutical Technology and Physical Chemistry, Faculty of Pharmacy and Food Sciences, University of Barcelona, Barcelona, Spain
[2] Department of Evolutionary Biology, Ecology and Environmental Sciences, Faculty of Biology University of Barcelona, Barcelona, Spain
[3] Department of Bioengineering, Faculty of Medicine, University International of Catalunya, Sant Cugat del Vallès, Spain.
[4] Institute of Nanoscience and Nanotechnology of the University of Barcelona (IN2UB), Barcelona, Spain

shsorous74@alumnes.ub.edu

Skin barrier dysfunction, characterized by alterations in the lipid organization of the stratum corneum, is a common feature of several dermatological conditions, including atopic dermatitis, acne, sensitive skin, and diabetic xerosis [1,2. In this context, nanostructured lipid-based systems, particularly liposomes, have emerged as promising candidates due to their biocompatibility, nanoscale architecture, and structural similarity to epidermal lipids [3,4]. These phospholipid vesicles can enhance skin hydration, promote lipid reorganization, and serve as multifunctional nanocarriers capable of improving the stability, delivery, and controlled release of bioactive compounds for skin barrier recovery.

Liposomes were prepared using a solvent-minimized and simplified method as an alternative to the thin-film hydration technique. Different formulations were designed by varying the proportions of hydrogenated lecithin, stearic acid (SA), and cholesterol, while maintaining constant amounts of Tween 80 and ethanol. Briefly, the lipid components were melted at 70 °C and mixed with a reduced volume of ethanol and Tween 80 until complete homogenization. The resulting lipid phase was then added to the aqueous phase and emulsified by a probe sonication to obtain nanosized liposomal dispersions. Liposomes were physicochemically characterized by dynamic light scattering (DLS) to determine particle size, polydispersity index (PDI), and zeta potential, while the final pH was also measured. The optimized liposomal formulation was subsequently incorporated into three gel matrices prepared in parallel, namely HPMC-Xanthan gum, Sepigel, and Tapioca-Xanthan gum, to obtain liposomal gels. Finally, the degradation behavior of the formulations was evaluated in PBS pH 5.5 under skin-mimicking conditions.

The prepared liposomal formulations exhibited nanoscale particle sizes below 120 nm across all batches, with narrow to moderate polydispersity indices (PDI range: 0.235–0.350) and negatively charged zeta potentials (–10.4 to –42.9 mV), indicating overall colloidal stability. The pH values ranged from 4.25 to 5.61, compatible with cutaneous application. Based on the combined criteria of particle size, PDI, and zeta potential, formulation F6 was selected as the optimized system, presenting a particle size of 113.1 nm, a PDI of 0.246, a zeta potential of –42.9 mV, and a pH of 5.02, and was subsequently incorporated into the gel matrices. The degradation behavior of the liposomal gels varied depending on the gel matrix composition. Sepigel-based liposomal gel exhibited the fastest degradation profile, reaching approximately 75% degradation within 10 minutes. In contrast, HPMC-Xanthan gum and Tapioca-Xanthan gum systems showed slower initial degradation rates of around 42% and 35%, respectively. After 40 minutes, only a minor fraction of the formulations remained, with residual non-degraded content of 16% for Sepigel, 10% for HPMC-Xanthan gum, and approximately 7% for Tapioca-Xanthan gum, indicating a matrix-dependent modulation of degradation kinetics.

The developed liposomal formulations demonstrated suitable nanoscale properties

and stability, with the optimized system successfully incorporated into gel matrices for topical application. The degradation behavior of the gels was strongly dependent on the polymeric network, supporting their potential as nanostructured topical systems for skin barrier repair.

References: [1] Elias, P. M., Journal of Investigative Dermatology, 2012. [2] Bouwstra, et al. Biochimica et Biophysica Acta, 2006. [3] Sguizzato, et al. International Journal of Molecular Sciences. 2021. [4] Musielak, et al. Cosmetics, 2024.

P.27. Advancing Topical Therapy: Antibiotic-Loaded Nanostructured Lipid Carriers Against Skin Infections.

Z. Talebian[1,2], S. Daneshjou[2], M. Mallandrich[1,3]

1 Department of Pharmacy and Pharmaceutical Technology, and Physical Chemistry, Faculty of Pharmacy and Food Sciences, University of Barcelona, Barcelona, Spain

2 Department of Nanobiotechnology, Faculty of Biological Sciences, Tarbiat Modares University, Tehran, Iran

3 Institute of Nanoscience and Nanotechnology of the University of Barcelona (IN2UB), Barcelona, Spain

zaratalebian@ub.edu

Bacterial infections have become a serious health threat due to the misuse of antibiotics and the emergence of antimicrobial resistance. The ineffectiveness of antibiotics, the emergence of antibiotic-resistant bacteria, and the increase in the number of multidrug-resistant bacterial strains have drawn the attention of researchers to create innovative methods to overcome this challenge. Nanotechnology is an efficient and effective solution to solve this problem. Loading antibiotics in nanoparticles can bring them to the site of infection in higher concentrations and thus increase their effectiveness. Nanostructured lipid carriers (NLCs) are lipid-based nanocarriers composed of a mixture of solid and liquid lipids. This structure provides higher drug loading capacity, improved solubility and stability, which leads to higher bioavailability. Additionally, they are biocompatible, biodegradable, and show low toxicity. The nanoscale size of these carriers increases surface area and promotes better interaction with biological membranes, facilitating improved penetration into target tissues such as infected skin or wounds. Encapsulation of antibiotics within NLCs also enables controlled and sustained drug release, which helps maintain therapeutic drug concentrations at the site of infection over extended periods. This sustained release profile can reduce dosing frequency, improve patient compliance, and minimize systemic side effects. Moreover, by localizing drug delivery and enhancing penetration into infected tissues, NLCs can potentially increase antimicrobial efficacy while reducing the risk of resistance development associated with sub-therapeutic dosing [1].

For synthesizing NLC, the melt emulsification and ultrasonication method was used. In brief, lipid and aqueous phases were prepared separately and heated to a certain temperature. The hot pre-emulsion was immediately subjected to probe-type ultrasonication. The resulting nano-emulsion was cooled in an ice bath. As it cooled, the lipid droplets recrystallized to form the final NLC. At this point, NLC were coated with hyaluronic acid (HA) to stabilize the NLC.

NLC showed a mean particle size of 33 nm before coating and 390 nm after the HA coating, with a polydispersity index (PDI) below 0.3 in both cases. The zeta potential of uncoated NLC was +11mV which shifted to –25 mV after coating. NLC showed high entrapment efficiency (>98 %) and drug loading of about 4%. The increase in particle size suggests successful surface coating; this fact is also confirmed by the change in zeta potential value. The PDI suggests that the system is uniform despite the size increase after coating [2].

The results confirm successful HA coating, evidenced by the increase in particle size and shift in zeta potential to negative values. The formulation maintained good uniformity, with high entrapment efficiency and adequate drug loading. Overall, the NLC system appears stable and suitable for the cutaneous delivery of antibiotics.

References:

[1] Henostroza et al. Int. J. Pharm. 2022. [2] Bonechi et al. Appl. Sci. 2021.

P.28. pH-Responsive Gelatin-Based Hydrogel Films for Targeted SCC Treatment in Chronic Wounds

M. C. Morán[1,2], F. Cirisano[3], M. Ferrari[3]
[1]Departament de Bioquímica i Fisiologia, Secció de Fisiologia– Facultat de Farmàcia i Ciències de l'Alimentació, Universitat de Barcelona, Avda. Joan XXIII, 27-31, 08028 Barcelona, Spain
[2]Institut de Nanociència i Nanotecnologia–IN2UB, Universitat de Barcelona, Avda. Diagonal, 645, 08028 Barcelona, Spain
[3]CNR-ICMATE Istituto di Chimica della Materia Condensata e di Tecnologie per l'Energia, via De Marini, 6, 16149 Genova, Italy
mcmoranb@ub.edu

Introduction: Chronic wounds are characterized by a persistent inflammatory state and an alkaline microenvironment that impairs healing and may promote the development of squamous cell carcinoma (SCC). These pathological conditions highlight the need for advanced biomaterials capable of responding to local stimuli to achieve controlled and localized therapeutic effects. In this context, pH-responsive systems represent a promising strategy for improving drug delivery in chronic wound environments. Recent advancements have highlighted the potential of gelatin-based nanoparticles as drug-delivery systems for chronic wound treatment [1,2]. Despite their promise, nanoparticles typically require a supporting scaffold or carrier for effective topical application. In contrast, hydrogel films may provide a solid or semi-solid matrix that can be directly applied to the wound bed.

Materials & Methods: Gelatin-based hydrogel films were developed using type A and type B gelatin with different gel strengths and loaded with 5-fluorouracil (5-FU) as a model antitumor drug. Films were prepared by solvent casting and characterized in terms of morphology, wettability, optical properties, swelling behavior, and drug release at pH 5.5, 7.4, and 9.0, simulating healthy skin and chronic wound conditions. Water vapor transmission rate (WVTR) was also evaluated to assess the suitability of the films for wound healing applications. Biocompatibility was determined through hemolysis assays, while cytotoxicity and selectivity were assessed using non-tumoral (3T3 fibroblasts and HaCaT keratinocytes) and tumoral (A431 carcinoma) cell lines.

Results and Discussion: The hydrogel films exhibited homogeneous structure, suitable transparency, and tunable surface properties depending on composition. A clear pH-responsive behavior was observed, with increased swelling and accelerated drug release under alkaline conditions, consistent with chronic wound environments. WVTR values were within the appropriate range to maintain a moist wound environment. All formulations showed non-hemolytic behavior, confirming good hemocompatibility. Unloaded films maintained high cell viability, demonstrating intrinsic biocompatibility. In contrast, 5-FU-loaded films induced significant cytotoxic effects in A431 carcinoma cells, while minimizing toxicity in healthy cell lines, indicating selective antitumor activity. Notably, the balance between controlled drug release, structural stability, and therapeutic selectivity could be finely tuned by adjusting the GA and GB gel strength [3]. These findings demonstrate that pH-responsive gelatin-based hydrogel films are promising platforms for localized SCC treatment in chronic wounds. Their ability to combine controlled drug delivery, environmental responsiveness, biocompatibility, and selective cytotoxicity supports their potential application in advanced wound care and targeted cancer therapy.

Acknowledgments: This work was conceived in the framework of the Cooperation Agreement between Faculty of Pharmacy and Food Science (UB)—Institute for Chemistry of Condensed Matter and Technologies for Energy (ICMATE-CNR) (Codi GREC 18407). This research has been partially supported by the project PID2022-136354NB-I00, funded by the Ministerio de Ciencia e Innovación (MCIN) and the Agencia Estatal de Investigación (AEI) (MCIN/AEI/10.13039/501100011033).

References:[1]https://doi.org/10.1016/j.msec.2021.112073. [2] https://doi.org/10.3390/antiox13030299. [3] https://doi.org/10.3390/pharmaceutics18010043.

P.29. NANOSTRUCTURED LIPID CARRIEDS AS NOVEL PSORIASIS TREATMENT: IN VITRO SAFETY AND ANTI-INFLAMMATORY EFFICACY

J. Madariaga-Burgos[1,2]; L. Bonilla-Vidal[1,2]; G. Esteruelas[1,2]; D. Lopez-Ramajo[3,4], Maria Luisa García[1,2], Marta Espina[1,2], Concepció Soler[3,4], Montserrat Pujol[1,2], Joan Manils[3,4,5], E. Sánchez-López[1,2]

[1] Department of Pharmacy, Pharmaceutical Technology and Physical Chemistry, Faculty of Pharmacy, University of Barcelona, 08028 Barcelona, Spain.
[2] Institute of Nanoscience and Nanotechnology (IN2UB), University of Barcelona, 08028 Barcelona, Spain.
[3] Departament de Patologia i Terapèutica Experimental and Hospital Universitari de Bellvitge-Bellvitge Institute for Biomedical Research, 08907 Barcelona, Spain.
[4] Immunity, Inflammation and Cancer Group, Oncobell Program, Institut d'Investigació Biomèdica de Bellvitge, Barcelona, Spain.
[5] Serra Húnter Programme, Immunology Unit, Department of Pathology and Experimental Therapy, School of Medicine, Universitat de Barcelona, Feixa Llarga s/n, 08907 L'Hospitalet de Llobregat, Spain

jmadariaga@ub.edu

Introduction

Clobetasol propionate (CP) is one of the most used drugs for treating inflammatory skin conditions such as atopic dermatitis and psoriasis, although its long-term treatment leads to serious adverse effects [1]. To improve drug permeation and retention and achieve a sustained effect, nanostructured lipid carriers (NLC) have emerged as promising candidates. Therefore, the aim of this work is the characterization of biopharmaceutical behaviour of previously developed CP loaded NLC (CP-NLC) and evaluation of toxicity, cellular uptake into keratinocytes and anti-inflammatory efficacy.

Materials and Methods

CP-NLC were obtained using high-pressure hot homogenization method and the formulation was optimized by a central composite factorial design [2]. *In vitro* release profile was evaluated by the indirect dialysis method, and stability was studied by the assessment of backscattering profile. Cell studies were carried out in HaCaT cells. Cell toxicity was evaluated by AlamarBlue viability assay, nanoparticle intake was evaluated by immunofluorescence and expression of inflammatory and NF-κB inhibition was assessed by the quantification of p-p65 by Western blot [3].

Results and Discussion

CP-NLC optimized formulation was stable up to two months. In respect to release profile, CP-NLC showed a sustained release of CP, reaching a 42 % of the drug released after 48 hours and fitting to Higuchi kinetic model. CP-NLC did not decreased cell viability after 48 hours and were internalized into HaCaT cells after 30 minutes (Figure 1). In addition, CP-NLC inhibited the expression of p-65, demonstrating its capacity of inhibition of the NF-κB inflammatory pathway in a more sustained way in comparison to CP alone.

Conclusion

CP-loaded NLCs were successfully characterized. The formulation showed a sustained release profile, was non-toxic and was capable of internalizing into HaCaT cells, showing maintained anti-inflammatory efficacy.

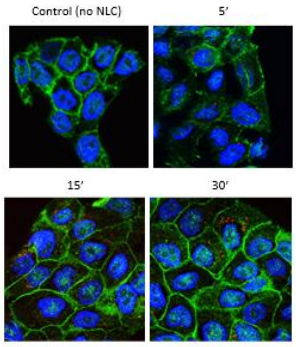

Figure 1. Cellular uptake of CP-NLC in HaCaT Cells (blue staining correspondS to DAPI, green staining corresponds to EGFR and red corresponds to CP-NLC).

References:
[1] doi:10.1038/S41572-025-00630-5.
[2] doi:10.1016/j.ijpharm.2024.124222.
[3] doi:10.3390/ijms24098053.

P.30. USE OF THP-1 CELL LINE TO EVALUATE THE LIGHT MODULATED IMMUNOTOXICITY OF METALLIC OXIDE NANOPARTICLES

A. S. Maddaleno[1,2], B. Maia-do-Amaral[1], L. Guardia-Escoté[3], M.P. Vinardell[1,2], E. Teixidó[3], M. Mitjans[1,2]

[1]Fisiologia, Departament de Bioquímica i Fisiologia, Facultat de Farmàcia i Ciències de l'Alimentació, Universitat de Barcelona

[2]Institut de Nanociència i Nanotecnologia, Universitat de Barcelona

[3]Toxicologia, Departament de Farmacologia, Toxicologia i Química Terapèutica, Facultat de Farmàcia i Ciències de l'Alimentació, Universitat de Barcelona.

adrianamaddaleno@ub.edu

Introduction: TiO_2 and ZnO nanoparticles (NPs) are widely used in our daily lives and in personal care products. However, there is still a need to address aspects of their toxic response [1] as their interactions with immune systems and immunocompetent cells. When these NPs contact or enter to our organism they can induce or modulate specific and/or unspecific immunological reactions as inflammation and hypersensitivity delayed reactions or allergic responses [2,3]. Moreover, studies have indicated these NPs hold the potential capacity to induce phototoxic reactions [1,4]. For this reason, the objective of the present study is to evaluate the use of THP-1 cell line as a model to determine the immunotoxicity of TiO_2 and ZnO NPs in the presence and absence of UVA light.

Material and Methods: Cytotoxicity and phototoxicity of commercial TiO_2 and ZnO NPs (21 nm; 50 nm and 100nm) was studied using the immunocompetent cell line THP-1. For comparative purposes, microsized particles of both oxide metals were also studied. Cells were exposed to a concentration of 100 µg/ml and cell viability was determined by the LDH and MTT assays after 24 hours of exposition. In parallel, the phototoxic potential was evaluated in the same conditions but cells were exposed concomitantly to the particles and to 2.5 J/cm^2 UVA light. Potential interferences and/or interactions of the NPs with the assays or reagents were considering. Cell morphology was checked at the optical microscopical level.

Results and Discussion: In general, low or no cytotoxic effect in the presence and absence of UVA light was recorded for any of the particles at the concentration assayed (100 µg/mL). Potential interactions of NPs with culture media usually consider NPs aggregation, dissolution and protein corona formation to understand their biological response [5]. However, in the case of ZnO particles, both microsized and nanosized, the presence of other components such as 2-mercaptoethanol (a reducing agent included to avoid cell apoptosis or macrophage differentiation) can mask the real effect of NPs. In this sense, we have found that ZnO reduces MTT in the absence of cells in dark conditions but not when irradiated, except in the case of ZnO 100 nm (Fig. 1). Further investigation of the immunotoxic effects of TiO_2 and ZnO will be focused in their capacity to induce the release of humoral mediators of inflammation as IL-8, TNF-α or IL-1β as well as their activity over human macrophages and the phagocytic function with special attention to potential interaction of the NPs with such cytokines as reported in the case of TiO_2 [6].

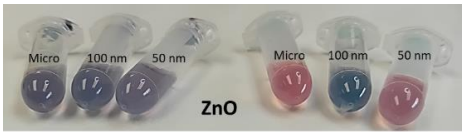

Figure 1. Reduction of MTT by the presence of ZnO particles in dark (left) and UVA light (right) conditions.

Acknowledgments: This work is part of the grant PID2020 funded by MICIU/AEI/10.13039/501100011033.

References: [1] doi: 10.1007/s13273-012-0021-.9 [2] doi: 10.3389/ftox.2024.1293147. [3] doi: 10.2147/IJN.S498690. [4] doi: 10.3390/nano15120951. [5] 10.1039/d0bm01086c. [6] doi: 10.22203/eCM.v035a02.

P.31. NANOCARRIER-MEDIATED DELIVERY OF AN ORGANOSELENIUM NUCLEOSIDE ANALOGUE: INSIGHTS INTO NONSPECIFIC CYTOTOXICITY, ANTITUMOR ACTIVITY, AND CELLULAR UPTAKE

B. C. Maia-do-Amaral[1,3], A. S. Maddaleno[1,2], M.P. Vinardell[1,2], D. R. Nogueira-Librelotto[3], M. Mitjans[1,2]

[1]Fisiologia, Departament de Bioquímica i Fisiologia, Facultat de Farmàcia i Ciències de l'Alimentació, Universitat de Barcelona; [2]Institut de Nanociència i Nanotecnologia, Universitat de Barcelona; [3]Labinvitro, Departamento de Farmacia Industrial, Universidade Federal de Santa Maria.

biancamaia.amaral@ub.edu

Introduction: Cancer is a leading global health concern, marked by uncontrolled cell growth [1]. Finding new treatments is vital, including discovering novel molecules, exploring combination therapies, and developing innovative drug delivery systems. Organoselenium compounds derived from zidovudine are promising nucleoside analogues with potential against tumor cells [2,3]. Developing nano-drug delivery platforms can reduce multidrug resistance (MDR) in cancer cells. Various nanocarriers with unique features have been studied for targeted delivery and improving the EPR effect. This enhances cell uptake by crossing barriers and bypassing efflux pumps, leading to tumor drug buildup [4,5]. Nanoparticle (NP) uptake by cells is essential for delivering active compounds into tumor cells to enable their cytotoxic effects. Without internalization, even highly therapeutic NPs may be ineffective as they remain outside cells [6]. For this reason, the objectives of the present study is to assess the antitumor activity of polymeric and lipid NPs loaded with an organoselenium nucleoside analogue (Di3a) on tumor cell lines, A549 (lung cancer) and NCI/ADR-RES (MDR ovarian adenocarcinoma), evaluate the nonspecific cytotoxic effects of NPs on a liver model (HepG2, human hepatocarcinoma) and immune cells (THP-1, human monocytes), and investigate the internalization of these NPs in both cancer cell lines (A549 and NCI/ADR-RES). **Material and Methods:** A549, NCI/ADR-RES, and HepG2 cells were seeded in 96-well plates at concentrations of 2,5 x 10^4, 1 x 10^5, and 9 x 10^4 cells/mL, respectively, and incubated for 24 hours at 37 °C in an atmosphere of 5% CO_2. The THP-1 cells, which are non-adherent cells, were seeded on the same day as the treatments (0.75 × 10^5 cells/mL). Polymer NPs (Di3a-77KL-NC and 77KL-NC) and lipid NPs (Di3a-77KL-NLC and 77KL-NLC), as well as the non-encapsulated Di3a, were diluted in concentrations ranging from 5 to 100 µg/mL. After 72 hours of incubation, the cells were incubated with 0.5 mg/mL MTT in DMEM for 3 hours at 37 °C in 5% CO_2. Then, the MTT solution was replaced with 100 µL of DMSO, and absorbance was measured at 550 nm to determine cell viability. For the cellular internalization assay, A549 and NCI/ADR-RES cells were incubated in 24-well plates for 24 hours at concentrations of 1×10^5 and 1.5×10^5 cells/mL, respectively, both on a round cover glasses 12mm. Polymeric and lipid NPs containing the fluorophore rhodamine B, at a concentration of 3 µg/mL, were applied for 4 or 24 hours. Subsequently, the cells were stained with DAPI to evaluate the intracellular localization of rhodamine B, and the samples were analysed by fluorescence microscopy. **Results and Discussion:** In the A549 cell line, the formulations Di3a-77KL-NC and Di3a-77KL-NLC significantly decreased cell viability in a dose-dependent way, with reductions ranging from about 12 to 75%, indicating increased cytotoxicity from nanoencapsulation. In NCI/ADR-RES cells, however, none of the treatments were able to significantly sensitize the cells. Lipid NPs showed dose-dependent toxicity in THP-1 cells, with viability ranging from ~20 to 90%. Polymeric NPs were non-toxic, maintaining over 100% viability. The non-encapsulated compound also showed no cytotoxicity, with viability near 100%. In HepG2 cells, no treatment induced over 50% cell death, and polymeric NPs maintained over 80% viability even at the

highest tested concentration. Internalization occurred in both cell lines. These results showed that biocompatibility varies depending on the nanocarrier type, with polymeric NPs being safer than lipid ones, and that NP antitumor activity and internalization data support their potential as delivery platforms for cancer adjuvant therapy.

Acknowledgments: This work is part of a doctoral research funded by 88881.218306/2025-01 PDSE scholarship – Brazil.

References: [1] Bray, F. el al. The ever-increasing importance of cancer as a leading cause of premature death worldwide. Cancer 2021, 127, 3029–3030. [2] Gu, Y. et al. Molecular mechanisms and therapeutic strategies in overcoming chemotherapy resistance in cancer. Mol. Biomed. 2025, 6, 2. [3] Wagner, M.S. et al. Revitalizing the AZT through the selenium: An approach in human triple negative breast cancer cell line. Front. Oncol. 2018, 8, 525. [4] Yadav, P. et al. Nanotechnology-based therapeutics to combat multidrug-resistant cancer. J. Nanobiotechnol. 2022, 20, 423. [5] Mir, S.A. et al. Role of nanotechnology in overcoming the multidrug resistance in cancer therapy: A review. Molecules 2022, 27, 6608. [6] Behzadi, S. et al. Cellular uptake of nanoparticles: Journey inside the cell. Chem. Soc. Rev. 2017, 46, 4218–4244.

NanoMagnetics

P.32. Lanthanoid 2D Metal Organic Frameworks: Exploring Luminescent Property

Abdullah [1,2], **E. Carolina Sañudo** [1,2]
1. Institut de Nanociències i Nanotecnologia, Universitat de Barcelona (IN2UB), 08028 Barcelona, Spain.
2. Departament de Química Inorgànica i Orgànica, Secció de Química Inorgànica, C/Martí i Franqués 1-11, 08028, Barcelona, Spain

abdullah@ub.edu/esanudo@ub.edu

Lanthanoid materials are of great interest due to their unique 4f electronic configurations, which result in sharp photoluminescent emissions[1]. The ideal format for investigating this property is two-dimensional (2D) metal-organic frameworks (MOFs), whose coordination environments around the lanthanoid centers are well-defined, enabling systematic control of luminescent responses through ligand choice and metal composition[2].

In this work, we will extend this family of smaller lanthanoid 2D MOFs of general formula $[Ln_{(x)}Ln'_{(1-x)}(MeCOO)(PhCOO)_2]$, synthesized through rapid, energy-efficient, and environmentally friendly routes (microwave and mechanochemical). New lanthanoid combinations will be explored, including single and mixed metal lanthanoid systems (50:50), using acetate and benzoate as organic linkers. Powder X-ray diffraction, scanning electron microscopy, and energy dispersive X-ray spectroscopy will be used to structurally characterize the materials. Photoluminescence spectroscopy will be employed to evaluate emission properties and energy transfer efficiency between lanthanoid pairs.

By systematically varying the lanthanoid composition, this work aims to establish structure-property relationships guiding the design of 2D MOFs with tunable luminescent responses for potential applications in sensing. Future directions will focus on exploring novel lanthanoid combinations to maximize energy transfer efficiency to improve luminescence.

References:

1. Bartolomé, E., et al., *Luminescent and magnetic [TbEu] 2D metal–organic frameworks.* Dalton Transactions, 2023. **52**(21): p. 7258-7270.
2. González, J., et al., *A multifunctional dysprosium-carboxylato 2D metall–organic framework.* Angewandte Chemie International Edition, 2021. **60**(21): p. 12001-12006.

P.33. Sustainable Synthesis and Structural Evaluation of Alkali-Lanthanide Nanostructured Materials for Energy Storage Applications

Francis Adjei [1], E. Carolina Sañudo [1,2]

[1] Departament de Química Inorgànica i Orgànica, Secció de Química Inorgànica, C/Martí i Franqués 1-11, 08028, Barcelona, Spain

[2] Institut de Nanociències i Nanotecnologia, Universitat de Barcelona (IN2UB), 08028 Barcelona, Spain

fradjeia70@alumnes.ub.edu

The development of cost-effective, structurally tunable nanomaterials is critical to advancing next-generation battery technologies[1]. Alkali-lanthanide-based coordination materials have attracted attention for their structural versatility and potential electrochemical functionality; however, their synthesis often relies on solvent-intensive methods and expensive rare-earth elements.

Here, we report the mechanochemical synthesis of alkali-lanthanide heterometallic coordination polymers incorporating sodium or lithium with terbium or yttrium, targeting their application in energy storage systems. Mechanochemistry offers a sustainable, solvent-minimized route that enables rapid formation of coordination frameworks with controlled composition[2]. Structural and physicochemical characterisation was performed using powder X-ray diffraction (PXRD) to assess phase formation and crystallinity, and infrared (IR) spectroscopy to confirm ligand coordination and bonding environments.

Currently, we are working on replacing costly lanthanide components with more abundant alternatives, particularly zirconium acetate, to develop analogous materials with comparable structural and functional properties while improving economic viability and scalability for industrial applications.

[1] M. H. Manik *et al.*, “Emerging nanomaterials for next-generation automotive energy storage systems,” *Energy Reports*, vol. 15, p. 109158, 2026, doi: https://doi.org/10.1016/j.egyr.2026.109158.

[2] F. Lorenzo *et al.*, “Mechanochemical Synthesis and Electron Crystallography Characterization of van der Waals Lanthanoid 2D Metal − Organic Frameworks,” 2025, doi: 10.1021/acs.inorgchem.5c01592.

P.34. MAGNONIC CRYSTALS IN NANOSTRUCTURED YIG: BAND ENGINEERING, MAGNON CONFINEMENT, AND CONDENSATION

Antoni Homar Genovart,[1] Pablo Cerrato-Serrano,[1,2] Antoni García-Santiago,[1,2] Joan Manel Hernàndez,[1,2] Marius V. Costache,[1,2]

[1]Department of Condensed Matter Physics, University of Barcelona (UB)
[2]Institut de Nanociència i Nanotecnologia (IN2UB), Universitat de Barcelona (UB)

ahomarge13@alumnes.ub.edu

Magnonics exploits spin waves, collective magnetic excitations known as magnons, as lowdissipation information carriers in nanoscale devices. Under resonant driving, magnonic systems can also achieve macroscopic quantum coherence through Bose-Einstein condensation (BEC). This work investigates magnonic crystals based on nanostructured Yttrium Iron Garnet (YIG) thin films, targeting two objectives: engineering controllable band gaps and realising magnon confinement and condensation via parametric pumping.

The structures consist of a YIG waveguide patterned with a one-dimensional periodic array of holes of varying geometry. Micromagnetic simulations are performed with mumax3 (M_{sat} = 1.38 × 10^5 A/m, A_{ex} = 3.4 × 10^{-12}J/m, α = 5 × 10^{-4}, B = 150mT), and the spin-wave dispersion $f(k)$ is extracted via two-dimensional Fourier analysis of the space- and time-resolved magnetisation following a broadband Gaussian pulse. Example below.

Increasing the hole width progressively lowers the lowest flat band frequency and opens tunable band gaps, providing precise control over the magnon density of states. A magnon cavity is then designed by adiabatically tapering the hole size towards the crystal centre, creating an effective potential well that spatially confines magnons, confirmed by the localisation of the spin-wave amplitude at the defect site.

Finally, parametric pumping at twice the confined mode frequency selectively populates the dispersion minimum, driving the system towards a macroscopically coherent magnon condensate. This last simulation is only performed on geometries whose dispersion relation does not exhibit the lowest flat band with large gap.

These results establish a systematic framework for band-structure engineering in magnonic crystals and a viable simulation-based route to room-temperature magnon BEC in geometries compatible with current nanofabrication.

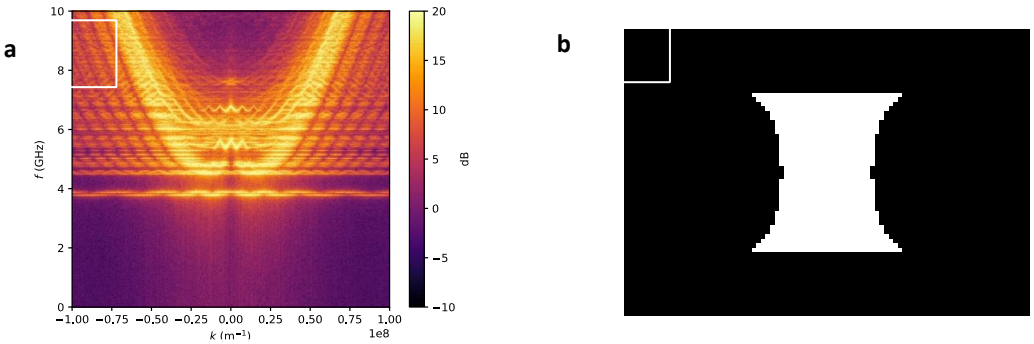

Fig. 4a): Spin wave dispersion relation of a one-dimensional YIG magnonic crystal.
Fig1b): Dumbbell-shaped unit cell with lattice parameter $\boldsymbol{a = 890}$nm and central constriction width $\boldsymbol{w = 190}$nm.

P.35. Enhanced Magnon Damping via Acoustic Fabry-Pérot Resonances in YIG/GGG Bilayers

Marc Batalla Estrada,[a] Pablo Cerrato-Serrano,[a,b] Antoni García-Santiago,[a,b] Joan Manel Hernàndez,[a,b] Marius V. Costache,[a,b]

[a]Department of Condensed Matter Physics, University of Barcelona (UB)

[b]Institut de Nanociència i Nanotecnologia (IN2UB), Universitat de Barcelona (UB)

mbatales31@alumnes.ub.edu

Magnons and phonons, the elementary excitations of spin waves and lattice vibrations, typically interact weakly. However, in yttrium iron garnet (YIG), strong magnetoelastic interaction enables these degrees of freedom to couple, facilitating the transfer of energy and information [1]. In this work, we investigate the influence of phonon-mediated relaxation on magnon damping in a 5µm YIG thin film grown on a Gadolinium Gallium Garnet (GGG) substrate.

By performing room-temperature Ferromagnetic Resonance (FMR) spectroscopy at low power, we demonstrate that the double-polished GGG substrate functions as an acoustic Fabry-Pérot cavity [2]. This mechanical confinement allows resonant phonons to couple intensely with both the fundamental and higher-order magnon modes. We show that this interaction manifests as periodic enhancements in magnetic damping and distinct frequency shifts, dictated by the spectral overlap between the acoustic modes of the substrate and the spin-wave modes of the film.

Notably, our results reveal that these resonant phonons significantly alter magnon dynamics even when their discrete signatures remain unresolved in the FMR linewidth. We provide a systematic characterization of these effects as a function of the external magnetic field and support our findings with a theoretical model that captures the linear magnetomechanical coupling. These insights into mode-specific relaxation are essential for defining the limits of coherence in hybrid magnetoelastic systems and modern magnonic technologies.

References:

[1] J-Y. Han, Z-P. Tian, Y-D. Cheng, H-B. Huang, X-L. Zhou, W-H. Wu, Y. Zhou and Q-L. Wang, J. Phys. B, 57, 025501 (2024)

[2] R. Schlitz, L. Siegl, T. Sato, W. Yu, G. E. W. Bauer, H. Huebl and S. T. B. Goennenwein, Physical Review B106, 014407 (2022)

P.36. ANTIFERROMAGNETIC SUPEREXCHANGE AND OXYGEN VACANCIES IN Co-DOPED V2O5 NANOPARTICLES: A DFT+U AND EXPERIMENTAL STUDY

J. Granados[1,2,3], J. D. Rueda[3], A. Cardona[3], M. A. Macías[3], R. J. Gonzalez[4], J. G. Ramirez[3], Y. R. Hernandez[3], and X. Batlle[1,2]

[1]Departament de Física de la Matèria Condensada, Universitat de Barcelona, 08028 Barcelona, Spain
[2]Institut de Nanociència i Nanotecnologia (IN2UB), Universitat de Barcelona, 08028 Barcelona, Spain
[3]Departamento de Fisica, Universidad de los Andes, Bogotá, Colombia
[4]Departamento de Fisica y Geociencia, Universidad del Norte, Barranquilla, Colombia

jgranaro19@alumnes.ub.edu

Vanadium pentoxide (V_2O_5) nanoparticles are promising candidates for photocatalysis and neuromorphic computing due to their sensitivity to thermal processing and defect engineering. This study investigates the synthesis and characterization of V_2O_5 nanoparticles doped with low concentrations of cobalt (Co), with a specific focus on the critical role of calcination temperature (400–500 °C).

Experimentally, we observe a significant reduction in the optical band gap as calcination temperature increases. Raman spectroscopy and X-ray diffraction analyses reveal that the lattice parameters and vibrational modes associated with the vanadyl oxygen (O1) fluctuate between 425 and 450 °C. Magnetic characterization using vibrating sample magnetometry (VSM) demonstrates temperature-dependent ferromagnetic and paramagnetic contributions in the undoped samples, whereas Co doping suppresses the net magnetization relative to the undoped, calcined baseline.

To investigate the local magnetic environment, we performed DFT+U calculations on a 96-atom supercell, which indicate that Co atoms preferentially integrate into lattice positions neighboring oxygen vacancies rather than occupying the vacancy sites. We attribute the observed optical shifts and structural fluctuations to structural relaxation associated with the formation of oxygen vacancies. Accordingly, the magnetic signals in the undoped nanoparticles are identified as arising from these intrinsic defects. Finally, based on the specific lattice configuration identified by DFT, the suppression of magnetization in the doped samples is explained by antiferromagnetic (AFM) superexchange coupling between the Co dopants and the vacancy-induced V^{4+} polarons.

References:

1. Correal, S., Hernández-Gómez, D., Esquivel, A.S. et al. Tuning electronic and magnetic properties through disorder in V2O5 nanoparticles. Sci Rep 13, 6752 (2023).

P.37. DIRECT IMAGING OF SINGLE-PARTICLE NÉEL AXES IN ANTIFERROMAGNETIC NANOPARTICLES

M. Garcia del Muro[1,2], J. Ara[1,2], C. Moya[2,3], A. I. Figueroa[1,2], M. Foerster[4], M. A. Niño[4], X. Batlle[1,2], A. Labarta[1,2] and A. Fraile Rodríguez[1,2]

[1]Departament de Física de la Matèria Condensada, UB, Martí i Franquès 1, 08028 Barcelona, Spain
[2]Institut de Nanociència i Nanotecnologia (IN2UB), UB, 08028 Barcelona, Spain
[3]Departament de Química Inorgànica i Orgànica, UB, Martí i Franquès, 1, 08028 Barcelona, Spain
[4]ALBA Synchrotron Light Source, CELLS, Cerdanyola del Vallès, E-08290 Barcelona, Spain

garciadelmuros@ub.edu

Nickel Ni oxide (NiO) nanoparticles (NP) are attracting great interest because their antiferromagnetic (AF) order and p-type semiconducting character are useful in electronics or catalysis applications. Unlike bulk NiO, a prototypical AF with zero net moment, nanoscale NiO often shows weak ferrimagnetism, finite coercivity, and superparamagnetic-like behaviour, usually attributed to finite-size and surface effects such as spin disorder, reduced coordination and Ni vacancies that destabilize AF order [1 and references therein]. In this work, we present a particle-by-particle analysis of the AF Néel axis in single-phase, highly crystalline 34 nm NiO NP synthesized via a chemical route, using synchrotron Photoemission Electron Microscopy with X-ray Magnetic Linear Dichroism (PEEM-XMLD). Our 3D nanoscale AF study extends earlier work on AF domain orientations in bulk and thin-film NiO, as well as our recent analysis of only a few particles [2]. By quantifying the XMLD contrast as a function of the polarization direction of the incident electric field (E - vector angle), we determine the Néel axes for tens of randomly dispersed individual NP. The AF axes are stable against room temperature thermal fluctuations and follow a stochastic distribution over the 12 easy directions of NiO, consistent with particle orientations on {200} or {220} facets seen in high-resolution transmission electron microscopy. Importantly, we observe a single-domain state, contrary to seminal predictions of the two-sublattice breakdown at this size [3], attributed to the excellent crystal quality and the absence of surface-induced uncompensated spins, in line with the missing macroscopic weak ferrimagnetism. Currently, we are investigating the emergence of thermally activated Néel vector fluctuations in single NiO NP during cooling across the Néel temperature, and identifying particularly stable orientations.

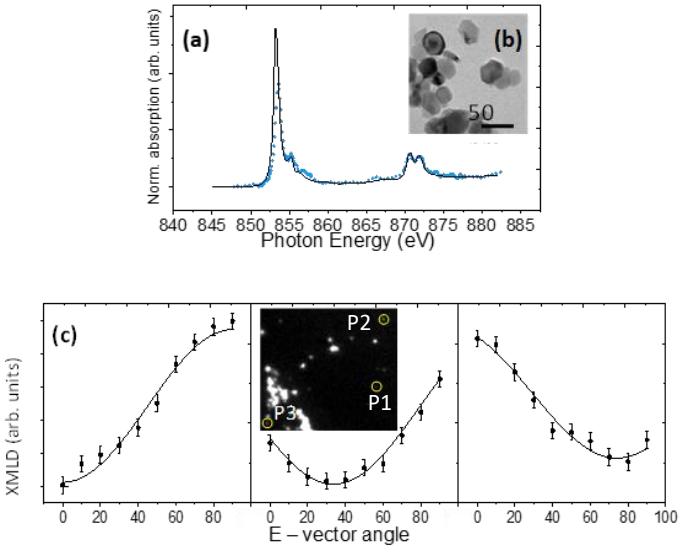

Figure 1. (a) X Absorption Spectra of a representative particle (blue symbols) fitted assuming an 80 % of pure NiO. (b) Representative low resolution TEM image, showing the faceted platelet-like shape, and (c) Experimental XMLD contrast (symbols) as a function of the E-vector angle for 3 particles (P1, P2 and P3) out of the 20 measured; fits (lines) yield the orientation of the AFM axis. Inset: elemental-contrast XPEEM image, scale bar corresponds to 1.5 mm.

[1] C. Moya, J. Ara, A. Labarta, and X. Batlle, et al, Magnetism, 2024, 4, 252.
[2] J. Ara, C. Moya, M. García del Muro, Adriana I. Figueroa, et al, Nanoscale, 2025, 17, 17719.
[3] R. H. Kodama, Salah A. Makhlouf, and A. E. Berkowitz, Phys. Rev. Lett. 79, 1393 (1997).

P.38. DESIGN AND SYNTHESIS OF SUPRAMOLECULAR SWITCHABLE MATERIALS

S. Tanyà[1], D. Aguilà[1,2], R. Díaz[1,2], V. Novikov[1,2], O. Roubeau[3], G. Aromí[1,2]

[1]Departament de Química Inorgànica i Orgànica, Universitat de Barcelona, Spain

[2]Institute of Nanoscience and Nanotechnology, University of Barcelona (IN2UB), Spain

[3]Instituto de Nanociencia y Materiales de Aragón (INMA), CSIC and Universidad de Zaragoza, Spain

stanyaro14@alumnes.ub.edu

Spin-crossover (SCO) compounds are a versatile class of switchable magnetic materials with strong potential for next-generation technological applications, as their properties can be finely tuned through subtle modifications of intermolecular interactions. Weak non-covalent forces (especially hydrogen bonding) play a crucial role in dictating supramolecular organization and, consequently, magnetic behavior. Building on this concept, recent strategies have focused on integrating SCO-active metal centers into supramolecular architectures to achieve enhanced control over structure-property relationships and to develop multifunctional materials.

In this context, we report the design and synthesis of a tailored ligand incorporating a pyrazolylpyridyl chelating unit alongside hydrogen-bond donor and acceptor functionalities, enabling the formation of Fe(II)-based SCO systems with rich supramolecular behavior. [1,2] These ligands were employed to construct a tetrahedral host supramolecular cage composed of four Fe(II) SCO centers, capable of encapsulating tetrahalometallate anions (MX_4^{2-}, M = Mn, Cu, Co, Zn; X = Cl, Br). The ligand, synthesized via a two-step Claisen condensation and cyclization route, was selected to promote both Fe-N coordination and intermolecular hydrogen bonding. The guest anions act as supramolecular templates, directing hydrogen-bond networks between ligands across different metal centers while contributing to charge balance within the assembly. Optimized layered crystallization conditions enabled the growth of high-quality single crystals, and X-ray diffraction studies at 100 K confirmed the formation of isostructural cages with Fe-N bond lengths consistent with a low-spin state in all Fe(II) centers.

Beyond structural characterization, current work explores how encapsulation influences guest-specific properties, including photoluminescence in Mn-based systems, quantum coherence in Cu analogues, and single-molecule magnet behavior in Co derivatives. These results highlight the effectiveness of combining SCO activity with host-guest chemistry to generate multifunctional materials, where cooperative magnetic switching and guest-dependent physicochemical properties are synergistically modulated through adaptable supramolecular interactions.

[1] H. H. Nielsen, P. Vilariño, G. Rodríguez, F. Trepard, O. Roubeau, G. Aromí, D. Aguilà. Dalton Trans. 2024, 53, 9792-9797.

[2] G. A. Craig, O. Roubeau, G. Aromí. Coord. Chem. Rev. 2014, 269, 13.

Figure. Host-guest system with a supramolecular SCO tetrahedral cage encapsulating tetrahalometallate anions

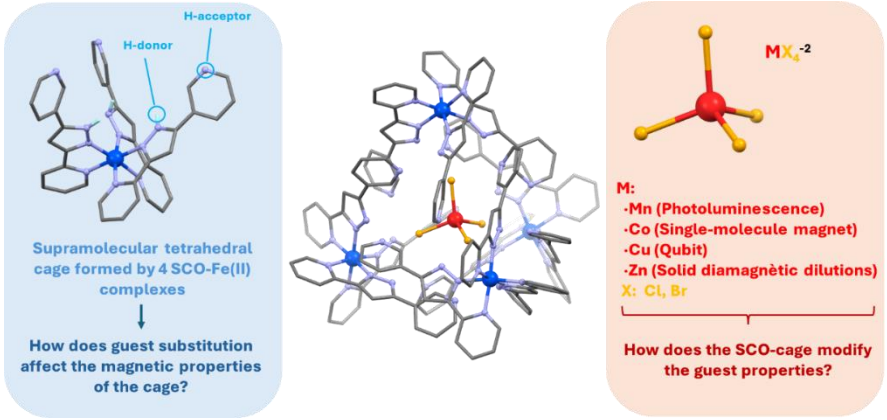

P.39. SYNTHESIS AND MAGNETIC CHARACTERIZATION OF A NOVEL SCHIFF BASE NITRIDOCHROMIUM(V) COMPLEX

S. Caballero[1], J. Mayans[1], A. Escuer[1]

[1]Departament de Química Inorgànica i Orgànica and Institut de Nanociència i Nanotecnologia, Universitat de Barcelona (IN2UB), Martí i Franquès 1-11, Barcelona, 08028, Spain

scaballerogutierrez@ub.edu

Paramagnetic coordination complexes have attracted considerable interest because of their potential applications in magnetic data storage, spin-based electronics, and quantum information processing [1]. In particular, molecule-based magnetic materials are promising candidates for spin qubits in quantum computing due to the versatility of coordination chemistry, which enables the incorporation of a broad variety of ligands and d- and f-block metal ions [2,3]. Among the most studied systems, S = 1/2 metal complexes such as those containing VO^{2+} and Cu^{2+} exhibit long coherence times [4]. In contrast, nitridochromium(V) complexes remain largely unexplored, and spin dynamics have only been investigated in one reported example [5].

Herein, we report the synthesis of a novel bicompartmental Schiff base complex featuring a high-valent Cr^{5+} center stabilized by a terminal nitride ligand in the inner coordination cavity, while the outer cavity remains available for the coordination of additional metal ions, such as Mn^{2+} or Ln^{3+}.

The mononuclear nitridochromium(V) complex was obtained through a modified synthetic procedure based on a previously reported nitrogen-transfer methodology [6]. The crystal structures of these nitride-containing complexes were successfully characterized, and preliminary magnetic measurements suggest the presence of slow magnetic relaxation behavior.

References:

[1] G. Aromí, D. Aguilà, P. Gàmez et al. *Chem. Soc. Rev.* **2012**, *41*, 537-546 . [2] J. M. Zadrozny, J. Niklas, O. G. Poluektvo, D. E. Freedman. *ACS Cent. Sci.*, ***2015,*** *1 (9), 488-492*. [3] R. Hussain, G. Allodi, A. Chiesa et al. *J. Am. Chem. Soc.* **2018***, 140,* 9814-9818 . [4] M. Atzori *et al*. J. Am. Chem. Soc. **2016,** *138* (7), 2154-2157. [5] T. Yamabayashi, Y..Horii, Z.-Y.Li, M. Yamashita, *Chem. Eur. J.*, **2024**, *30*, e202303082. [6] T. Birk, J. Bendix, *Inorg. Chem.* **2003**, *42*, 7608-7615

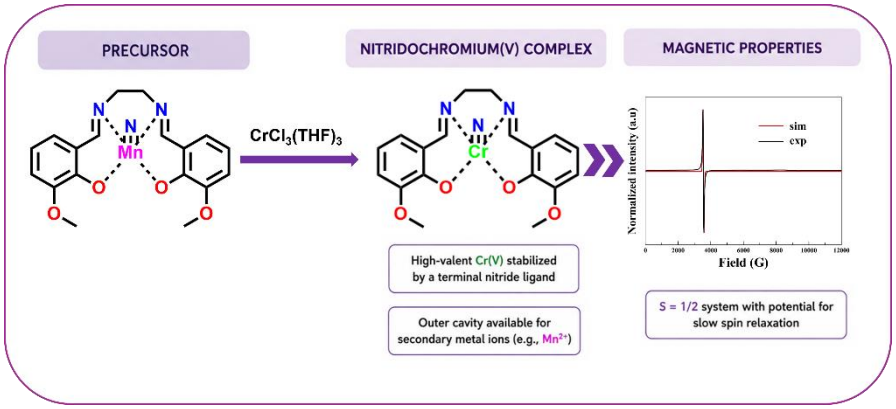

P.40. Mechanochemical synthesis of new Van der Waals nanomaterials based on Lanthanide 2D MOFs

F.Z. BELGHAIT[1], C. SAÑUDO[1,2],

1. Departament de Química Inorgànica i Orgànica, Secció de Química Inorgànica, C/Martí i Franqués 1-11, 08028, Barcelona, Spain

2.Institut de Nanociències i Nanotecnologia, Universitat de Barcelona (IN2UB), 08028 Barcelona, Spain.

Fbelghbe247@alumnes.ub.edu

In the fast-moving world of chemical synthesis, **mechanosynthesis** is stepping into the spotlight as a revolutionary strategy. This method fundamentally reimagines how we trigger chemical changes by swapping out traditional heat or chemical catalysts for **mechanical force** to build sophisticated new materials. **Sustainability at the Core:** By cutting out the need for dangerous solvents and energy-heavy procedures, it paves the way for a greener, more resource-conscious future. **Simplified Efficiency:** The use of straightforward techniques allows for more efficient production while unlocking entirely new chemical frontiers. **A Paradigm Shift:** More than just a trend, mechanosynthesis represents a serious move toward redefining the limits of chemistry through environmentally responsible innovation[1-3].

This study aims to obtain MOF Type I using mechanochemistry with the larger lanthanoids with different derivatives of carboxyates acide for studying the Van Dar Waals interaction MOF $[Ln(MeCOO)(RCOO)_2]n$. The materials were successfully assembled under solvent-minimized conditions, highlighting the potential of mechanochemistry as an environmentally friendly alternative to conventional solution-based methods.

The resulting 2D MOFs exhibit structurally organized layered architectures in which weak interlayer interactions promote van der Waals-type stacking, making them promising candidates for the development of low-dimensional functional nanomaterials. Structural and physicochemical characterization confirms the formation of crystalline phases and provides insight into the relationship between lanthanide coordination behaviour and framework assembly.

References:

[1] J. F. Reynes, F. Leon, and F. García, "Mechanochemistry for Organic and Inorganic Synthesis," Oct. 02, 2024, *American Chemical Society*.

[2] M. M. Mokhtar, T. Heppler, and J. Mack, "Mechanochemically mediated electrosynthesis: unveiling a new pathway for redox reactions under mechanochemical conditions," *Green Chemistry*, vol. 27, no. 34, pp. 10106–10116, Aug. 2025.

[3] N. Fantozzi, J. N. Volle, A. Porcheddu, D. Virieux, F. García, and E. Colacino, "Green metrics in mechanochemistry," Sep. 11, 2023, *Royal Society of Chemistry*.

P.41. PHONON-MEDIATED RELAXATION AND MODE-SPECIFIC MAGNETOELASTIC COUPLING IN YIG/GGG ACOUSTIC CAVITY

P. Cerrato-Serrano[1,2], C. López-Arenas Rovira[1], M. Batalla-Estrada[1], A. García-Santiago[1,2], J. M. Hernàndez[1,2], M. V. Costache[1,2]

[1]Departament de Física de la Matèria Condensada, Universitat de Barcelona (UB)
[2]Institut de Nanociència i Nanotecnologia (IN2UB), Universitat de Barcelona (UB)

pablo.cerrato@ub.edu

The damping of magnons (spin excitations within a crystal lattice) is a critical parameter in magnetism, as it dictates spin precession coherence and magnon lifetimes. Low damping is a prerequisite for modern magnonic applications, ranging from the exploration of novel states of matter [1] to the development of hybrid systems and high-sensitivity sensors [2]. Consequently, identifying and controlling damping mechanisms is essential for advancing these technologies.

In this work, we investigate the influence of phonon-mediated relaxation on magnon damping in a series of four Yttrium Iron Garnet (YIG) thin films of varying thicknesses grown on Gadolinium Gallium Garnet (GGG) substrates.

We demonstrate that due to the strong magnetoelastic coupling in YIG, the double-polished GGG substrate functions as an acoustic Fabry-Pérot cavity. This mechanical confinement allows phonons at resonant frequencies to couple intensely with the film's magnetization. This interaction manifests as both enhanced magnetic damping and a distinct frequency shift in the magnon resonance. Notably, our results reveal that these resonant phonons significantly alter magnon dynamics even when their discrete signatures remain invisible in the Ferromagnetic Resonance (FMR) transmission spectrum. We provide a systematic characterization of these damping and shift effects as a function of the external magnetic field and YIG layer thickness, offering insights into the limits of coherence in magnetoelastic systems.

[1] A. Rückriegel and P. Kopietz, Phys. Rev. Lett., 115, 157203 (2015).

[2] J-Y. Han, Z-P. Tian, Y-D. Cheng, H-B. Huang, X-L. Zhou, W-H. Wu, Y. Zhou and Q-L. Wang, J. Phys. B, 57, 025501 (2024).

P.42. POLARIZATION-DEPENDENT SURFACE LATTICE RESONANCES IN PLASMONIC BAR-DIMER CHAINS

Beñat Albizbeaskoetxea[1,2], A. I. Figueroa[1,2], X. Batlle[1,2], A. Labarta,[1,2] A. Fraile Rodríguez[1,2]

[1]Departament de Física de la Matèria Condensada, Universitat de Barcelona

[2]Institut de Nanociència i Nanotecnologia (IN2UB), Universitat de Barcelona

(balbizbeaskoetxea@ub.edu)

Plasmonic nanosystems are relevant not only for their fundamental properties but also for out of equilibrium phenomena, such as hot carrier generation at metal–insulator interfaces, symmetry breaking, geometric frustration, and chirality, and they have recently emerged as promising topological photonic platforms [1]. In this work, we design and optimize 1D plasmonic lattices, in which the unit nanostructure is composed of two bars, tilted toward each other and separated by a gap. This system exhibits hybrid dark/bright excitation modes that depend on the polarization of the incident radiation. The dark component leads to a relatively strong, high-Q absorption feature, which we enhance by spectrally separating the broader mode from the narrower absorption resonance.

The distance between unit cells (i.e. the lattice pitch) in the chain tunes the excitation of the surface lattice resonance (SLR), a hybrid mode of localized surface plasmons and lattice diffraction orders. The combination of SLRs with the dark high Q resonance yields narrow, tunable modes suitable for applications such as refractive index sensing [2], enhanced lasing [3], and selective light harvesting [4]. We optimize the unit structure through extensive FDTD simulations of the absorption, scattering, and near-field maps, first sweeping the bar length, gap, and tilt angle within the unit dimer (Fig. 1(a)), under perpendicular excitation linearly polarized along the X and Y axes. We then incorporate a metal-insulator-metal (MIM) configuration and vary the spacer thickness to tune the coupling within the cavity and thereby enhance light absorption at the relevant resonance. Finally, we introduce periodicity along the X direction and simulate the chain structure, varying the lattice pitch a to study the polarization-dependent SLR behavior and its impact on the reflectance and the near-field. As an example, Fig. 1(b) shows reflectance spectra for an optimized geometry, displaying the characteristic Fano lineshape associated with the hybridization of the SLR mode and the localized plasmon resonance of the bar dimer. The corresponding near field maps in Fig. 1(c) reveal a higher excitation of the bar dimer for X-polarization at the SLR wavelength due to the larger dipole moment induced along the chain axis.

References:

[1] Marie S. Rider, et al. ACS Photonics 9 (5), 1483 (2022) [2] J. Rodríguez-Álvarez, et al, Nanomaterials 11, 1217 (2021). [3] Zhou, W. et al. Nature Nanotech 8, 506–511 (2013). [4] Mandal, P. Plasmonics, 17, 1247 (2022)

Fig. 1. (a) Geometry of the tilted-bar plasmonic dimer with key parameters (top) and schematic of the plasmonic chain in a MIM configuration (bottom). (b) Simulated reflectance spectra (curves vertically shifted for clarity) for selected lattice pitches on a MIM stack with a 100 nm spacer, under X- (top) and Y-polarized (bottom) excitation. (c) Near-field intensity for both polarizations, evaluated at the SLR wavelength for a pitch of 1400 nm.

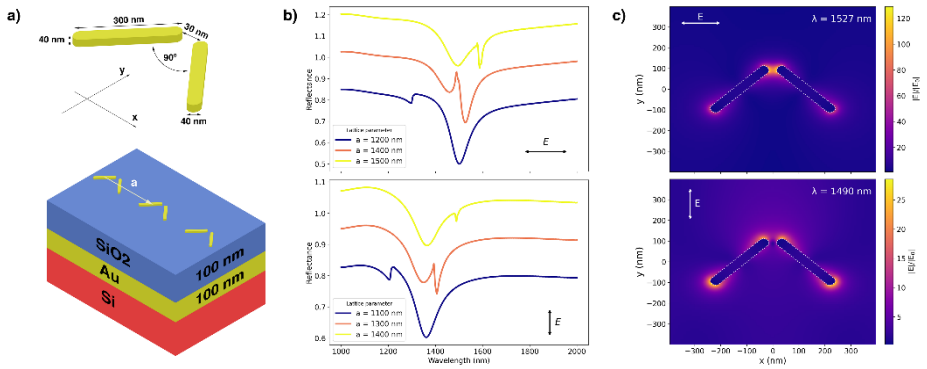

P.44. Fe_3O_4 NPs IN FENTON-LIKE DYE DEGRADATION: LINKING STRUCTURE TO CATALYTIC PERFORMANCE

C. Moya[1,2*], J. Ara[1,3], J. A. Ruiz[1,3], A. Labarta[1,3], X. Batlle[1,3]

[1]Institut de Nanociència i Nanotecnologia (IN2UB), Universitat de Barcelona, 08028 Barcelona, Spain
[2]Departament de Química Inorgànica i Orgànica, C/ Martí i Franquès 1–11, 1era planta, 08028 Barcelona, Spain
[3]Departament de Física de la Matèria Condensada, Universitat de Barcelona, Martí i Franquès 1, 08028 Barcelona, Spain
carlosmoyaalvarez@ub.edu

The removal of organic dyes from wastewater remains an important environmental challenge due to their high chemical stability and widespread industrial use [1,2]. In this context, magnetite nanoparticles (Fe_3O_4 NPs) have attracted considerable attention as catalysts for Fenton-like processes because of their ability to generate highly reactive oxygen species for pollutant degradation (see Figure 1). However, the performance of Fe_3O_4-based catalysts strongly depends on multiple interconnected factors, including iron speciation, active-site accessibility, surface interactions, and reaction conditions [3, 4].

This work provides a critical analysis of Fe_3O_4-based Fenton-like systems, with emphasis on how structural features, surface engineering strategies, and reaction conditions determine catalytic performance. This analysis is supported by the discussion of representative Fe_3O_4-based materials reported over the past decade, enabling the identification of key trends and design principles. Key factors examined the role of Fe^{2+}/Fe^{3+} ratios, morphology, surface functionalization, porous supports, and hybrid systems, as well as to the influence of pollutant properties on catalyst–interface interactions. By establishing structure–condition–performance relationships, this work aims to guide the rational design of efficient and practical Fe_3O_4-based catalysts for water remediation.

Special emphasis is placed on environmentally relevant operating conditions, including near-neutral pH, low oxidant concentrations, visible-light activation, and realistic water matrices. In addition, catalyst stability, iron leaching, magnetic recoverability, scalability, and the use of low-cost or waste-derived materials are considered as key parameters for practical implementation.

Overall, Fe_3O_4-based Fenton-like catalysts represent a versatile platform for water remediation. This analysis highlights the importance of establishing structure–performance relationships and standardized evaluation protocols to support the development of efficient and scalable catalytic systems.

References

[1] Firmansyah, M.; et al. Sep. Purif. Technol. 2025, ***360***, 131111.
[2] Swaminathan, P.; et al. Sustainable Chem. Environ. 2024, ***8***, 100171.
[3] Machado, F.; et al. Int. J. Environ. Sci. Technol. 2023, ***20*** (12), 13995–14032.
[4] Ribeiro, J.; et al. Catalysts 2024, ***14*** (9),1-18.

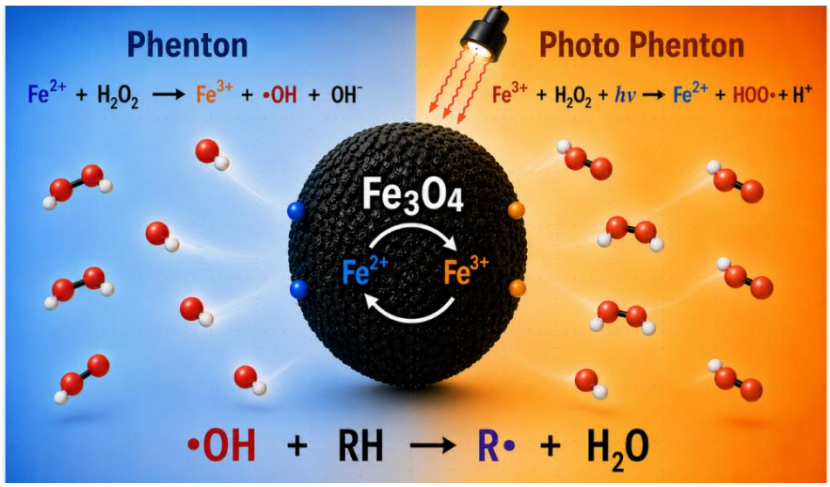

Figure 1. Schematic illustration of the Fenton and photo-Fenton processes on Fe_3O_4 NPs. Fe^{2+}/Fe^{3+} redox cycling promotes reactive radical generation for dye degradation.

P.44. TOPOLOGICAL MAGNETIC TEXTURES IN THREE-DIMENSIONAL IRON OXIDE NANOFLOWERS

A. I. Figueroa,[1,2] R. Ferrer Santos,[1] J. M. Pérez Zegarra,[1] A. E. Herguedas Alonso,[3,4,5] A. Hierro Rodríguez, [4,5] J. A. Ruiz-Torres[1,2], C. Moya,[1,2] L. Aballe,[3] C. Fernández,[3] M. Puerto Morales,[6] A. Labarta,[1,2] X. Batlle[1,2], and A. Fraile Rodríguez[1,2]

[1]Departament de Física de la Matèria Condensada, Universitat de Barcelona, 08028 Barcelona, Spain
[2]Institut de Nanociència i Nanotecnologia (IN2UB), Universitat de Barcelona, 08028 Barcelona, Spain
[3]ALBA Synchrotron Light Facility, CELLS, 08290 Barcelona, Spain
[4]Departamento de Física, Universidad de Oviedo, 33007 Oviedo, Spain
[5]CINN (CSIC – Universidad de Oviedo), 33940 El Entrego, Spain
[6]Department of Nanoscience and Nanotechnology, Instituto de Ciencia de Materiales de Madrid (ICMM-CSIC), 28049 Madrid, Spain

aifigueroa@ub.edu

Magnetic iron oxide nanoflowers (IONFs) are excellent candidates for biomedical and environmental applications due to their superior performance compared to single-core magnetic nanoparticles [1]. Previous studies have shown that, despite their relatively large size, IONFs exhibit nearly zero remanence and coercivity while maintaining high saturation magnetization [2]. Their internal crystalline texture stabilizes magnetic vortices via dipolar interactions and inter-core exchange coupling, yielding a super-ferromagnetic state of the entire aggregate [2,3,4]. Yet a 3D spatial mapping of these internal magnetic textures has remained elusive. In this work, we present a deep characterization of the 3D magnetization textures within individual 200 nm IONFs to bridge the gap between crystalline correlations and macroscopic magnetic response. Using tomographic reconstructions from synchrotron-based transmission X-ray microscopy with X-ray magnetic circular dichroism contrast, we resolved the internal magnetization arrangement of a series of individual particles, providing robust statistics. Our analysis reveals distinct families of magnetic textures, classified by the morphology of their magnetization streamlines. We show that these textures are governed by magnetic vorticity, which enables the nearly demagnetized remanent state observed experimentally. Among 33 analyzed IONFs, about 42 % exhibit a topological charge of Q = 0 (vortices) and 58% host $Q \approx \pm 0.5$ (meron-like tubes). Occasional point singularities with larger topological charge ($Q > \pm 0.5$) were identified in a few particles (<5 %). Electron tomography of the same individual IONFs at ELECMI indicates that these textures are influenced by the particles' internal morphology, with some particles being nanoporous and others more compact. This study provides fundamental insight into the topological complexity of 3D nanostructured magnets and establishes a framework for tailoring the magnetic performance of IONFs through textural engineering.

[1] Batlle, X. et al. JMMM. **543**, 168594 (2022). [2] Moya, C. et. al. Nanoscale, **16**, 1942-1951 (2024). [3] Bender, P. et al. J. Phys. Chem C. **122**, 3068 (2018). [4] Jefremovas, E. M., et al. Small Sci., 6, e202500490 (2026).

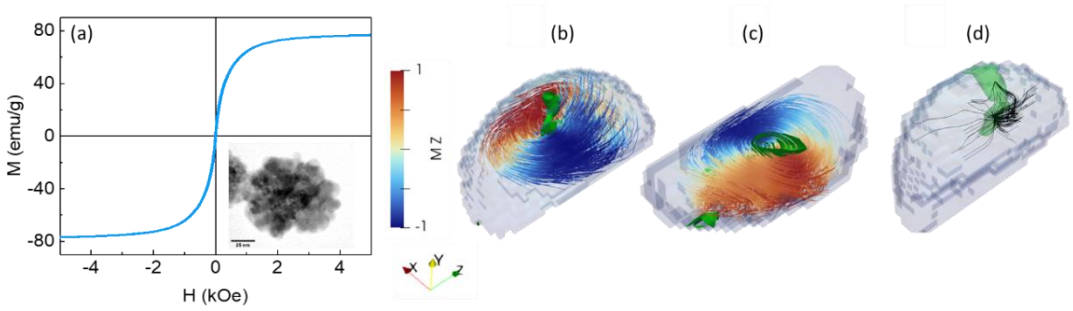

Figure 1: (a) Effective superferromagnetic behavior in IONF. Inset: high-resolution transmission electron microscopy image of an IONF forming a multicore, petal-like nanostructure. Representative examples of 3D magnetic textures identified: (b) vortices, $Q \approx 0$ (42 %) and (c) non-trivial textures, $Q \approx \pm 0.5$ (58 %). Colored lines represent magnetization streamlines, and green isosurfaces correspond to high-vorticity regions. The emergent field emanating from a point singularity in occasional IONFs is depicted in (d).

P.45. The coupling of ferroelectric polarization and oxygen vacancy migration enables electrically controlled thermal memories.

Dídac Barneo[1,2], Miquel Royo[3], Rafael Ramos[4,5], Jesús Carrete[6], Hugo Romero-Bernad[6], Ricardo Jiménez[7], Víctor Leborán[4], César Magén[6,8], Noa Varela-Domínguez[4,5], Miguel Algueró[7], Riccardo Rurali[3], José A. Pardo[6,9,10], Francisco Rivadulla[4,5], Eric Langenberg[1,2,*]

[1]Departament de Física de la Matèria Condensada, Universitat de Barcelona, 08028 Barcelona, Spain. [2]Institut de Nanociència i Nanotecnologia (IN²UB), Universitat de Barcelona, 08028 Barcelona, Spain. [3]Institut de Ciència de Materials de Barcelona, ICMAB-CSIC, Campus UAB, 08193 Bellaterra, Spain, [4]Centro Singular en Química Biolóxica e Materiais Moleculares (CiQUS), Universidade de Santiago de Compostela, 15782 Santiago de Compostela, Spain. [5]Departamento de Química-Física, Universidade de Santiago de Compostela, 15782-Santiago de Compostela, Spain. [6]Instituto de Nanociencia y Materiales de Aragón (INMA), CSIC-Universidad de Zaragoza, 50009 Zaragoza, Spain. [7]Instituto de Ciencia de Materiales de Madrid (CSIC), 28049 Madrid, Spain. [8]Departamento de Física de la Materia Condensada, Universidad de Zaragoza, 50018 Zaragoza, Spain. [9]Departamento de Ciencia y Tecnología de Materiales y Fluidos, Universidad de Zaragoza, 50018 Zaragoza, Spain. [10]Laboratorio de Microscopías Avanzadas, Universidad de Zaragoza, Campus Río Ebro, 50018 Zaragoza, Spain

eric.langenberg@ub.edu

The coupling between electric, ionic, and thermal phenomena in functional oxides offers new opportunities for active control of heat transport in solid-state devices. These devices, based on opening and closing thermal current pathways, enable the active route of thermal energy on demand, which is critical for applications such as thermal energy storage and management, solid-state refrigeration -and thermal regulation- technologies, thermoelectric systems for energy harvesting, or even storing and processing information via heat currents. In this work [1], we demonstrate electrically controlled and non-volatile thermal conductivity (κ) switching in epitaxial ferroelectric $Hf_{0.5}Zr_{0.5}O_2$ thin films, positioning hafnia-based oxides as promising platforms for thermal memories and multifunctional thermal devices. Using frequency-domain thermoreflectance (FDTR) measurements under applied electric fields, we show that the cross-plane κ of metal/$Hf_{0.5}Zr_{0.5}O_2$/Y_2O_3:ZrO_2 heterostructures exhibits a pronounced hysteretic dependence on the electric field. This behavior enables two distinct and non-volatile thermal states, corresponding to high (ON) and low (OFF) thermal conductivity, which remain stable after removal of the external stimulus. The κ_{ON}/κ_{OFF} ratio we report is of approximately 1.6, and switching between states can be achieved using voltages below ±5 V, compatible with thin-film device integration. The observed κ hysteresis closely correlates with the ferroelectric coercive fields of $Hf_{0.5}Zr_{0.5}O_2$, revealing a connection between polarization and heat transport. Structural analysis confirms that the ferroelectric orthorhombic phase is preserved in both thermal states, excluding electric-field-induced phase transitions as the operating mechanism. Instead, we identify the dominant process as the electrically driven migration of oxygen vacancies, which act as highly efficient phonon scattering centers. Ferroelectric polarization creates an electrostatic barrier that controls the redistribution and retention of these vacancies, stabilizing non-equilibrium defect configurations and enabling a non-volatile thermal response. Both κ_{ON} and κ_{OFF} states show excellent temporal stability over several days at room temperature, indicating a strong suppression of vacancy back-diffusion in the absence of an applied field. While the thermal switching speed is limited by ionic transport in the solid electrolyte electrode, the robustness, reversibility, and low operating voltages highlight the technological relevance of this approach.

References: [1] D. Barneo et al. Adv. Materials **38**, e19670 (2026)

P.46. Site-Dependent Lanthanide Anisotropy in Rigid Polyoxometalate Frameworks Governs Single-Molecule Magnet Relaxation

Abir Dhaou,[1,2*] Jesús Jover,[1,3] Sonia Abid,[2] E. Carolina Sañudo[1,4]

[1] Departament de Química Inorgànica i Orgànica, Secció de Química Inorgànica, Universitat de Barcelona, Av.Diagonal 645, 08028 Barcelona, Spain

[2] University of Carthage, Faculty of Sciences of Bizerte, LR13ES08, Laboratory of Chemical Materials, 7021, Bizerte, Tunisia.

[4] Química Física and Institut de Química Teòrica i Computacional (IQTCUB), Universitat de Barcelona, Martí i Franqués 1, 08028 Barcelona Spain

[4] Institut de Nanociència i Nanotecnología, Universitat de Barcelona (IN2UB), C/Martí i Franques 1-11, Barcelona, 08028, Spain

abir.dhaou@ub.edu

Controlling magnetic anisotropy in lanthanide systems remains a key challenge for the development of high-performance single-molecule magnets (SMMs). Here, we report a polyoxometalate (POM)-based approach to organize 4f ions within rigid coordination frameworks that directly influence magnetic relaxation. A series of lanthanide POM coordination polymers (1Gd, 2Tb, 2Dy, and 2Er) was synthesized, featuring square-antiprismatic environments around the metal centers. Magnetic measurements indicate that all compounds behave as magnetically isolated lanthanide systems due to large Ln···Ln separations.

While Gd(III) and Tb(III) derivatives show paramagnetic behavior, Dy(III) and Er(III) compounds exhibit slow relaxation of magnetization. In particular, 2Dy displays complex multi-channel relaxation arising from two crystallographically inequivalent Dy(III) sites. Ab initio calculations reveal strong axial anisotropy and reduced quantum tunneling, explaining the observed dynamics. In contrast, 2Er exhibits field-induced SMM behavior associated with weaker anisotropy.

These findings highlight the crucial role of site-dependent anisotropy in tuning magnetic relaxation and provide insights for the rational design of lanthanide-based SMMs.

P.47. Synthesis, Structural Elucidation, Magnetic Behavior, and DFT Investigation of a Copper Cyclohexaphosphate Framework with Molecular Docking Insights

Chaima Arfa,[a,b] Sonia Abid, [b] E. Carolina Sañudo [a,c]

[a] Departament de Química Inorgànica i Orgànica, Secció de Química Inorgànica, Universitat de Barcelona, Av.Diagonal 645, 08028 Barcelona, Spain
[b] University of Carthage, Faculty of Sciences of Bizerte, LR13ES08, Laboratory of Chemical Materials, 7021, Bizerte, Tunisia.
[c] Institut de Nanociència i Nanotecnología, Universitat de Barcelona (IN2UB), C/Martí i Franques 1-11, Barcelona, 08028, Spain

arfaarfachaima@ub.edu

Abstract

Metal phosphates represent a versatile class of inorganic materials with rich structural diversity and promising functional properties [1]. Among them, cyclohexaphosphates stand out due to their high thermal and hydrolytic stability, as well as their strong ability to coordinate metal centers [2].

In this work, we report the synthesis and comprehensive characterization of a novel copper cyclohexaphosphate compound. The crystal structure, determined by single-crystal X-ray diffraction, reveals that cyclohexaphosphate ring anions are interconnected with copper coordination polyhedra via Cu–O–P bridges, forming extended one-dimensional ribbon-like architectures.

Spectroscopic analysis using infrared measurements confirmed the characteristic vibrational modes of the phosphate groups. The optical behavior was examined through fluorescence studies, indicating potential photoactive properties. Magnetic measurements revealed the presence of significant magnetic interactions, highlighting the role of copper centers in governing the compound's magnetic behavior.

To further understand its electronic features, density functional theory calculations were performed, providing insights into the electronic structure, HOMO–LUMO energy gap, density of states, and nonlinear optical properties. Additionally, molecular docking studies were carried out to evaluate possible interactions with biological targets, suggesting potential relevance in bioactive applications.

Overall, this study demonstrates that the synthesized copper cyclohexaphosphate combines structural complexity with multifunctional properties, making it a promising candidate for applications in materials science and related fields.

Keywords

Copper-cyclohexaphosphate; X-ray diffraction; Hirshfeld surface; DFT, density of states (DOS), magnetic measurements.

Reference

[1] Rosario M. P. Colodrero, Pascual Olivera-Pastor, Aurelio Cabeza and Montse Bazaga-García, Materials.,15(2022)1292.

[2] U. Schülke, R. Kayser, Zur thermischen Dehydratisierung von Lithiumdihydrogen phosphat, -hydrogendiphosphat und -cyclophosphat-Hydraten, Z. Anorg. Allg. Chem. 531(1985)167–176.

P.48. METALLOPORPHYRINS AS BUILDING BLOCKS FOR MOLECULAR MULTIQUBIT ARCHITECTURES.

J. Torrent[1], A. de Juan[2], D. Gonzalez-Rodríguez[2], V. Novikov[1], A. Escuer[1], J. Mayans[1]

[1]Departament de Química Inorgànica i Orgànica, Secció Inorgànica and Institute of Nanoscience and Nanotecnology, Universitat de Barcelona, Barcelona 08028, Spain

[2]Nanostructured Molecular Systems and Materials group, Organic Chemistry Department, Universidad Autónoma de Madrid, Madrid 28049, Spain; Institute for Advanced Research in Chemical Sciences (IAdChem), Universidad Autónoma de Madrid, Madrid 28049, Spain;

joan.torrent@ub.edu

The implementation of highly coherent molecular spin quantum bits into the field of quantum information science is one of the main challenges the field of molecular magnetism is currently facing. Tackling this challenge involves the integration of single molecule qubits into multiqubit systems. In such a context, metalloporphyrins stand out as excellent building blocks due to both their long coherence times[1] and chemical tunability[2], the latter allowing their scaling up from single metalloporphyrin units into multiqubit architectures[3]. To achieve this, this work explores two different directions: (i) The integration of metalloporphyrins into metal-organic frameworks (MOFs) featuring lanthanide ions (Fig. 1a), and (ii) the design of cofacial bisporphyrin cages[4] with guest binding capabilities (Fig. 1b,c). In the first approach, the MOF scaffold allows embedding metalloporphyrin units in a rigid and controlled environment. Furthermore, the presence of lanthanides allows the inclusion of a second qubit unit into the system. In the second, the bisporphyrin cage allows the precise control of qubit-qubit distances, as well as the inclusion of guests into the cage, which has been shown to enhance the qubit performance of the cage. The spin dynamics of these systems have been studied by means of SQUID magnetometry (Fig. 1d) and pulse EPR spectroscopy (Fig. 1e,f), which reveals the presence of quantum coherence for both lanthanide and metalloporphyrin moieties in both MOF and cage environments. Furthermore, the inclusion of a fullerene guest into the cage results in a significant increase of the qubit coherence lifetime. These results highlight the potential of metalloporphyrin-based qubits as platforms to achieve potential multiqubit systems.

References: [1] *Chem. Sci.,* 2019, **10**, 1702-1708. [2] *J. Am. Chem. Soc.,* 2018, **140**, 12090-12101. [3] *J. Am. Chem. Soc.,* 2026, **148**, 10408-10420. [4] *J. Am. Chem. Soc.,* 2025, **147**, 918-931.

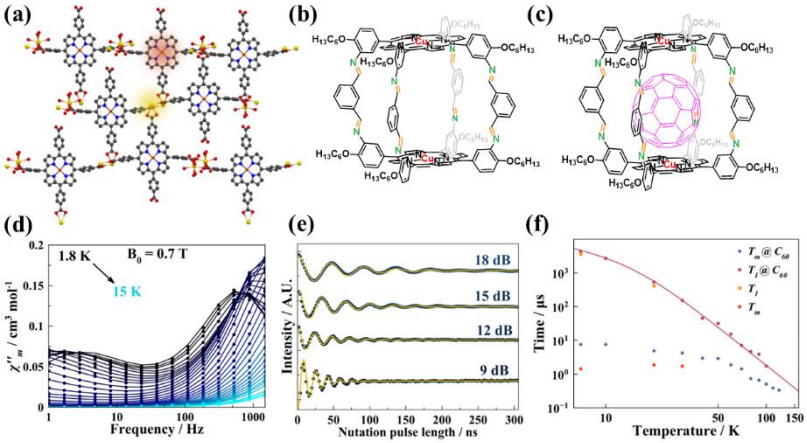

Figure 1: (a) Lanthanide-metalloporphyrin MOFs present in this work. **(b)** Cu^{II} bisporhyrin cage, and its capability to act as a host to guests such as fullerenes **(c)**. **(d)** Lanthanide metalloporphyrin MOFs AC SQUID magnetometry measurements. **(e)** and **(f)** Results from pulse EPR measurements on the aforementioned systems.

P.49. High-Sensitivity Characterization of Magnetic Dynamics via Cylindrical Cavity Ferromagnetic Resonance

B. Segret [a], Pablo Cerrato-Serrano,[a,b] Antoni García-Santiago,[a,b] Joan Manel Hernàndez, [a,b] Marius V. Costache, [a,b]

[a] Department of Condensed Matter Physics, University of Barcelona (UB)
[b]Institut de Nanociència i Nanotecnologia (IN2UB), Universitat de Barcelona (UB)
Universitat de Barcelona

bsegrebr7@alumnes.ub.edu

We explore ferromagnetic resonance (FMR) utilizing an electromagnetic cavity as an alternative to conventional broadband coplanar waveguides. By confining the microwave field, the resonant cavity enhances sensitivity and enables high-resolution probing of magnetic dynamics. This work investigates cavity–spin interactions, performs resonance measurements, and analyzes linewidths and mode structures to refine techniques for the characterization of ferromagnetic materials. The study began by characterizing the eigenmodes of a cylindrical copper cavity (radius: 1 cm, variable height) across a frequency range of 5 GHz to 25 GHz. Absorption was observed at discrete resonant frequencies, with the fundamental mode identified near 9 GHz. Due to the cavity geometry and the spatial distribution of the microwave magnetic field, specific modes were selected for FMR measurements based on their coupling efficiency to the sample and the measurement circuit. Two materials were investigated: a 5 µm-thick yttrium iron garnet (YIG) film grown on a gadolinium gallium garnet (GGG) substrate, and a disk-shaped ferrite sample. The YIG film exhibited sharp, well-defined resonances with narrow linewidths, indicative of low magnetic damping, while the ferrite sample displayed broader resonance characteristics.

An external static magnetic field, modulated via Helmholtz coils, was applied to tune the system into resonance. At the resonance condition, the cavity response was modified as the resonator mode hybridized with the magnetic excitations. The resulting spectra are analogous to the frequency response of two coupled harmonic oscillators.

Preliminary results underscore the efficacy of cavity-based FMR for studying low-loss magnetic systems. While shifts in the cavity resonance frequency have been successfully quantified, detailed analysis of the resonance linewidths and intrinsic magnetic parameters is currently ongoing. These findings demonstrate the high sensitivity of resonant cavities for advanced magnetic materials characterization. Examples of the measured data can be seen in figures 1 and 2.

Figure 1

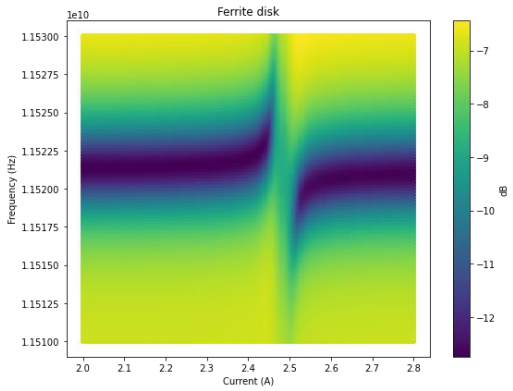

Figure 2

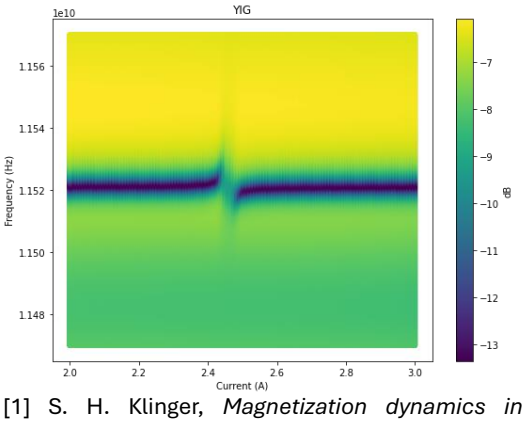

[1] S. H. Klinger, *Magnetization dynamics in coupled magnetic Systems*. [2] A. Blais, *Circuit Quantum Electrodynamics*. [3] B. Bhoi et al, *Study of photon-magnon coupling in a YIG-film split-ring resonant system*

P.50. COHERENCE OF TWO Ce(III) QUBITS EMBEDED IN [LuCeLu] ASSEMBLIES

José Serrano-Guarinos [ab], Zahra Hosseinzadeh [ab], Abinash Swain [ab], David Aguilà [ab], Leoní A. Barrios [ab], Yulia Nelyubina [c], Olivier Roubeau [d], Valentin Novikov [ab], Guillem Aromí [ab]

[a]Department of Inorganic and Organic Chemistry, University of Barcelona, Barcelona, Spain.
[b]Insitute of Nanotecnology and Nanocience (IN2UB), Universitat de Barcelona, Barcelona, Spain.
[c]Nesmeyanov Institute of Organoelemtns, Russian Academy of Sciences, Moscow, Russia.
[d]Insitute of nanoscience and materials of Aragon (INMA), CSIC – University or Zaragoza, Zaragoza, Spain.

jose.serranog@ub.edu

Spin states in molecular systems constitute a promising platform for the physical implementation of qubits and quantum logic gates within emerging quantum technologies. This approach benefits from the versatility of chemical design, which enables atomistic control over key magnetic and electronic properties while ensuring high structural reproducibility across identical molecular units. Such tunability allows precise engineering of coherence, coupling interactions, and environmental effects that are critical for quantum information processing. [1] Previous work from our research group claimed that a trinuclear molecular complex of composition [ErCeEr] can operate as a platform for implementing a quantum error-correction circuit, highlighting the potential of heterometallic molecular architectures for scalable quantum operations. [2]

In this work, we develop a new synthetic approach towards [LuCeLu] compounds and provide a detailed investigation of the spin dynamics of two cerium(III)-based qubits embedded in a heterometallic molecular assembly of composition [LuCeLu] in solid policrystalline state through magnetization measurements, NMR, and pulsed EPR.

[1] Aromí, G., Aguilà, D., Gamez, P., Luis, F. Roubeau, O. Chem. Soc. Rev. 41, 537–546 (2012).

[2] Macaluso, E. et al. Chem. Sci. 11, 10337–10343 (2020).

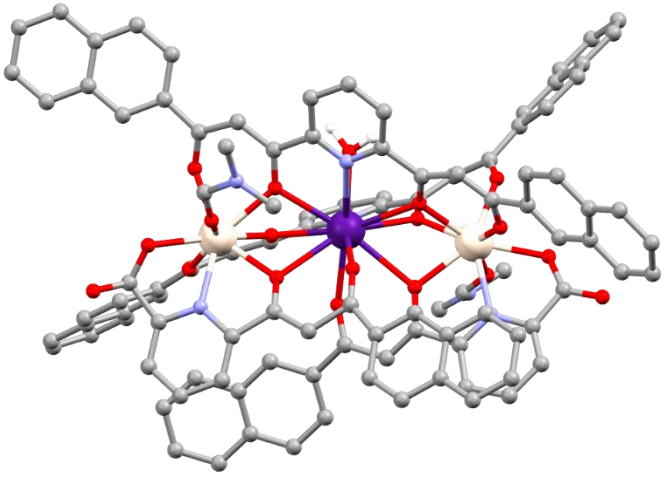

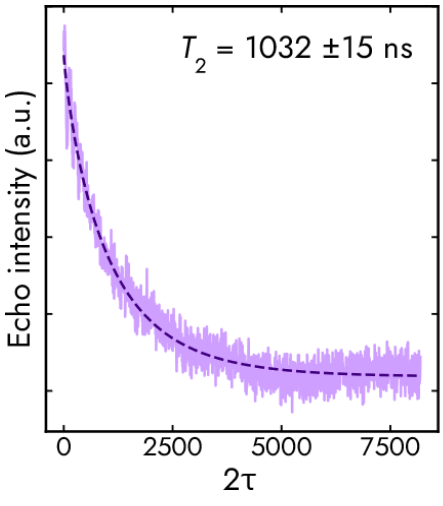

Figure 1: Crystal structure of $[LuCeLu(LA)_2(LB)_2(DMF)_2(H_2O)](NO_3)$ (**[Ce1]**) (left) and stretched exponential fitting of a Hahn echo experiment of **$[Ce_{0.01}1]$** at 4 K.

NanoPhotoElectro

P.51. GUIDED PHOTOLUMINESCENCE SPECTROSCOPY OF 2D MATERIALS INTEGRATED ON SI3N4 WAVEGUIDES

V. Gonzalez-Morote[1], D. Navarro-Urrios[1], A. Gertych[2], M. Zdrojek[2], M. Sledzinska[3]

[1]MIND-IN2UB, University of Barcelona, Spain
[2] Faculty of Physics, Warsaw University of Technology, Poland
[3] Institute of Nanoscience and Nanotechnology (ICN2), Spain
vgonzalezmorote@ub.edu

The family of two-dimensional (2D) transition metal dichalcogenides (TMDs), such as MoS_2 and WS_2, has emerged as a very attractive platform for integrated optoelectronic devices due to their strong excitonic response and efficient interaction with confined optical fields [1,2]. Here, we investigate TMD flakes integrated on Si_3N_4 waveguides using guided photoluminescence as an internal broadband probe of their effective optical absorption. Broadband photoluminescence is generated in the Si_3N_4 waveguide under 405 nm excitation, couples to the guided modes, and propagates through regions covered by the 2D material, where it undergoes wavelength-dependent evanescent absorption.

Figure 1 summarizes the experimental approach and the main results. The interaction mechanism is illustrated in Fig. 1a, while Fig. 1b shows the expected spectral reshaping of the guided PL after propagation through the TMD-covered region. Raman spectroscopy confirms the identity of the investigated MoS_2 and WS_2 flakes through their characteristic vibrational fingerprints (Fig. 1c). In addition, the Raman peak separations extracted from the spectra provide further information on the samples (Fig. 1d): for MoS_2, the separation $\Delta\omega^{MoS_2} = \omega_{A_{1g}} - \omega_{E^1_{2g}}$ shows a broader distribution for the irregular flake than for the smoother one, indicating stronger local thickness variability and reduced homogeneity [3], while for WS_2 the spacing between the A_{1g}peak and the $2LA(M)/E^1_{2g}$feature is included as an additional Raman fingerprint. This structural variability is reflected in the guided optical response: the normalized spectra show distinct effective absorption onsets for MoS_2 and WS_2, with the WS_2-covered waveguide shifted toward higher photon energies, as well as clear differences between the two MoS_2 samples (Fig. 1e). These results demonstrate guided photoluminescence in Si_3N_4 waveguides as a simple on-chip method to probe 2D material optical response under integrated photonic conditions, supporting the development of compact waveguide-integrated photodetectors [2].

References:

[1] K. F. Mak and J. Shan, *Nat. Photonics* **10**, 216–226 (2016). [2] J. F. Gonzalez Marin et al., *npj 2D Mater. Appl.* **3**, 14 (2019). [3] C. Lee et al., *ACS Nano* **4**, 2695–2700 (2010).

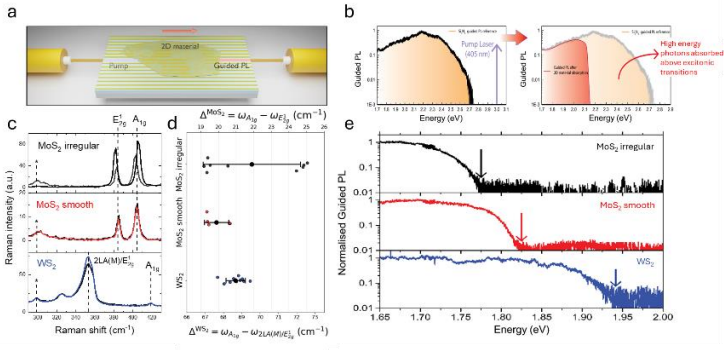

Figure 1. ***Guided photoluminescence spectroscopy of Si_3N_4 waveguides interfaced with MoS_2 and WS_2.*** *(a) Schematic of the interaction mechanism. (b) Conceptual spectral evolution. (c) Representative Raman spectra confirming the identity of MoS_2 and WS_2; the characteristic in-plane $E^1_{2g}$and out-of-plane A_{1g}Raman modes are indicated, while the asterisk marks a substrate-related feature. (d) Raman peak separation for two MoS_2 samples. (e) Normalized guided photoluminescence spectra showing material-dependent effective absorption onsets for MoS_2 and WS_2, as well as differences between smooth and irregular MoS_2 flakes.*

P.52. RGB Mueller Matrix Microscopy: Advantages of Simultaneous Polarimetric Imaging at Three Wavelengths.

Shuang Chen[1], Oriol Arteaga [2]
[1] Dep. Fisica Aplicada, PLAT Group, IN2UB, Universitat de Barcelona
[2] Institute of Nanoscience and Nanotechnology (IN2UB), Universitat de Barcelona

schen@ub.edu

We present an RGB Mueller matrix microscope with a color polarization camera to perform simultaneous polarimetric imaging at three wavelengths. This configuration, shown in Fig. 1, offers three major advantages over conventional monochromatic systems: (i) real-time color visualization before full data acquisition, (ii) simultaneous multispectral retrieval of Mueller matrices enabling improved parameter estimation, and (iii) accurate determination of retardances exceeding π, thus eliminating the phase ambiguity inherent to single-wavelength measurements.

Results obtained from a quarter-wave, a half-wave, and a full-wave plates (Fig. 2) validate the accuracy and robustness. This instrument demonstrates the significant potential for quantitatively investigating the microstructure and mechanical properties of highly birefringent biological sample.

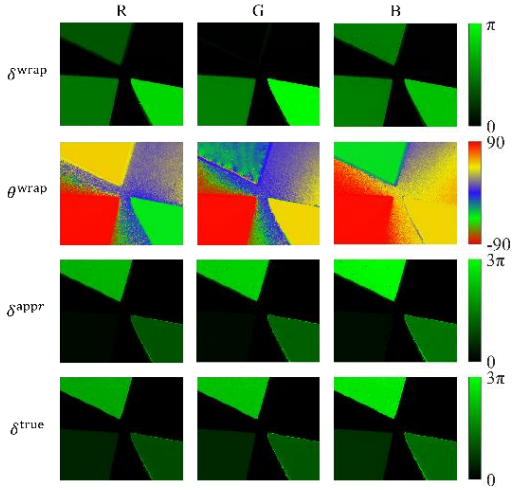

Fig. 2: Comparison of retardances in RGB channels.

References:

[1] Shuang Chen, and Oriol Arteaga. "RGB Mueller matrix microscopy: Advantages of simultaneous polarimetric imaging at three wavelengths." *Optics & Laser Technology* 201 (2026): 115216.

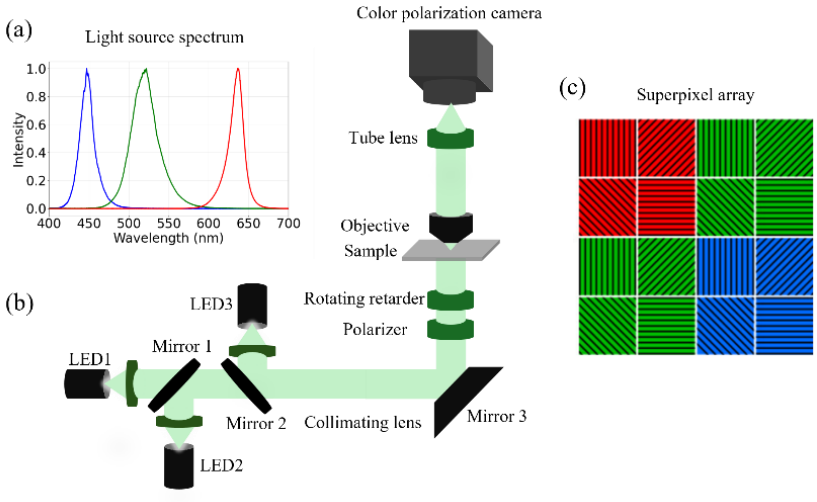

Fig. 1: RGB Mueller Matrix Microscopy [1].

P.53. Chip-Sized Lensless Holographic Microscope for Real-Time Biosensing in Angiogenesis Models

S. Moncada-Madrazo[1,2], S. Moreno[1,2], J. Canals[1,2], O. Caravaca[1,2], N. Castro[3], J.R. Azcón[3,4], A. Vilà[1,2], A. Diéguez[1,2]

[1]Dept. of Electronic and Biomedical Engineering of Universitat de Barcelona,

[2] Institute of Nanoscience and Nanotechnology (IN²UB) of Universitat de Barcelona,

[3]Institute for Bioengineering of Catalonia (IBEC), The Barcelona Institute of Science and Technology (BIST),

[4] Institució Catalana de Recerca i Estudis Avançats (ICREA)

sofia.moncada@ub.edu

Conventional optical microscopes are important tools for biological imaging, but their size, cost, and reliance on complex optical components limit their use in compact and high-throughput experimental platforms. This is especially relevant in emerging bioengineering applications involving microfluidic devices and nano-engineered cell culture systems. In this work, we present a chip-sized lensless digital holographic microscope (CSM) for real-time and label-free optical biosensing [1].

The CSM integrates a CMOS image sensor and an LED microdisplay within a compact 10 × 6 × 3.4 cm aluminum enclosure and operates without lenses, filters, or mechanical alignment. Illumination transmitted through the sample generates holographic interference patterns, which are recorded directly by the CMOS sensor. These holograms are computationally reconstructed using custom backpropagation algorithms with twin-image suppression [2], resulting in high-contrast images of biological structures. The short distance between CMOS and microdisplay enables a compact system and supports the parallel implementation of multiple units for scalable biosensing.

The CSM was used to monitor angiogenic network formation in a HUVEC tube formation assay on Matrigel, which is a standard *in vitro* vascular model [3]. Two experiments were evaluated: a 24 h endpoint assay at different VEGF-165 concentrations (0, 20, 40, and 50 ng/mL), and a continuous time-lapse mode that acquired images every 30 min at 40 ng/mL. The reconstructed holograms were processed with a custom Python pipeline to quantify angiogenesis-related parameters, including total tube length, mean mesh area, and junction count. Continuous monitoring enabled detection of transient vascular dynamics, such as peaks in tube length and junction count, between 0 and 6 h, which are not easily captured by conventional endpoint assays. Figure 1 illustrates the capture process for a sample. Figure 1A shows the control image taken with a conventional inverted microscope, Figure 1B the same sample taken with the CSM, Figure 1C the annotated image, and Figure 1D the analyzed image.

The CSM represents a compact, low-cost optical biosensing platform for continuous *in vitro* biological monitoring. Its scalable architecture may facilitate future integration with microfluidic and nano-engineered cell culture platforms, opening possibilities for applications such as real-time monitoring of cellular responses to nanoparticles, nanotoxicology screening, and vascularization studies in organ-on-chip systems.

References

[1] Moncada-Madrazo, S. et al. In-incubator continuous and endpoint monitoring of angiogenesis using a chip-sized holographic microscope. *Biosens. Bioelectron.* 303, 118579 (2026). doi: 10.1016/j.bios.2026.118579

[2] Latychevskaia, T.; Fink, H.-W. Practical algorithms for simulation and reconstruction of digital in-line holograms. *Appl. Opt.* 54, 2424 (2015). doi: 10.1364/AO.54.002424

[3] Staton, C.A.; Reed, M.W.R.; Brown, N.J. Current methods for assaying angiogenesis in vitro and in vivo. *Int. J. Exp. Pathol.* 90, 195–221 (2009). doi: 10.1111/j.1365-2613.2008.00633.x.

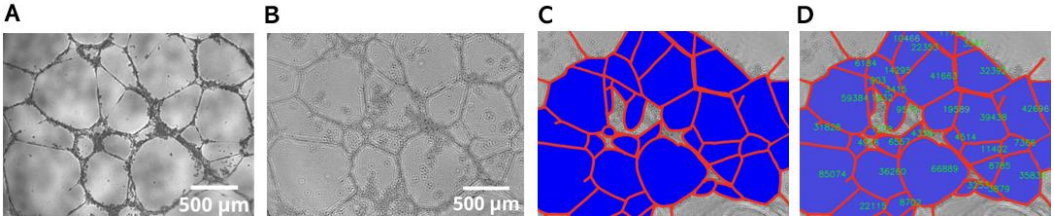

Fig. 1. Representative images from the CSM analysis pipeline: (A) control sample imaged with a conventional inverted microscope, (B) same sample imaged with the CSM, (C) annotated image with meshes (blue) and tubes (red), and (D) quantified areas of meshes (green).

P.54. DEPTH SENSIBLE INSTRUMENT FOR MUELLER MATRIX IMAGING

I.Pardo[1], E. Pascual[1], O. Arteaga[1]

[1]PLAT group, Dep. Física Aplicada, IN2UB, Universitat de Barcelona

iago.pardo@ub.edu

We introduce an optical imaging system that combines Spatial Frequency Domain Imaging (SFDI) with Mueller Matrix polarimetry to achieve depth-resolved, polarization-sensitive characterization of turbid media. This system enables the acquisition of Mueller matrices at multiple spatial frequencies, probing different optical depths within the sample.

Mueller Matrix imaging provides a comprehensive description of the polarization properties of light after interaction with a sample, encoding information on anisotropy, birefringence, depolarization, and structural orientation [1]. When combined with SFDI, which projects sinusoidal patterns of varying spatial frequencies onto the sample, it becomes possible to selectively modulate photon penetration depth [2]. Low spatial frequencies probe deeper layers due to broader photon diffusion, while high frequencies restrict the light–tissue interaction to more superficial structures.

This approach allows for the separation of polarization phenomena that may originate at different depths, revealing layered structures or subtle changes in tissue organization not detectable by conventional polarization imaging.

This method opens new possibilities in some fields such as biomedical optics, especially for non-invasive assessment of layered biological tissues such as skin, where birefringent and depolarizing behaviors can vary significantly with depth [3].

References:

[1] Chipman, R. A., Lam, W. S. T., & Young, G. P. (2018). *Polarized Light and Optical Systems*. CRC Press. [2] Cuccia, D. J., Bevilacqua, F., Durkin, A. J., & Tromberg, B. J. (2009). Quantitation and mapping of tissue optical properties using modulated imaging. *Journal of Biomedical Optics*, 14(2), 024012. [3] Pierangelo, A., et al. (2012). Ex vivo characterization of human colon cancer by Mueller polarimetric imaging. *Optics Express*, 19(2), 1582–1593.

Fig 1: Measurement of a chicken breast sample using different spatial frequencies and analysis of Mueller Matrix elements as a function of penetration depth.

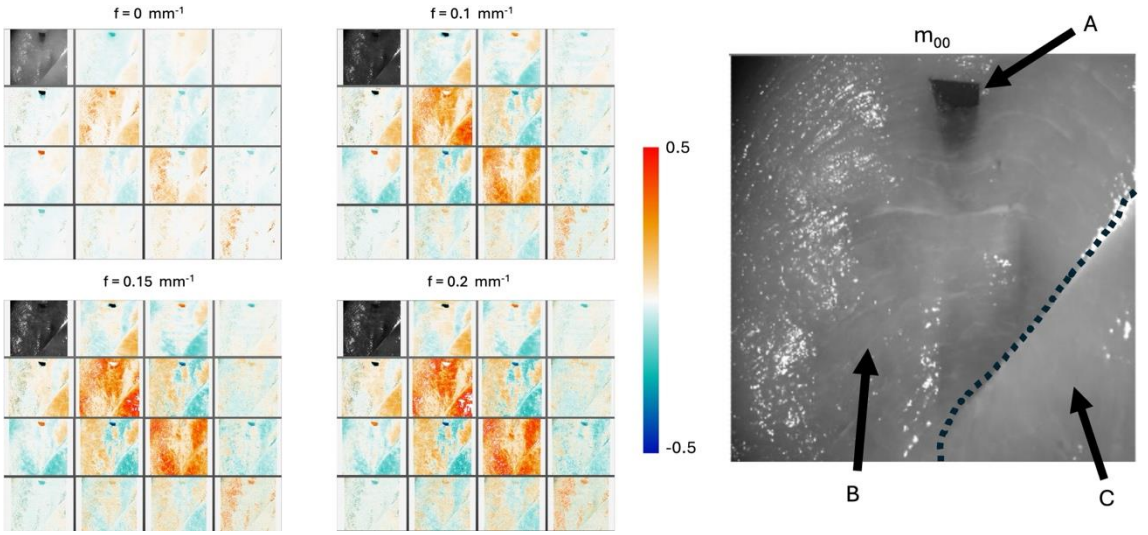

P.55. High Dynamic Range enhancement in Mueller matrix polarimetry

Lourdes Camblor-Navarro[1,2], Iago Pardo[1,2], Oriol Arteaga [1,2]

[1]Dep. Física Aplicada, PLAT group, Universitat de Barcelona, Barcelona, 08028, Spain
[2]Institute of Nanoscience and Nanotechnology (IN2UB), Universitat de Barcelona, Barcelona, 08028, Spain

lourdescamblor@ub.edu

Mueller matrix (MM) polarimetry is an effective, non-invasive tool for retrieving information from complex media [1]. However, the finite dynamic range of optical detectors poses a significant challenge when measurements involve strong intensity contrasts, where bright regions risk saturation while dark regions suffer from poor signal-to-noise ratio [2]. To address this challenge, this article presents a straightforward, high dynamic range methodology that does not require non-linear algorithms [3]. The proposed technique relies on the direct addition of raw intensities captured at multiple exposure times prior to the calculation of the MM. By extending the effective well-depth of the detector, this technique allows the 16 MM elements to be calculated across different hardware configurations with a significantly improved signal-to-noise ratio in low-intensity regions while eliminating artifacts caused by saturation. This approach offers a simple yet efficient solution for the characterization of samples, eliminating the need for hardware modifications or software trade-offs.

References:

[1] H. He, R. Liao, N. Zeng, P. Li, Z. Chen, X. Liu, H. Ma, Mueller matrix polarimetry—an emerging new tool for characterizing the microstructural feature of complex biological specimen, Journal of Lightwave Technology 37 (2018) 2534–2548.

[2] G. C. Holst, T. S. Lomheim, CMOS/CCD Sensors, JCD Publishing: Oviedo, FL, USA, 2007.

[3] F. Banterle, A. Artusi, K. Debattista, A. Chalmers, Advanced high dynamic range imaging, AK Peters/CRC Press, 2017.

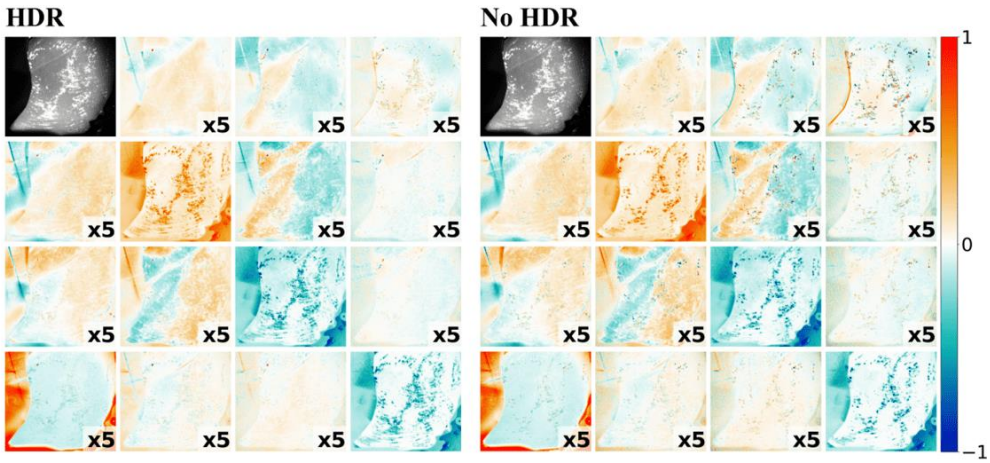

Figure 1. Normalized MMs with off-diagonal scaled for both the HDR and no-HDR measurements of our sample. In the top left corner of the MM, we can see the unnormalized M00 calculated with a single exposure time.

P.56. Truxene-based MOFs for the detection of greenhouse gases

Sergi González-Martínez[1,2,3],Yuzelfy Mendoza-Gamero[1,2,3], Albert Romano-Rodríguez[1,2], Daniel Sainz-García[2,3], Mauricio Moreno-Sereno[1,2].

[1]Dept Electronic and Biomedical Engineering, Universitat de Barcelona, Barcelona, Spain.
[2]Institute of Nanoscience and Nanotechnology (IN²UB), Universitat de Barcelona, Barcelona,Spain.
[3] Dept Inorganic and Organic Chemistry, Universitat de Barcelona, Barcelona, Spain.

sergigonzalez@ub.edu

Introduction

Rising greenhouse gas emissions and the growing demand for fossil-based chemicals are major environmental challenges today. Hence, controlling these emissions and developing sustainable materials is essential to reduce environmental damage. Sensitive, selective, and energy-efficient technologies must be designed for effective gas monitoring.

This study focuses on the development of advanced metal-organic frameworks (MOFs)[1]. MOFs are highly porous materials with suitable electrical conductivity. These properties make them effective and selective gas sensing materials. Therefore, MOFs show strong potential for environmental and energy-related applications.

Materials & Methods

This project proposes the synthesis of 2Dc-MOFs using ligands based on truxene. To be more concrete, truxene core has been chosen because of its highly and extended π-conjugation and favourable charge-transport characteristics. The ligand that is used for MOF materials is 2,3,7,8,12,13-hexahyrdoxyltruxene (HHTx) which was synthesized via 2 steps synthesis according to the literature [2]. The resulting MOFs have been characterised through SEM, EDS and PXRD to confirm its morphology, components and its crystallinity.

Results and Discussion

We present the effective synthesis of the formation of the HHTx, as well as the synthesis of their MOFs. What is more, we also present the electronic properties of Cu-HHTx and its sensitivity towards CO_2 and CH_4.

References: [1]: P. Apostol, et. al., *J. Am. Chem. Soc.* 2023, 145, 24669−24677 [2] : Q. Zhao, et. al., *ACS. Appl. Mater. Interfaces,* **2020**, 12, 7504-7509.

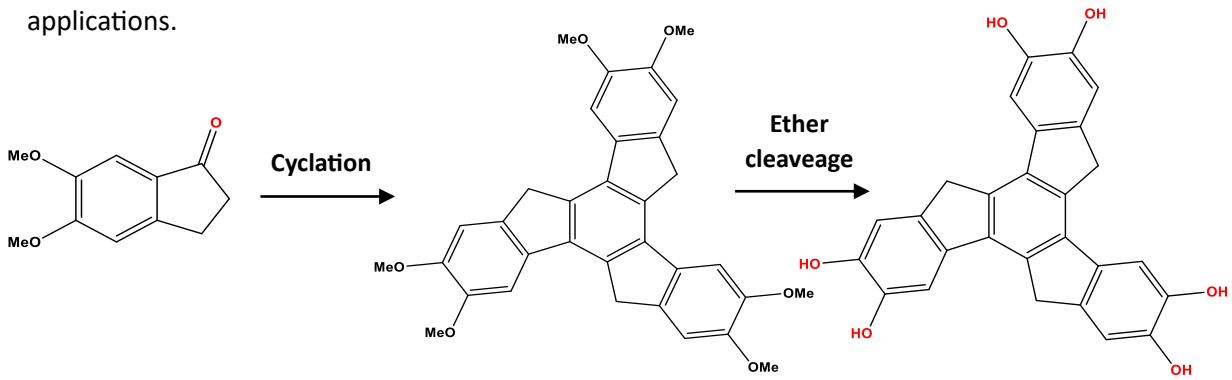

P.57. INKJET-PRINTED HEXAGONAL BORON NITRIDE MEMRISTORS FOR IN-MEMORY COMPUTING AND HARDWARE SECURITY

P. Aran[1], J. Castillo[1,3], G.Vescio[2], F. Palacio[1], B.Garrido[1], S. Hernández[1], A. Cirera[1]

[1]Department of Electronic and Biomedical Engineering, Universitat de Barcelona, Barcelona, Spain

[2]Department of Electronic Engineering, Universitat Politècnica de Catalunya, Barcelona, Spain

[3]Department of Systems, Universidad de Nariño, San Juan de Pasto, Colombia

paranvil20@alumnes.ub.edu

The exponential increase in energy consumption resulting from the development of artificial intelligence systems poses a substantial sustainability challenge [1]. Memristors emerge as the fundamental electronic device capable of enabling low-power neuromorphic applications. In specific, inkjet-printed memristors stand out due to their low material waste process, economic viability, and compatibility with flexible substrates, facilitating the development of flexible and biocompatible applications [2,3].

In this work, we present and hexagonal boron nitride (h-BN) based inkjet-printed memristor. The results obtained from the electrical characterization of the devices show volatile and non-volatile resistive switching (RS) behaviour. At higher currents (above 10 µA) the devices show stable non-volatile RS with a high HRS/LRS ratio. The same devices when operated at much lower currents (below 1 µA) exhibit volatile RS. Endurance tests have been conducted under a current-controlled approach were a Howland-based current source is utilized. Both in the non-volatile and volatile regime a remarkable endurance on inkjet-printed memristors is achieved of 60,000 and 2 million cycles with minimum overlap. The obtained results not only demonstrate exceptional endurance, reliability and operation under low currents but also opens the avenue for the implementation of current-controlled neuromorphic applications.

To demonstrate the applicability of this approach, a current-controlled stateful logic-in-memory NOR gate is presented. The MAGIC gates are subject to stringent operational voltage pulse conditions [4], which are challenging to meet due to the inherent variability of resistive switching devices. Consequently, the number of experimental demonstrations of these gates is limited. Our proposed NOR gate addresses this issue by employing a current-controlled approach, which expands its operational window significantly. The proposed NOR gate has been experimentally validated using inkjet-printed h-BN memristors, achieving 120 consecutive cycles without any computational errors.

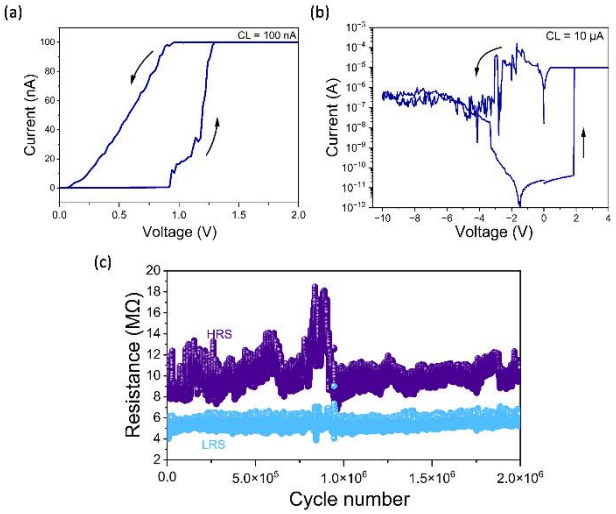

Figure 1. (a) and (b) current-voltage curves depicting the volatile and non-volatile resistive switching characteristics of the fabricated memristors, respectively, with current compliance levels of 100 nA and 10 µA. (c) Endurance test conducted under a volatile regime, demonstrating a remarkable endurance of 2 million cycles on inkjet-printed memristors.

References: [1]Mehonic A, Kenyon AJ. Brain-inspired computing needs a master plan. Nature 2022;604:255–60. https://doi.org/10.1038/s41586-021-04362-w. [2]Franco M, Kiazadeh A, Martins R, et al. Printed Memristors: An Overview of Ink, Materials, Deposition Techniques, and Applications. Adv Electron Mater 2024;10:2400212. https://doi.org/10.1002/aelm.202400212. [3] Pazos S, Xu X, Guo T, et al. Solution-processed memristors: performance and reliability. Nat Rev Mater 2024;9:358–73. https://doi.org/10.1038/s41578-024-00661-6. [4]Kvatinsky S, Belousov D, Liman S, et al. MAGIC—Memristor-Aided Logic. IEEE Trans Circuits Syst II Express Briefs 2014;61:895–9. https://doi.org/10.1109/TCSII.2014.2357292.

P.58. Engineering optomechanical coupling and phononic confinement of flexural modes with symmetry-broken cavities

D. Alonso-Tomás[1], B. Lu[2], G. Arregui[3], S. Lepeshov[2], S. Stobbe[2], D. Navarro-Urrios[1]

[1]MIND-IN2UB, Departament d'Enginyeria Electrónica i Biomédica, Facultat de Física, Universitat de Barcelona, Martí i Franquès 1, Barcelona 08028, Spain
[2]Department of Electrical and Photonics Engineering, Technical University of Denmark, Kongens Lyngby, Denmark
[3]Swiss Federal Institute of Technology Lausanne (EPFL), CH-1015 Lausanne, Switzerland

david.alonso@ub.edu

The confinement and controlled coupling of mechanical modes are central goals in cavity optomechanics, with applications in multimode interactions, signal transduction, and phononic networks. Periodic nanostructures provide powerful routes to localize mechanical excitations, as shown in optomechanical crystals and related phononic platforms [1]. Structured beam-based unit cells can also tailor flexural-wave bandgaps through geometry alone [2]. Motivated by these ideas, we develop an optomechanical platform designed to enhance, confine, and couple flexural modes.

First, we engineer an optomechanical cavity with a deliberate geometrical asymmetry, Fig. 1(a), to enhance the coupling to flexural modes. The optical field is localized in the cavity region, Fig. 1(b), while the first flexural modes show displacement antinodes near the cavity center, Fig. 1(c), enabling efficient transduction. We then introduce a periodic unit cell, Fig. 1(e), that opens a phononic bandgap for flexural excitations, allowing confinement around individual cavities and controlled coupling between nearby cavities, Fig. 1(d). By varying the number of unit cells between cavities, we observe the expected splitting between symmetric and antisymmetric hybridized modes, Fig. 1(f). The experimental spectra agree well with numerical simulations, demonstrating a simple route to engineer coupled flexural modes in optomechanical devices.

[1] M. Eichenfield *et al*., *Nature* **462**, 78–82 (2009).
[3] C. L. Willey *et al*., *Phys. Rev. Applied* **18**, 014035 (2022).

Fig. 1: (a) SEM image of the optomechanical cavity. **(b)** Simulated electric-field distribution of the optical mode. **(c)** Solid displacement fields of the first three flexural modes with an antinode at the cavity center. **(d)** SEM image of two mechanically coupled cavities. **(e)** Unit cell of the periodic structure providing phononic confinement. **(f)** Frequencies of the hybridized symmetric and antisymmetric modes as a function of the number of unit cells between cavities.

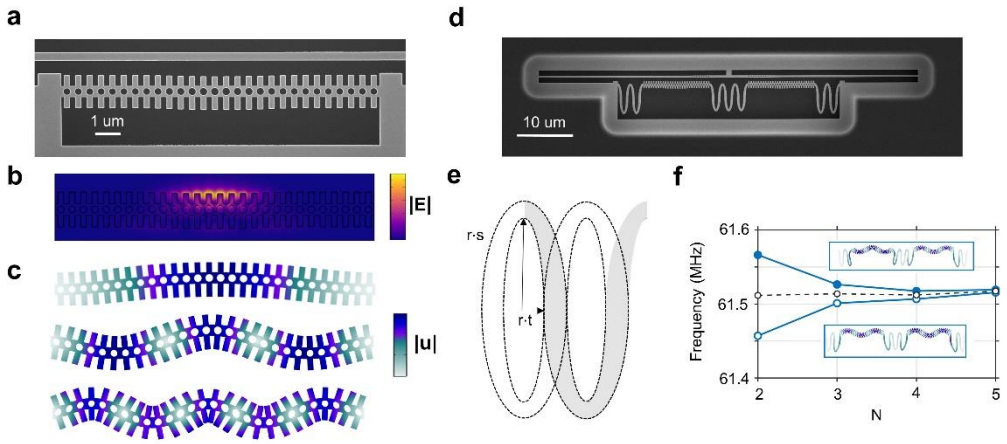

P.59. From Robust Colorimetric Inks to Vapochromic Multifunctional Surfaces for Indoor Air Quality Monitoring

Yansheng Chen[1], Olga Casals Guillen[1] , María Gonzalez Gómez[1],Ismael Benito Altamirano[2], Cristian Fabrega Gallego[1]

[1]IN²UB, Dept. Of Electronics and Biomedical Engineering. Falculty of Physics, University of Barcelona
[2]Universitat Oberta de Catalunya, Rambla del Poblenou, 154-156 Spain

yanshengchen@ub.edu ismael.benito@ub.edu olga.casals@ub.edu lugosagonzalez@ub.edu cfabrega@ub.edu

Introduction

Continuous Indoor Air Quality (IAQ) monitoring is critical for public health. However, conventional sensors (e.g., NDIR, MOx) are frequently limited by high cost, high power consumption, and poor selectivity at trace levels. Colorimetric sensors present a highly selective, room-temperature, and mass-producible alternative, but their real-world application has historically been hindered by environmental noise, particularly humidity interference. This project bridges past achievements in overcoming these limitations for single-target gases (CO_2 and Formaldehyde) with a future vision: evolving these robust systems into AI-driven, multi-gas capable Vapochromic Multifunctional Optical Sensing Surfaces.

Materials & Methods

Phase I: Completed Work (Single-Target Sensors)
We formulated selective colorimetric inks comprising polymer matrices (HEC or EC), primary amines (DETA or aPEG), and pH-sensitive dyes[i][ii]. The sensing mechanism relies on the nucleophilic attack of the amine by the target gas, generating a localized pH shift and an optical color change. The signal was acquired using an off-the-shelf LED-photodetector module (MAX30105). To handle environmental noise, statistical tools (ANOVA, t-tests) and Multivariable Linear Regression (MLR) models were developed to decouple and compensate for humidity.

Phase II: Proposed Work (Multifunctional Surfaces)
Future work will integrate Metal-Organic Frameworks (MOFs, such as ZIF-8, MIL-53(Al)-TDC, and Ti-MOF) into multilayered stacked surfaces (e.g., applying a MOF sieving overlayer onto an HKUST-1 sensing ink[iii]). MOFs will act both as vapochromic materials and tunable sieving overlayers. To process the resulting multidimensional datasets (combining steady-state optical signals and transient features), advanced Machine Learning and multivariate analysis pipelines will be deployed ***(Fig 1)***.

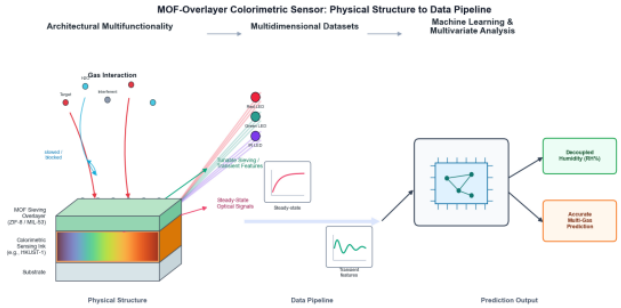

Fig 1A MOF sieving overlayer modulates gas transport to the colorimetric ink, generating both transient and steady-state optical features. Machine learning algorithms process this multidimensional dataset to achieve decoupled humidity compensation and precise multi-gas detection.

Results and Discussion

Past Achievements: We successfully developed ultra-low-cost sensors for CO_2 (150–1500 ppm)[1] and formaldehyde (80–660 ppb)[2]. For the cumulative formaldehyde sensor, a multivariable linear regression model—incorporating target concentration, relative humidity, and their interaction terms (CH_2O•RH)—successfully explained 94% of the sensor's response variance[2]. This proved that the synergy of

smart inks, low-cost optoelectronics, and statistical compensation algorithms can effectively neutralize humidity interference (e.g., imine hydrolysis at high RH) and maintain high accuracy over 7-day stability tests.

Future Direction: Building on this successful data-driven decoupling, we will transition to Architectural and Intrinsic Multifunctionality. Instead of treating environmental factors purely as noise, multi-wavelength optical interrogation will be used to simultaneously extract multi-parameter information (e.g., gas concentration + RH) from a single layer. Furthermore, by adding MOF sieving layers, we will modulate gas diffusion and transport kinetics. This co-engineering of surface architecture and machine learning will deliver a new paradigm of low-power, highly selective, multi-gas intelligent sensing platforms without the need for bulky sensor arrays.

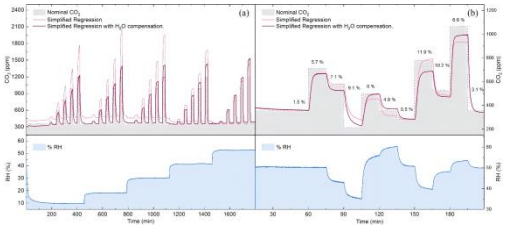

Fig 2 Validation of the CO2 colorimetric sensor: predicted concentrations demonstrating the successful decoupling and compensation of humidity interference under variable RH conditions.

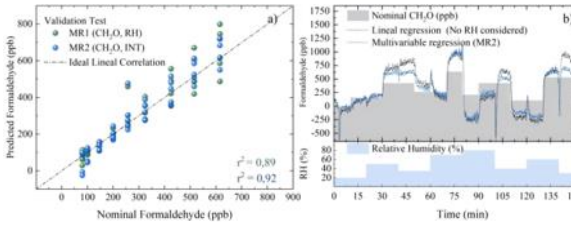

Fig 3 Validation of the cumulative formaldehyde colorimetric sensor: the multivariable regression model (MR2, blue) successfully decouples and compensates for severe humidity interference, maintaining highly accurate CH2O predictions at ppb levels compared to a standard uncompensated model (black).

[1] González-Gómez, M., Benito-Altamirano, I., Prades, J. D., Casals, O. & Fàbrega, C. Ultralow-cost and selective water-based colorimetric ink for indoor CO_2 monitoring. IEEE Sens. J. 25(11), 18722-18730 (2025).

[2] González-Gómez, M., Zymohliad, A., Benito-Altamirano, I., Casals, O., Prades, J. D. & Fàbrega, C. A cost-effective colorimetric sensor for ppb-level indoor formaldehyde monitoring. (In review).

[3] González-Gómez, M., Martínez Medina, E., Kovač, J., Casals, O., Martínez López, M., Xuriguera-Martín, E. & Fàbrega, C. A low-cost colorimetric HKUST-1 sensor for ppm-level humidity detection. Sens. Actuators B Chem. 441, 137973 (2025).

NanosMat

P.60. MULTIFUNCTIONAL BIOMIMETIC POLLEN-BASED CATALYSTS FOR WATER REMEDIATION AND BIOMASS VALORIZATION

Jordi Rigual-Miret[1,2], Queralt Baustista[1,2], Elvira Gómez[1,2], Albert Serrà[1,2]

[1] Grup d'Electrodeposició de Capes Primes i Nanoestructures (Ge-CPN), Departament de Ciència de Materials i Química Física, Secció de Química Física, Universitat de Barcelona, Barcelona, Spain
[2] Institute of Nanoscience and Nanotechnology (IN²UB), Universitat de Barcelona, Barcelona, Spain

j.rigual@ub.edu

The removal of persistent organic pollutants (POPs) and the sustainable upgrading of biomass-derived molecules require multifunctional catalytic materials capable of operating under mild, energy-efficient conditions.

This work introduces the application of bio-templated and multifunctional pollen catalysts for both advanced water decontamination and biomass valorization. Nine distinct biohybrid catalysts were synthesized by depositing Ni, Ru, or Cu onto *Salix caprea*, *Sambucus nigra, and Helianthus annuus* pollen templates via electroless deposition. The intrinsic hierarchical porosity and high surface area properties of pollen were preserved after metal deposition. In water treatment applications, these catalysts demonstrated excellent performance in UV/visible-light-assisted peroxymonosulfate (PMS) activation. Among them, Cu-coated *Helianthus annuus* pollen achieved near-complete degradation of sulfamethoxazole [1] within 60 min and up to 75 % total organic carbon (TOC) removal, maintaining >90 % efficiency in complex aqueous matrices. Additionally, the materials exhibited dual functionality by promoting the degradation of polystyrene (PS) microplastics, inducing significant particle size reduction and surface erosion via sulfate radical pathways. Beyond environmental remediation, the biohybrid catalysts were successfully applied to biomass valorization reactions. Under photo-thermocatalytic conditions, nickel-coated pollen showed outstanding activity and selectivity in the conversion of levulinic (LA) acid into γ-valerolactone (GVL), achieving nearly complete LA conversion and GVL yields above 70 %, with minimal by-product formation.

Overall, this work demonstrates that metal-functionalized pollen synthesized via electroless deposition constitutes a versatile, low-cost, and sustainable catalytic platform, capable of addressing both water decontamination and biomass valorization challenges, in line with circular economy and green chemistry principles.

[1] Bautista, Q., Rigual, J., Lloreda, J., Fons, A., Nogués, J., Gómez, E., Sepúlveda, B. & Serrà, A. (2026). Synergistic photothermal/photocatalytic activation of peroxymonosulfate using $SrFe_{12}O_{19}$@Ni-P core@shell microparticles for energy efficient water remediation. Chemical Engineering Journal, 173570.

Acknowledgements: The authors would like to express their gratitude to the Departament de Recerca i Universitats, particularly the Departament d'Acció Climàtica, Alimentació i Agenda Rural, as well as the Fons Climàtic de la Generalitat de Catalunya (project 2023 CLIMA 00009 AGAUR) for their support. Authors thank the CCiT-UB for the use of their equipment.

P.61. SYNTHESIS AND COMPLEXATION OF A FORGOTTEN PHOSPHACYCLE: THE PHOSPHORINANE

A. Vila,[1,2] **A. Grabulosa**[1,2]

[1]Universitat de Barcelona, Departament de Química Inorgànica i Orgànica, Secció de Química Inorgànica
[2]Institut de Nanociència i Nanotecnologia de la Universitat de Barcelona (IN²UB)

avilagaj7@alumnes.ub.edu

Introduction

The importance of chirality in organic chemistry and biology has driven the development of enantioselective homogeneous catalysis with transition metals, which relies on enantiopure ligands, particularly phosphorus-based [1]. A crucial subset of ligands bears a phosphorus atom embedded into a carbocycle, forming a phosphacycle, which have provided excellent ligands, especially for hydrogenation. Hence, phospholanes (5-membered phosphacycles) and phosphepines (7-membered analogues) are commonly encountered in the literature [2],[3]. Surprisingly, phosphorinanes (6-membered phosphacycles) are rare in general and almost unknown in homogeneous catalysis. For this reason, this work focused on the synthesis of two novel phosphorinanes having a 1,8-dimethylnapthalene (DMNp) scaffold and their complexation to a ruthenium(II) organometallic moiety.

Materials and methods

For the synthesis of phenylphosphorinane-borane (**1·BH₃**), two different approaches have been followed: (*i*, not shown in the scheme): cyclisation of dilithiated DMNp with dichlorophenylphosphane and (*ii*, shown): cyclisation of 1,8-bis(chloromethyl)naphthalene ($DMNpCl_2$) with bis-deprotonated phenylphosphane-borane (**1a**) [4]. Methylphosphorinane-borane (**2·BH₃**) has been prepared from phosphinic acid **2a** by reduction with phenylsilane, boronation, deprotonation and alkylation. Borane groups were removed to give **1** and **2**, which were reacted with [RuCl(*m*-Cl)(h^6-*p*-cymene)]$_2$ to yield **Ru1** and **Ru2**, respectively.

Results and discussion

The synthesis of **1** via route *i* appears to be more challenging and is still being optimized. Despite this, both **1** and **2** have been successfully synthesized and fully characterized, as well as their ruthenium(II) complexes, which can already be used for its further studies in homogeneous catalysis. In the near future, **1·BH₃** and **2·BH₃** will be subjected to desymmetrization reactions to access to enantiopure ligands.

References

[1] Grabulosa, A., RSC Catalysis Series, 2011, Cambridge: Royal Society of Chemistry. [2] Tang, W. and X. Zhang, Angew. Chem. Int. Ed., 2002. **41**(9): p. 1612–1614. [3] Tang, W., et al., Angew. Chem. Int. Ed., 2003. **42**: p. 3509–3511. [4] Slootweg, C., et al., Chem. Eur. J., 2020. **26**(68): p. 15944–15952.

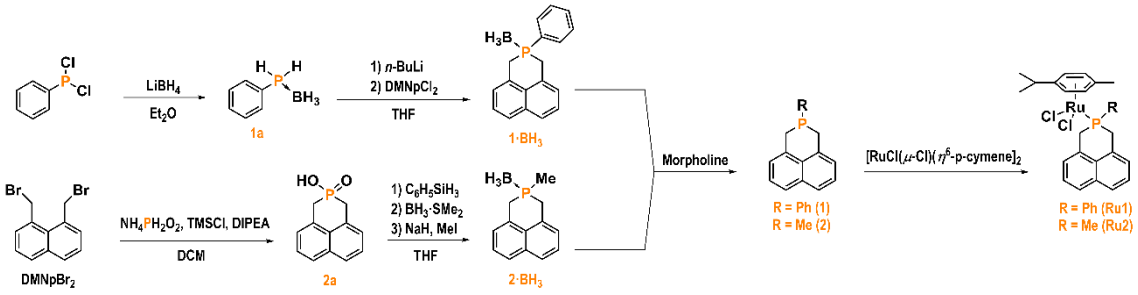

P.62. LUMINESCENCE CYCLOMETALLATED PLATINUM COMPOUNDS WITH PEGYLATED ANCILLARY LIGANDS.

O. Rodríguez[1], A. Lazaro[1], L. Rodriguez[1]

[1]Departament de Química Inorgànica i Orgànica, Secció de Química Inorgànica, Martí i Franquès 1-11, 08028, Barcelona, Spain

orodriga39@alumnes.ub.edu

Several studies have reported luminescent platinum (II) compounds for various applications, such as sensors, biomedical applications and OLED devices. Luminescence plays a very important role in all of them. For example, photodynamic therapy degrades cancer cells via reactive oxygen species (ROS) generated by irradiating a luminescent compound. It is also essential in the development of OLED devices, whose efficiency is increased thanks to the phosphorescence of these compounds (Figure 1).[1]

The luminescence of platinum compounds can be modulated by varying the type of ligands and supramolecular contacts in order to shift the emission towards the near infrared. The strategies that can be used for the design of these compounds are based on including conjugated π ligands and providing planarity to the structure to facilitate the formation of aggregates through Pt···Pt interaction (figure 2) or other type of weak intermolecular contacts.[2]

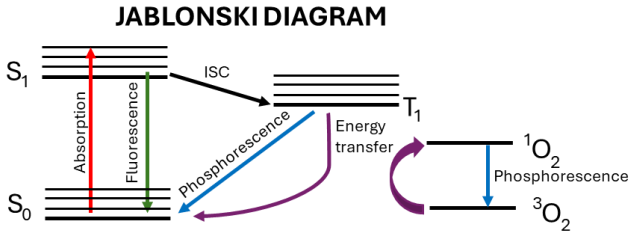

Figure 1: Jablonski diagram

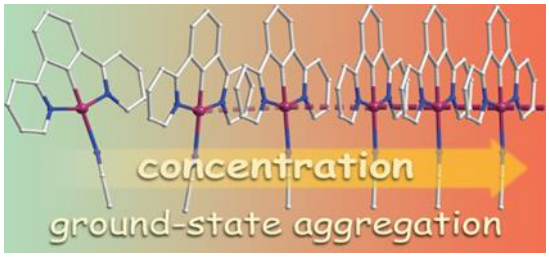

Figure 2: Apoptosis and necroptosis of a cancer cell by oxigen singlet.[4]

In this work, (C^N^N) type cyclometallated platinum compounds have been synthesized, where the ancillary ligand will be varied in order to be coordinated to the platinum metal centre compound via an alkynyl or a pyridine unit. The structures are based on conjugated π ligands, with the aim of shifting the emission towards the red or near-infrared. Furthermore, polyethylene glycol (PEG) chains have been introduced to impart an amphiphilic character to the structure (Figure 3), allowing partial or total solubility in water. This amphiphilic nature will enable the luminescent study to be extended across various solvents and broaden the application of platinum compounds in biomedical research.[3]

[1] Mackay, F. S.; Woods, J. A.; Heringova, P.; Kasparkova, J.; Pizarro, A. M.; Moggach, S. A.; Parsons, S.; Brabec, V.; Sadler, P. J. *Proc. Natl. Acad. Sci. U. S. A.* **2007**, *104*, 20743–20748. [2] Hattori, S.; Shinozaki, K.; *ChemPhotoChem*. **2025**, *9*. [3] Lázaro, A.; Balcells, C.; Quirante, J.; Badia, J.; Baldomà, L.; Ward, J. S.; Rissanen, K.; Font-Bardia, M.; Rodríguez, L.; Crespo, M.; Cascante, M.; *Chem. Eur. J.* **2020**, *26*, 1947–52. [4] Sivchik, V. V.; Grachova, E. V.; Melnikov, A. S.; Smirnov, S. N.; Ivanov, A.; Hirva, P.; Tunik S. P.; Koshevoy, I. O.; *Inorg. Chem*. **2016**, *55*, 3351-3363.

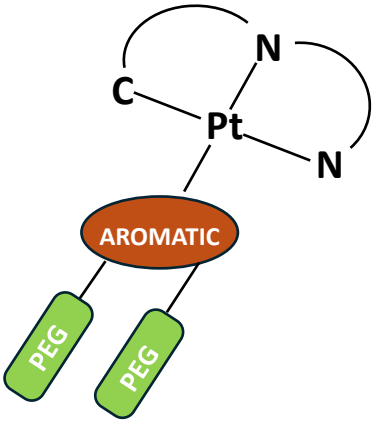

Figure 3: Proposed structure of the compounds

P.63. PLAYING WITH AUROPHILIC INTERACTIONS IN GOLD(I) AND GOLD(II) LUMINESCENT COMPOUNDS

A. Fabregas[1], A. Pinto[1], L. Rodríguez[1]

[1] Departament de Química Inorgànica i Orgànica, Secció de Química Inorgànica, Martí i Franquès 1-11, 08028, Barcelona, Spain

afabrega38@alumnes.ub.edu

Luminescent gold(I) compounds have attracted considerable attention due to strong spin-orbit coupling (SOC) arising from the heavy atom effect of gold. Different chromophore ligands and phosphines are used to enhance the luminescence properties.[1]

In this work, we explore a novel class of geminal gold(I) compounds, in which two gold centers are bound to the same carbon atom of a chromophoric unit. These systems enable tunable emission across a wide range through ligand modification and aurophilic interactions which exhibit strong luminescence in the solid state.[2]

The presence of these aurophilic interactions provide an excellent platform for the exploration and development of new emissive gold(II) compounds. Aurophilic interactions favour the oxidation process by preorganising the starting $[Au(I)]_2$ complexes and lowering their redox potential, enabling the possibility to $[Au(II)]_2$ species.[3]

Having this in mind, we have proceeded to the oxidation of gold(I) compounds to their corresponding gold(II) derivatives using $PhICl_2$ as an oxidant at low temperature and under dark conditions due to the photosensitivity of these complexes.

[1] A. De Aquino, J. S. Ward, K. Rissanen, G. Aullón, J. C. Lima, L. Rodríguez. *Inorg. Chem.* 2022, *61*, 20931−20941.

[2] X. Y. Zhai, L. Zhao. *Nature Commun.* 2025, *16*, 405.

[3] A. Portugués, D. Bautista, J. Gil-Rubio. *Chem. Eur. J.* 2021, *27*, 15815–15822.

Figure 1. Scheme reaction of the formation of gem-digold(I) complexes with dibenzofuran and fluorene as chromophores.

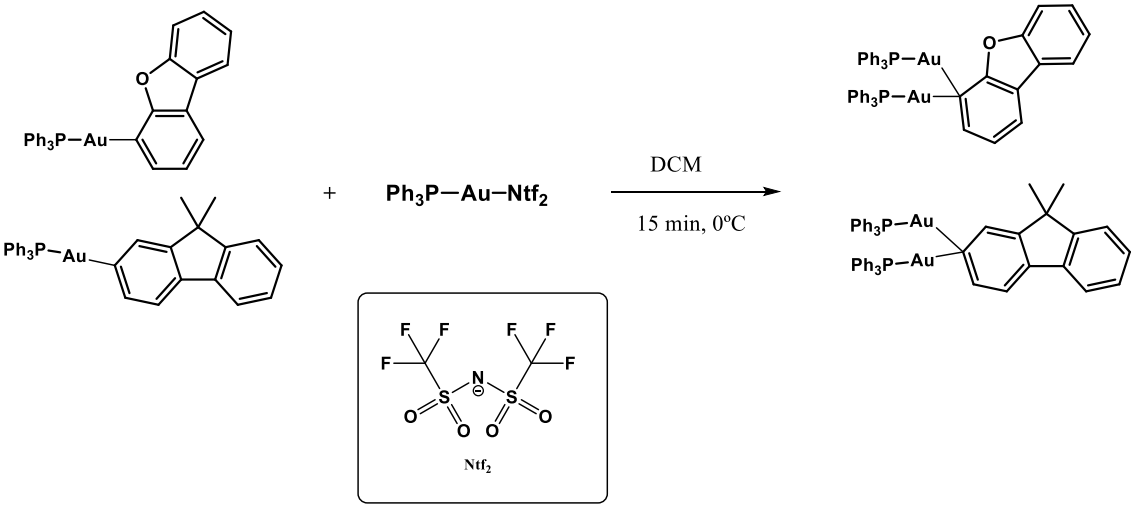

P.64. Insights into Inductively Coupled Plasma Chemical Vapor Deposition and Water Functionalization of Vertical Graphene Nanowalls

I.M. Toliou[1,2], S. Majumdar[1,2], R.A. Rovira[1,2], S. Chaitoglou[1,2*]

[1]*Department of Applied Physics, University of Barcelona, C/Martí i Franquès, 1, 08028 Barcelona, Catalunya, Spain*
[2]*ENPHOCAMAT Group, Institute of Nanoscience and Nanotechnology (IN²UB), University of Barcelona, C/ Martí i Franquès, 1, 08028 Barcelona, Catalunya, Spain*

[*]ilektratoliou@ub.edu
[*]stefanoschaitoglou@ub.edu

Vertical graphene nanowalls (VGNWs) have emerged as promising supports for electrochemically active materials owing to their intrinsic physicochemical properties[1], including high electrochemical surface area, electrical conductivity and chemical stability. Precise synthesis and functionalization control will unlock their use in future energy harvesting systems. Here, we report a systematic investigation on the C_2H_2/H_2/Ar gas mixture variation during inductively coupled plasma chemical vapor deposition (ICP-CVD)[2]. Subsequently, water plasma functionalization under different pressure and power conditions was used to modify their surface chemistry through the controlled incorporation of oxygen-containing groups[3]. The effects of growth conditions and water plasma functionalization were examined by SEM, Raman and X-Ray photoelectron (XPS) spectroscopy, cyclic voltammetry (CV), and Electrochemical Impedance Spectroscopy (EIS). Results show that control in growth conditions and water-plasma treatment strongly influence the structural order and defect density of the nanowalls. Raman analysis showed that variations in the growth gas mixture affected disorder and crystallinity, while plasma power determined whether water-plasma treatment promoted oxygen functionalization or etching. Finally, water plasma treatment results in a 1.4-fold increase in the double-layer capacitance (Cdl) from 5.44 to 7.66 mF cm^{-2}, indicating increased electrochemically accessible surface area.

References

(1) Bertran-Serra, E.; Musheghyan-Avetisyan, A.; Chaitoglou, S.; Amade-Rovira, R.; Alshaikh, I.; Pantoja-Suárez, F.; Andújar-Bella, J.-L.; Jawhari, T.; Perez-del-Pino, A.; Gyorgy, E. Temperature-Modulated Synthesis of Vertically Oriented Atomic Bilayer Graphene Nanowalls Grown on Stainless Steel by Inductively Coupled Plasma Chemical Vapour Deposition. *Appl. Surf. Sci.* **2023**, *610*, 155530.

(2) Ishikawa, K. Effects of Plasma Ions/Radicals on Kinetic Interactions in Nanowall Deposition: A Review. *Adv. Eng. Mater.* **2024**, *26* (16), 2400679.

(3) Hussain, S.; Amade, R.; Jover, E.; Bertran, E. Functionalization of Carbon Nanotubes by Water Plasma. *Nanotechnology* **2012**, *23* (38), 385604.

P.65. Nanostructured Electrocatalyst for Tunable Biomass Valorization

P. Vilariño[1,2], E. Gómez[1,2], A. Serrà[1,2]

[1]Grup d'Electrodeposició de Capes Primes i Nanoestructures (Ge-CPN), Departament de Ciència de Materials i Química Física, Universitat de Barcelona, Martí i Franquès, 1, E-08028, Barcelona, Catalonia, Spain.
[2]Institute of Nanoscience and Nanotechnology (IN2UB), Universitat de Barcelona, Barcelona, Catalonia, Spain.

pol.vilarino@ub.edu

Abstract:

Electrocatalytic upgrading of biomass-derived molecules offers a sustainable route to renewable fuels and green chemicals. Levulinic acid (LA), obtained from lignocellulosic biomass, is a versatile precursor that can be selectively transformed into γ-valerolactone (GVL) or 4-hydroxyvaleric acid (HVA), valuable intermediates for solvents, fuels, and polymer building blocks. Here we establish a unified multiscale framework linking electrode fundamentals, interfacial engineering, and advanced nanostructured architectures to direct LA electrohydrogenation. Baseline studies on glassy carbon and controlled electrolyte environments reveal the decisive roles of proton availability, solvent, and temperature in the LA→HVA→GVL pathway with Ni-based electrocatalysts, while bimetallic CuNi and trimetallic CuNiRu systems exhibit markedly enhanced activity compared to Ni alone. Transitioning to vertically aligned graphene nanowalls (GNWs) decorated with CuNi or CuNiRu enables tunable product switching: at 5 °C, >95% HVA is obtained, whereas at 50 °C GVL selectivity exceeds 90%. The CuNiRu–GNW platform reaches 96.6% conversion and 98.5% selectivity, highlighting the synergy between high-surface-area carbon supports and Ru-mediated hydrogen activation. Finally, hierarchical Ni@Ru electrodes fabricated via the Dynamic Hydrogen Bubble Template (DHBT) and stabilized by a DTAC molecular shield provide macroporous transport channels, proton-throttling, and exceptional acid stability. Applied to LA, HMF, and FF, the Ni@Ru–DTAC system delivers high Faradaic efficiencies (~80–90%), excellent chemoselectivity, and intrinsic scalability. Overall, coupling interfacial regulation, nanostructure engineering, and temperature control enables robust and selective electrochemical biomass valorization.

P.66. NiX/Al_2O_3 CATALYSTS FOR METHANATION OF RESIDUAL CO_2 FROM BIOGAS UPGRADING

J. Lloreda[1,2,3], J. Serafin[2,4], X. Vendrell[2,4], V. Abad[3], E. Gómez[1,2], A. Serrà[1,2]

[1]Grup d'Electrodeposició de Capes Primes i Nanoestructures (GE-CPN), Departament de Ciència de Materials i Química Física, Universitat de Barcelona, Martí i Franquès 1, E-08028, Barcelona, Espanya
[2]Institut de Nanociència i Nanotecnologia (IN2UB), Universitat de Barcelona, Barcelona, Espanya
[3]Consorci per a la Gestió dels Residus del Vallès Oriental, Camí Ral s/n, E-08401, Granollers, Espanya
[4]Grup de Química de l'Estat Sòlid (QES), Departament de Química Inorgànica i Orgànica, Universitat de Barcelona, Martí i Franquès 1, E-08028, Barcelona, Espanya

juditlloreda@ub.edu

The transition towards renewable energy systems has intensified interest in upgrading biogas to biomethane, a grid-compatible and storable fuel. Nevertheless, this process inevitably produces a CO_2-rich off-gas stream. Valorizing this residual carbon dioxide is therefore a key strategy to enhance overall carbon efficiency and achieve a closed carbon cycle. In this framework, catalytic CO_2 methanation, commonly referred to as the Sabatier reaction, is considered a promising pathway [1]. In this context, Ni-based catalysts supported on alumina have emerged as promising materials due to their favorable balance between activity, cost, and scalability, maintaining efficient operation at atmospheric or moderately elevated pressures [2]. Moreover, the robustness of these well-established catalysts allows them to tolerate impurities typically present in biogas-derived streams, thereby facilitating their implementation under real operating conditions.

In this work, NiX/Al_2O_3 catalysts (X = none, Co, Cu or Fe) were synthesized following a standard wet impregnation method [3], employing different metal compositions while keeping the total metal loading constant at 10 wt%. To evaluate the general behavior of the supported-metal catalysts, monometallic Ni/Al_2O_3 was prepared as a reference, whereas the bimetallic catalysts were synthesized with an equimolar (50-50) metal ratio. Morphological characterization of the fresh catalysts confirmed the formation of metallic nanoparticles dispersed over the micrometric γ-Al_2O_3 surface, as well as their homogeneous distribution across the support. Catalytic experiments were conducted in a fixed-bed stainless-steel reactor using a CO_2:H_2 molar feed ratio of 1:3. This deliberately chosen sub-stoichiometric ensures complete CO_2 conversion while maintaining efficient hydrogen utilization, aligning the operating conditions more closely with practical industrial applications. Initial experiments were performed at atmospheric pressure over a temperature range of 150 to 550 °C, with increments of 50 °C.

For all four catalysts, methane production strictly followed the hydrogen conversion pathway. For both Ni/Al_2O_3 and NiFe/Al_2O_3, significant hydrogen and carbon dioxide conversions began at approximately 250 °C and reached maximum values at 400 °C (~60% and ~50%, respectively). At higher temperatures, a decrease in H_2 consumption accompanied by an increase in CO_2 conversion was observed, indicating a shift in the dominant reaction pathway towards CO formation. NiCo/Al_2O_3 exhibited a comparable trend, however maximum conversions were reached at 450 °C, with slightly lower H_2 and CO_2 conversions of approximately 50%. In contrast, NiCu/Al_2O_3 displayed clearly different catalytic behavior. CO_2 conversion was consistently higher than H_2 conversion, while overall product formation was significantly lower. Additionally, CO production began at lower temperatures. Among the three bimetallic formulations evaluated, Ni-Fe and Ni-Co were chosen for further optimization. Since increasing pressure enhances methanation reaction rates and improves selectivity towards CH_4, another set of experiments was performed at higher pressures of 2, 3 and 4 bar. Finally, catalyst stability under

continuous operation conditions was assessed at both atmospheric and pressurized conditions at a controlled temperature of 400 °C.

References: [1] Wang, W.; et al. *ACS Catal.* **2025**, *15*, 10868. [2] Yin, S.; et al. *Chem. Eng. J.* **2025**, *504*, 158723. [3] Bian, Z.; et al. *Int. J. Hydrogen Energy*. **2021**, *46*, 31041.

Acknowledgments: With the support of the Industrial Doctorates Program of the Department of Research and Universities of the Generalitat de Catalunya (project 2022 DI 00035). The authors acknowledge financial support through the AGAUR grant, 2021SGR00936 and project 2023 CLIMA 00009, supported by the Department of Research and Universities, the Department of Climate Action, Food and Rural Agenda, and the Climate Fund of the Generalitat de Catalunya. The authors would also like to thank the CCiT-UB for the use of their equipment.

P.67. Luminescent Gold(I) Complexes for Molecular Recognition of Environmental Contaminants

M. Mustak Ahmed[1], A. Pinto[1], A. Lázaro[1], I. Angurell[1,2], L. Rodríguez[1,2]

1 Departament de Química Inorgànica i Orgànica, Secció de Química Inorgànica, Martí i Franquès 1-11, 08028, Barcelona, Spain
2 Institut de Nanociència i Nanotecnologia de la Universitat de Barcelona (IN²UB)

mdahmeda101@alumnes.ub.edu

Environmental contamination by hazardous species such as polyaromatic hydrocarbons (PAHs), anions, and metal cations poses a raising challenge for water systems, environmental safety and public health. There is an increasing demand for sensitive, rapid, and cost-effective detection technologies capable of identifying these at low concentrations. In this context, luminescent materials offer a promising platform for the development of next-generation sensing systems.

This study focuses on the rational design and synthesis of luminescent systems based on gold(I) organometallic complexes that give rise to functional fluorescent materials when they are linked into a polymeric structure. Phosphine ligands incorporating chromophoric units such as carbazole and pyrene were synthesized and coordinated to Au(I) centers to obtain a series of Au(I) complexes [1]. In parallel, a light active molecular probe was synthesized via a Sonogashira coupling strategy and integrated into a fluorescent cellulose matrix [2,3]. Consequently, the presence of a terminal alkyne functionality facilitates coordination to gold(I), allowing for the creation of hybrid luminescent systems for sensing applications. All systems were characterized using ^{1}H and ^{31}P NMR, IR, UV-Vis and photoluminescence measurements.

Photophysical investigations demonstrate that coordination to gold(I) substantially alters the emission properties of these systems, resulting in enhanced excited-state interactions and tunable luminescence. These materials display pronounced sensitivity to their chemical environment, as interactions with target analytes produce quantifiable changes in emission intensity and spectral characteristics. Consequently, these responses facilitate the selective detection of environmental contaminants via luminescence signaling at low concentrations.

Overall, this work illustrates how molecular design and metal coordination can be combined to create efficient and adaptable sensing platforms. And this highlights their potential for real world applications in environmental monitoring.

References:

[1] A. P. Atencio, S. Burguera, G. Zhuchkov, A. de Aquino, J. S. Ward, K. Rissanen, J. C. Lima, I. Angurell, A. Frontera and L. Rodríguez, Tuning luminescence in gold(I)-phosphine complexes: structural, photophysical, and theoretical insights, **Inorg. Chem. Front., 2025, 12, 3041-3054.** DOI: 10.1039/d4qi03225j.

[2] P. McNeice, G. H. ten Brink, U. Gran, L. Karlson, R. Edvinsson and B. L. Feringa, Cellulose modification for sustainable polymers: overcoming problems of solubility and processing, **RSC Sustainability, 2024, 2, 369-376**. DOI: 10.1039/D3SU00317E.

[3] S. Rykowski, D. Gurda-Woźna, M. Orlicka-Płocka, A. Fedoruk-Wyszomirska, M. Giel-Pietraszuk, E. Wyszko, A. Kowalczyk, P. Stączek, K. Biniek-Antosiak, W. Rypniewski and A. B. Olejniczak, Design of DNA Intercalators Based on 4-Carboranyl-1,8-Naphthalimides: Investigation of Their DNA-Binding Ability and Anticancer Activity, ***Int. J. Mol. Sci.*, 2022, 23**, **4598**. DOI: 10.3390/ijms23094598.

P.68. Graphene Nanowalls-Guided Growth of Vertically Aligned Carbon Nanotubes on Flexible Carbon Substrate for High-Performance Supercapacitive Electrodes

Yang Ma [*a b], **Shubhadeep Majumdar** [a b], **Ghulam Farid** [a b], **Enric Bertran-Serra** [a b], **Stefanos Chaitoglou** [*a b], **Roger Amade-Rovira** [* a b]

[a] Department of Applied Physics, University of Barcelona, C/Martí i Franquès, 1, 08028 Barcelona, Catalunya, Spain

[b] ENPHOCAMAT Group, Institute of Nanoscience and Nanotechnology (IN2UB), University of Barcelona, C/Martí i Franquès, 1, 08028 Barcelona, Catalunya, Spain

ymamaxxx147@ub.edu; r.amade@ub.edu; stefanoschaitoglou@ub.edu.

Introduction

Flexible supercapacitors require electrode architectures that simultaneously combine mechanical compliance, efficient electron transport, rapid ion diffusion, and high electrochemically accessible surface area. Herein, we report a flexible hierarchical carbon electrode in which carbon nanotubes (CNTs) are grown on vertical graphene nanowalls (GNWs) on Papyex, yielding a CNTs/GNWs/Papyex architecture. The introduction of the GNWs interlayer fundamentally alters CNTs growth behavior, converting the disordered and locally agglomerated nanotube network formed on bare Papyex into a more uniform, vertically aligned, and hierarchically porous structure. Comprehensive structural characterization reveals that the GNWs scaffold not only improves CNTs organization and interfacial integration, but also enriches the surface with oxygen-containing functional groups that enhance electrolyte affinity and electrochemical activity. In particular, CNTs/GNWs/Papyex exhibits the lowest Raman I_D/I_G ratio, indicating a more ordered sp^2 carbon framework, while the integrated morphological and chemical evidence supports a coupled chemical and geometric interplay that suppresses Fe/Al catalyst coarsening, thereby promoting dense and uniform CNTs nucleation. Benefiting from the synergistic integration of continuous conductive pathways, open ion-transport channels, and oxygen-functionalized active sites, the hierarchical electrode delivers a volumetric capacitance of 96.3 mF cm^{-3} at 0.8 mA cm^{-2}, representing an 11.2-fold enhancement over CNTs/Papyex, together with 90% capacitance retention after 6000 charge-discharge cycles. This work provides a mechanistic strategy for engineering catalyst-support interactions on flexible carbon substrates and offers a promising route toward advanced hierarchical carbon electrodes for flexible energy-storage applications.

Keywords: Vertical graphene; Guided-growth carbon nanotubes; Chemical vapor deposition; Catalyst-support interaction; Supercapacitive performance

P.69. DEVELOPMENT OF LUMINESCENT Pt(II) SUPRAMOLECULAR POLYMERS AND MATERIALS.

R. Ñañez[1], A. Lázaro[1], A. Pinto[1], L. Rodríguez[1]

[1]Department of Inorganic and Organic Chemistry, Inorganic Chemistry Section, Universitat de Barcelona, Martí y Franquès 1, 08028 Barcelona, Spain

rnanezaz7@alumnes.ub.edu

Luminescent polymeric materials have been widely studied due to their potential applications in sensors[1], bioimaging[2] and optoelectronics[3]. However, conventional systems based on π-conjugated polymers, despite their high emission efficiency, usually suffer from complex synthesis, poor water solubility and susceptibility to aggregation-caused quenching. In contrast, nonconventional luminescent polymers (NLPs) have emerged as a promising alternative due to their easier synthesis, good processability and biocompatibility.[4] Unlike traditional systems, NLPs exhibit luminescence from clustering of nonconjugated electron-rich functional groups within synthetic or natural polymeric matrices, including poly(amidoamine), starch, and bovine serum albumin.

Cellulose, an abundant and chemically versatile biopolymer, provides an excellent platform for functionalization due to its high density of hydroxyl groups, good mechanical strength, and intrinsic permeability to small molecules. Covalent incorporation of luminescent units into a cellulose backbone results in improved stability, homogeneity and control of the luminescent properties compared to physical loading.

Platinum(II) complexes bearing tridentate NCN-type cyclometalating ligands (Pt-NCN) exhibit intense luminescence with tunable emission colors. Their strong spin-orbit coupling efficiently promotes intersystem crossing, leading to high phosphorescence quantum yields and long-lived triplet emissions.

In this work, a hybrid luminescent polymer based on sulfonated cellulose has been developed through the covalent integration of a modular emissive unit consisting of a luminescent linker and a Pt–NCN complex. Cellulose has been chemically modified via sulfonation using 1,3-propanesultone to enhance its solubility and reactivity, enabling subsequent functionalization. The designed linker facilitates the attachment of the platinum complex to the polymer backbone, resulting in a renewable hybrid system that combines the structural advantages of cellulose with the photophysical properties of metal-based emitters. This approach provides a promising platform for the development of advanced luminescent materials with potential applications in sensing and photonic systems.

[1] Kim, H. N.; Ren, W. X.; Kim, J. S.; Yoon, J. *Chem. Soc. Rev.* **2012**, *41*, 3210–3244.
[2] Yuan, Y.; Xu, S.; Cheng, X.; Cai, X.; Liu, B. *Angew. Chem. Int. Ed.* **2016**, *55*, 6457–6461.
[3] Grimsdale, A. C.; Chan, K. L.; Martin, R. E.; Jokisz, P. G.; Holmes, A. B. *Chem. Rev.* **2009**, *109*, 897–1091.
[4] Bauri, K.; Saha, B.; Banerjee, A.; De, P. *Polym. Chem.* **2020**, *11*, 7293–7315.

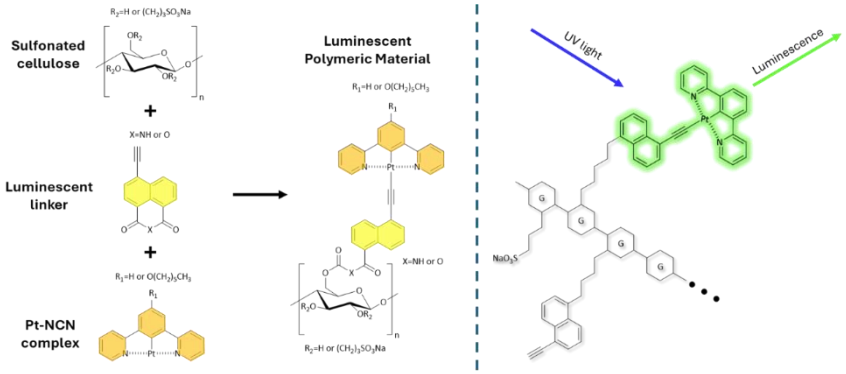

Figure 1. Schematic representation of the synthesis of the luminescent polymeric material (left) and luminescent phenomena under UV light exposure (right).

NanoEnergy

P.70. Role of acidic ion-exchange resin morphology on the production of butyl levulinate from glucose

P.A. Bohórquez, J.H. Badia, R. Bringué, R. Soto, E. Ramírez
Universitat de Barcelona, Barcelona, Spain

pbohorji10@alumnes.ub.edu

Introduction

Alkyl levulinates (ALs) are versatile bio-based compounds particularly attractive as renewable additives in automotive and aviation fuels, where they enhance performance while reducing carbon emissions. In addition, ALs show potential applications in the pharmaceutical, cosmetic, agricultural, and food industries [1]. Among them, butyl levulinate (BL) is considered a promising diesel blend component due to its favorable physicochemical properties. Previous studies demonstrated that sulfonic ion-exchange resins, especially Dowex 50Wx2, are highly effective catalysts for the direct one-pot synthesis of BL from fructose and 1-butanol, achieving yields up to 81.7% at 140 °C [2,3]. Resin morphology in the swollen state was found to strongly influence catalytic performance. However, glucose, the main monomer of cellulose and a much more abundant feedstock, remains scarcely studied because its conversion requires an additional isomerization step to fructose. This work evaluates the feasibility of producing BL directly from glucose and 1-butanol using sulfonic ion-exchange resins, correlating swollen-state morphology with catalytic activity and selectivity.

Materials and Methods

Batch experiments were conducted over 6 h using glucose as the substrate at an initial concentration of 10 wt.%. The reaction medium consisted of a 50 mL mixture of γ-valerolactone (GVL, 95%, CymitQuimica) and 1-butanol (BuOH) with a BuOH:GVL ratio of 70:30 wt.%. All experiments were performed under identical operating conditions: 150 °C, 500 rpm stirring rate, and 1 wt.% catalyst loading. Eight acidic ion-exchange resins (IERs) were evaluated as catalysts, selected to cover a broad range of structural properties.

Results and Discussion

A strong relationship was found between the IERs' morphological features and the obtained yield of butyl levulinate (BL). Firstly, acid capacity seems essential for achieving a significant conversion of cellulose-derived glucose into BL. As shown in Fig. 1, A-46 exhibits a significantly lower yield than the other resins, which strongly correlates with its much lower acid capacity. The relationship between the swollen pore volume and the density of acid sites also appears relevant to produce the desired product, as shown in Fig. 2. Finally, Fig. 3 correlates the polymer chain concentration with the BL yield, showing that excessively high polymer chain concentrations negatively affect the accessibility of catalytic sites and diffusion of reactants, ultimately leading to lower BL production.

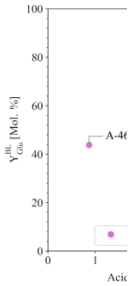

Fig. 1. Acidity vs Yield

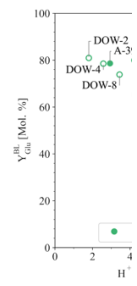

Fig. 2. Acid Site Density vs Yield

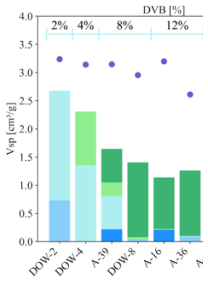

Fig. 3. Polymer Chain Concentration vs Yield

References

1 Kim, S. *et al. Chem. Eng. J.* 533, 174833 (2026) **2** Bringué, R. *et al. Ind. Eng. Chem. Res.* 63, 16701–16709 (2024) **3** Ramírez, E. *et al. Appl. Catal. Gen.* 612, 117988 (2021)

P.71. Tailoring the performance of Al-doped ZnO-based dielectric-metal-dielectric transparent electrodes for solar cells

U. Aziz[1,2], A. L. Muñoz-Rosas[1,2], J. M. Asensi[1,2], J. Bertomeu[1,2], J. López-Vidrier[1,2]

[1]Multiferroic and Photovoltaic Materials for Renewable Energies (MAMFER), Universitat de Barcelona, Barcelona (Spain)
[2]Institute of Nanoscience and Nanotechnology (IN2UB), Universitat de Barcelona, 08028 Barcelona - Barcelona (Spain)

umeraziz@ub.edu

Abstract

Solar cells require a proper transparent electrode able to extract the photogenerated charge while not compromising on their transmittance and reflectance. In conventional photovoltaics, and widespread in optoelectronics, indium-doped tin oxide (ITO) is commonly used as a transparent conductive electrode [1]. However, because of In being classified as a critical raw material, dielectric-metal-dielectric (DMD) layered structures have emerged as candidates to substitute ITO for this function, where a sub-10 nm thin metal layer helps enhancing the conductivity while barely affecting transparency [2].

Here, magnetron sputtered DMD structures have been investigated for solar cell applications. ZnO and Al-doped ZnO-based films were selected as dielectric materials, whereas Al-doped Ag films were employed as the metal. The optical and electrical properties of the layers have been determined via UV-Vis-NIR spectroscopy and a 4-probe setup, respectively, and they have been correlated to the material structure and composition using X-ray diffraction, scanning electron microscopy, and atomic force microscopy. We proved that the co-sputtering of Ag and Al produces the necessary coalescence of the M layer for improved charge transport. In addition, different chamber environment during deposition (from oxidized to reduced) has been shown to provide different characteristics of the D layer. Finally, Haacke's figure of merit is employed to compare the performance of the different DMD structures under test [3].

References:

[1] Xu, H., et al., (2026). Tailoring indium-reduced AZO-ITO composite films for superior transparent conductive oxide films in silicon heterojunction solar cells. Solar Energy Materials and Solar Cells, 299, 114222.

[2] Tom, T., Ros, et al., 2020. Influence of co-sputtered Ag: Al ultra-thin layers in transparent V_2O_5/Ag: Al/AZO hole-selective electrodes for silicon solar cells. Materials, 13(21), p.4905.

[3] Haacke, G. (1976). New figure of merit for transparent conductors. Journal of Applied Physics, 47(9), 4086-4089.

P.72. HETEROGENEOUS MULTILAYER PIEZOELECTRIC CERAMICS

A. Rodríguez[1], X. Vendrell[1], J. Garcia[2]

[1]Department of Inorganic and Organic Chemistry & Institute of Nanoscience and Nanotechnology (IN2UB), Universitat de Barcelona, Barcelona, Spain
[2]Department of Physics, Universitat Politècnica de Catalunya, Barcelona, Spain

andres.rodriguez@ub.edu

Enhancing the electromechanical coupling of piezoelectric ceramics is traditionally pursued through compositional modifications; additionally, the improvements achieved by new formulations are often incremental and increasingly difficult to attain.[1] At the same time, the growing demand for efficient mechanical-to-electrical energy conversion motivates the exploration of alternative strategies to improve functional performance.[2] In this work, bulk laminated heterostructures are fabricated from commercial PZT-based microparticulate powders (PZ24, PZ26, PZ27, supplied by Ferroperm), selected for their well-established and distinct electromechanical properties, and its piezoelectric and electromechanical behavior is studied.

Disk-shaped samples were fabricated by sequential powder stacking, followed by uniaxial and isostatic pressing, and a final sintering thermal process, obtaining dense laminated structures. Bipolar strain–electric field hysteresis loops were measured using a conventional Sawyer–Tower configuration. Electromechanical coupling constants under radial mode excitation were calculated from resonance and antiresonance frequencies, determined by measuring electrical impedance as a function of frequency under an applied AC voltage.

The heterostructured samples exhibit a maximum strain comparable to the highest-performing constituent material, while showing significantly reduced losses, indicating an overall enhancement of the piezoelectric response. Moreover, geometrically homogeneous multilayers show no substantial improvement in electromechanical coupling, whereas heterogeneous configurations lead to a remarkable enhancement. The highest effective coupling coefficient is obtained for the PZ24/26/27 (1/1/2) configuration, where the PZ27 layer has twice the thickness of the others.

Multilayer ceramics demonstrate enhanced piezoelectric response, reduced losses, and an effective electromechanical coupling coefficient exceeding that of the individual materials, resulting in improved macroscopic energy conversion. This behaviour cannot be explained by a simple averaging of properties, highlighting the decisive role of the multilayer architecture approach. These results establish a practical framework for designing high-efficiency bulk piezoelectric materials, particularly for energy harvesting applications, through the combination of compositions with tailored electromechanical properties.

References:

[1] Sahu, R. K., Asthana, S. J. Alloys Compd. 2025, 1010, 178227.

[2] Pradeesh, E. L., Udhayakumar, S., Vasundhara, M. G., Kalavathi, G. K. Microsyst. Technol. 2022, 28(8), 1797-1830.

Transversal Proposals

P.73. 2D-GADOLINIUM DILUTED METAL ORGANIC FRAMEWORKS ON FLEXIBLE SUBSTRATES. (NanoMagnetics&NanosMat)

Eva Tormos Feliu[a,b] **E. Carolina Sañudo**[a,b*] **Stefanos Chaitoglou**[ac]

a . Institut de Nanociències i Nanotecnologia, Universitat de Barcelona (IN2UB), 08028 Barcelona, Spain.
b. Departament de Química Inorgànica i Orgànica, Secció de Química Inorgànica, C/Martí i Franqués 1-11, 08028, Barcelona, Spain
c. Departament de Física Aplicada, C/Martí i Franqués 1-11, 08028, Barcelona, Spain

eva.tormos@ub.edu

The integration of lanthanoid ions into metal organic frameworks (MOFs) offers a promising platform for designing advanced materials with magnetic properties, which can be explored for application in emerging spintronics technologies[1].

The large intrinsic magnetic moment of lanthanoid coupled with the spatial ordering and bottom-up assembly of MOFs enables the desired suppression of spin relaxation and decoherence.

Previous studies in our group have revealed that the Gd ions in Gd-based MOFs exhibit favorable characteristics as molecular qubits[2]. With this finding as a starting point, we propose the synthesis of magnetically diluted La/Gd-based MOFs with varying Gd doping levels to study their qubit performance (including relaxation time (T_1) and phase memory (T_m)).

Moreover, while it is challenging, achieving effective surface deposition control is essential for certain application. This study also evaluates the deposition of MOF onto a flexible substrate (Kapton tape) combining physisorption (drop casting and Scotch tape methods) and chemisorption (immersion growth). The difference in binding strength will help us study how changes in the electronic structure during chemisorption affect magnetic behavior.

References

1.A Multifunctional Dysprosium-Carboxylato 2D Metall–Organic Framework Chem. Int. Ed. 2021, 60, 12001–12006
2.Magnetic and luminescent lanthanoid (Ln = Tb, Dy) 2D MOFs on functionalized silicon. J. Mater. Chem. C, 2025, 13, 21015

P.74. CHEMIRESISTIVE GREENHOUSE GAS DETECTION WITH TRIPHENYLENE- AND TRIPTYCENE-DERIVED MOFS. (NanoPhotoElectro&NanosMat)

Y. Mendoza-Gamero[1,2,3], A. M. Leyu[1,3], A. Romano-Rodriguez[1,2], D. Sainz-Garcia[2,3]

[1] Electronic and Biomedical Engineering Department, Universitat de Barcelona, Barcelona, Spain
[2] Institute of Nanoscience and Nanotechnology (IN2UB), Universitat de Barcelona, Barcelona, Spain
[3] Inorganic and Organic Chemistry Department, Universitat de Barcelona, Barcelona, Spain

yuzelfymendoza@ub.edu

Conductive metal-organic frameworks (MOFs) based on π-conjugated ligands have emerged as promising candidates for gas sensing due to their tuneable porosity, accessible active sites, and intrinsic charge transport properties. Triphenylene-based MOFs have demonstrated chemiresistive responses toward polar analytes, although detection of weakly interacting gases such as CO_2 and CH_4 remains challenging, especially in the presence of water [1,2].

Our work focuses on the synthesis of triphenylene-based MOFs (Cu- and Ni-HTAT) and their comparison with a series of triptycene-derived frameworks (M-HHTT; M = Cu, Ni, Zn, Co). By introducing a rigid 3D scaffold with intrinsic free volume, we investigate how modifying ligand dimensionality influences gas diffusion and adsorption, clarifying the role of framework topology in modulating the electrical response to non-polar analytes in realistic environments.

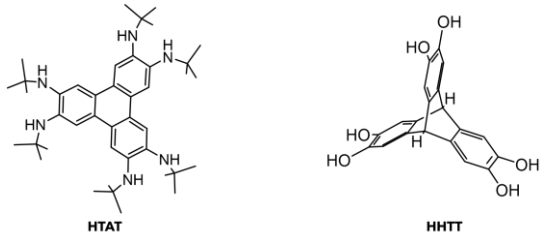

Figure 5. Chemical structures of the triphenylene-based (HTAT) and triptycene-based (HHTT) ligands

The triphenylene-based (HTAT) ligand was synthesized via bromination followed by Pd-catalyzed Buchwald-Hartwig amination. The triptycene-derived hexahydroxy (HHTT) ligand was prepared through Cu(I)-assisted methoxylation of a brominated triptycene precursor, followed by demethylation with boron tribromide [3,4]. Both ligands were characterized by NMR, ATR-FTIR, and ESI-MS.

MOFs (M-HTAT and M-HHTT) were obtained by solvothermal coordination and deposited onto platinum or gold interdigitated electrodes by drop casting. Sensing experiments were performed in a miniaturized chamber with mass-flow controllers delivering CO_2 and CH_4 pulses in synthetic air at 0-40% relative humidity, recording resistance changes in real time.

PXRD confirms crystalline MOF formation for both HTAT- and HHTT-based systems. Under CO_2 and CH_4 exposure, HTAT-based MOFs show a chemiresistive response that depends on relative humidity: with increasing humidity the baseline resistance decreases, which is consistent with transport dominated by planar π-conjugated pathways. HHTT-based MOFs display a similar trend with differences in signal modulation attributable to their three-dimensional structure.

In this work, we will present the synthesis of the ligands, triphenylene and triptycene, the preparation and structural characterisation of the corresponding MOFs prepared thereof, and the study of their chemiresistive response towards gas exposure, with particular emphasis on the influence of relative humidity.

References

[1] M. G. Campbell et al., J. Am. Chem. Soc. 137, 13780 (2015); doi: 10.1021/jacs.5b09600
[2] I. Fort-Grandas et al., ACS Small (2026, under review)
[3] S. Gonell et al., Angew. Chem. Int. Ed. 52, 7009 (2013); doi: 10.1002/anie.201302686
[4] Y. Lin et al., RSC Adv. 6, 32598 (2016); doi: 10.1039/C6RA01536K

P.75. Hexahydroxytriptycene-Based Metal-Organic Frameworks and Their Application in Catalysis (NanoPhotoElectro&NanosMat)

Abrha Mengstu Leyu[1,3], Yuzelfy Mendoza Gamero[1,2,3], Albert Romano-Rodriguez[1,2], Daniel Sainz-García[2,3].

[1]Dept Electronic and Biomedical Engineering, Universitat de Barcelona, Barcelona, Spain.
[2]Institute of Nanoscience and Nanotechnology (IN²UB), Universitat de Barcelona, Barcelona, Spain.
[3] Dept Inorganic and Organic Chemistry, Universitat de Barcelona, Barcelona, Spain.

aleyuley197@alumnes.ub.edu

Introduction

In modern chemical processes, catalysts play a crucial role by lowering the activation energy required for reactions, hence increasing reaction rates and enabling highly selective transformations. Homogeneous catalysts present challenges in terms of separation from mixtures, limited potential for recovery and reuse, and high operational costs. These limitations raise environmental concern due to waste generation and necessitate additional purification steps. To address these issues, heterogeneous catalysts have been developed. In addition to easier separation, enhanced recyclability and greater stability, their robustness and cost-effectiveness make them attractive for more sustainable and economically viable chemical process. Due to their high surface area, adjustable porosity, and presence of open metal sites, metal organic frameworks (MOFs) have emerged as promising heterogeneous catalysts. Hexahydroxytriptycene (HHTT) provides a rigid, π-conjugated structure with multiple coordination sites, enabling the formation of robust frameworks with transition metals. In this work, Ni, Cu, Zn, and Co-based HHTT MOFs were synthesized and evaluated for catalytic applications. Epoxide alcoholysis reactions were selected as model reactions due to their industrial relevance in chemical synthesis.

Materials & Methods

HHTT-based MOFs were synthesized using Ni^{2+}, Cu^{2+}, Zn^{2+}, and Co^{2+} metal salts via a solvothermal method. The obtained materials were characterized by powder X-ray diffraction (PXRD), Fourier-transform infrared spectroscopy (FTIR), scanning electron microscopy (SEM), transmission electron microscopy (TEM) and thermogravimetric analysis (TGA). Catalytic activity was evaluated in the alcoholysis of cyclohexene oxide with methanol (nucleophile) reaction in a covered gass reactor. Reaction aliquots were withdrawn at selected time intervals, diluted in pentane, and analyzed by gas chromatography (GC-FID), and conversion and selectivity were calculated using an internal standard method (toluene).

References [1] M. Mohammadikish, M. Masteri-Farahani, *Coord. Chem. Rev.*, 2026, **556**, 217684. [2] A. Banan, *Results Chem.*, **2026**, 21, 103064. [3] S. Kargar, D. Elhamifar, *Nanoscale Adv.*, **2025**, **7**, 4194–4204. [4] M. M. Ahmad, M. Roushani, S. Farokhi, *J. Electroanal. Chem.*, **2024**, 197, 1–8. [5] A. Santiago-Portillo, S. Naval, *Mol. Catal.*, **2024**, 564, 114288. [6] A. Jahanbani, Y. Mansoori, S. Fekri, *J. Organomet. Chem.*, **2026**, 1053. [7] L. Chen, Z. Gao, Y. Li, *Catal. Commun.*, **2015, 245**, 122–128. [8] J. Gabriel Flores, J. L. Obeso, V. Martínez, N. Martínez, E. González, I. A. Ibarra, *RSC Adv.*, 2023, **13**, 27174–27179.

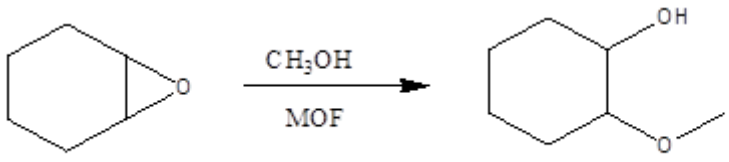

P.76. TOWARDS PHOSPHORUS-BASED MOFs FOR GAS SENSING (NanoPhotoElectro&NanosMat)

Judith Capdevila-Resa,[1,2,3] Albert Romano-Rodriguez,[1,3] Arnald Grabulosa[2,3]

[1]Universitat de Barcelona, Departament d'Enginyeria Electrònica i Biomèdica, Facultat de Física. [2]Universitat de Barcelona, Departament de Química Inorgànica i Orgànica, Facultat de Química.

[3]Institut de Nanociència i Nanotecnologia de la Universitat de Barcelona (IN2UB).

judith.capdevila@ub.edu

INTRODUCTION

Gas detection requires materials capable of interacting with gas molecules and converting these interactions into a measurable signal [1]. Metal–Organic Frameworks (MOFs) are promising candidates for this purpose because of their permanent porosity, high surface area, and tuneable chemical structure. Most of the described MOFs are built from nitrogen- or oxygen-based ligands, while phosphorus-containing MOFs (P-MOFs) remain largely unexplored and circumscribed to the field of catalysis, despite their potential to provide distinct coordination environments and electronic properties [2]

MATERIALS AND METHODS

This project proposes the design and synthesis of P-MOFs using ligands based on the triphenylene scaffold, a widely used building block in conductive MOFs due to its extended π-conjugation and favourable charge-transport properties. The incorporation of phosphorus-donor functionalities into triphenylene-based ligands could combine conductivity with unconventional coordination chemistry.

The resulting ligands will be coordinated to selected metal ions to obtain the corresponding MOFs, which will subsequently be characterized using standard structural and spectroscopic techniques. Their potential for gas sensing will be then evaluated by integrating them into miniaturized sensor platforms.

RESULTS AND DISCUSSION

We present the effective synthesis of some of phosphorus-based ligands, as well as the preliminary results on the synthesis of the proposed P-MOFs and their conductive properties. The aim is using them as chemoresistive and optical gas sensors for industrial gases, like CO and NO_x.

References:

[1] Dai et al., *Chem. Soc. Rev.*, 2020, 49, 1756–1789.
[2] Chen et al., *Angew. Chem. Int. Ed.*, 2024, 63, e202315075.

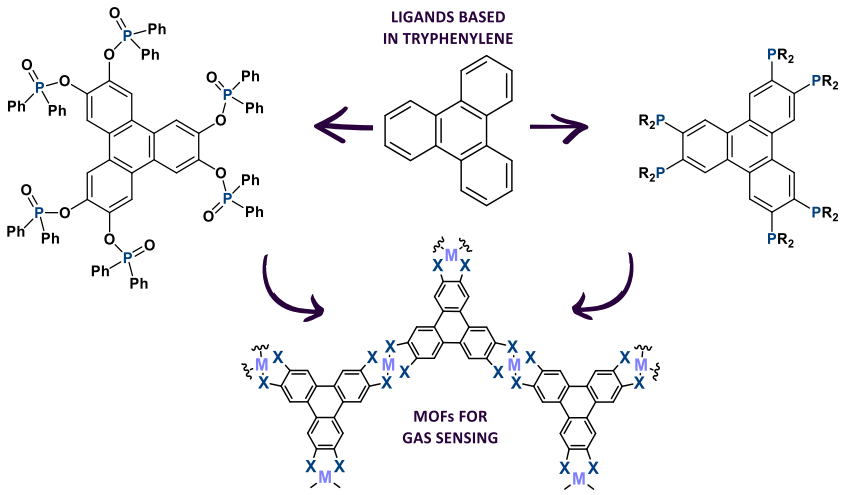

Institut de Nanociència
i Nanotecnologia
UNIVERSITAT DE BARCELONA